

Vacuum Systems

Lecture 4

V. Baglin

CERN TE-VSC, Geneva



Outline

1. Synchrotron radiation and photodesorption
2. Vacuum instability and ion stimulated desorption
3. Particle losses and ion stimulated desorption
4. Electron cloud and related surface parameters

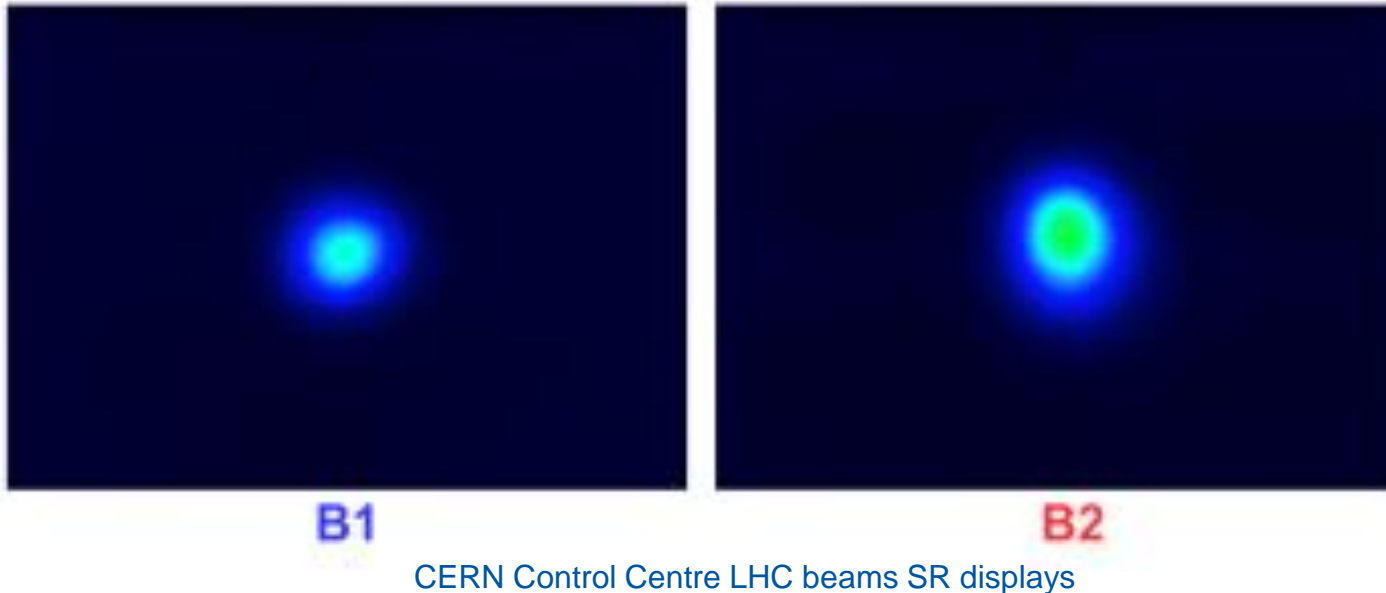
1. Synchrotron radiation and photodesorption

1.1 Synchrotron radiation

Synchrotron radiation: visible light

- In synchrotron, particles can radiate light by synchrotron radiation
- Can be use for diagnostics purposes :

LHC SYNCHROTRON LIGHT MONITORS



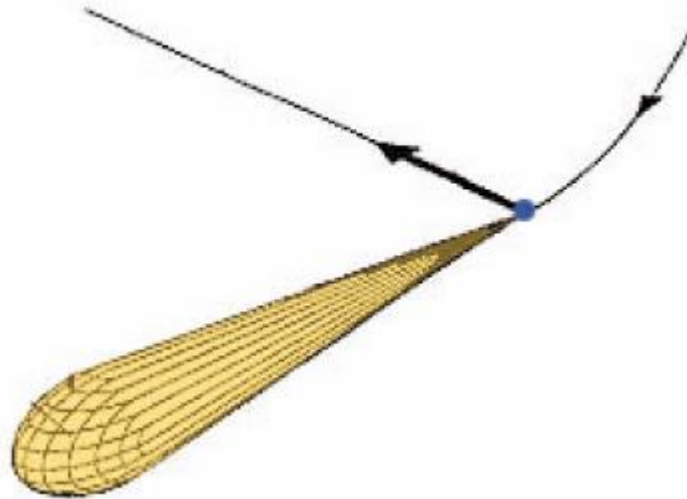
- But particles loose energy by synchrotron radiation → should be compensated by RF system
- Beam emittance shrink by synchrotron radiation
- Power is dissipated on the machine elements
- **Molecules are desorbed** from the vacuum chamber wall due to synchrotron radiation

Synchrotron Radiation

- A charged particle which is accelerated produce radiation
- The power of the centripetal radiation is larger than the longitudinal radiation (factor γ^3)
- For a relativistic particle, the radiation is highly peaked (opening angle $\sim 1/\gamma$)
- The radiation energy range from infra-red to gamma rays: from meV to MeV

References :

- K. Hübner, CAS 1984, CERN 85-19
- R.P. Walker, CAS 1992, CERN 94-01
- A. Hofmann, CAS 1996, CERN 98-04
- L. Rivkin, CAS 2008



Critical energy

- The critical energy split the power spectrum in two equals parts

$$\varepsilon_c = \frac{3}{2} \frac{hc}{2\pi} \frac{\gamma^3}{\rho}$$

$$\text{Electrons : } \varepsilon_c [\text{eV}] = 2.218 \cdot 10^3 \frac{E[\text{GeV}]^3}{\rho[\text{m}]}$$

$$\text{Protons : } \varepsilon_c [\text{eV}] = 3.5835 \cdot 10^{-7} \frac{E[\text{GeV}]^3}{\rho[\text{m}]}$$

- 90 % of the emitted photons have an energy lower than the critical energy
- Magnetic rigidity:

$$B \rho = \frac{p}{e} \approx \frac{E}{e c}$$

$$\frac{1}{\rho} \approx \frac{3}{10} \frac{B[\text{T}]}{E[\text{GeV}]}$$

$$\varepsilon_c \propto \frac{E^3}{\rho} \propto B E^2$$

Dissipated power

- The energy emitted by the synchrotron radiation per turn and per particle is:

$$\Delta E = \frac{e^2}{3\epsilon_0} \frac{\gamma^4}{\rho} = \frac{4\pi}{3} r m_0 c^2 \frac{\gamma^4}{\rho}$$

with $r = \frac{1}{4\pi\epsilon_0} \frac{e^2}{m_0 c^2}$ (classical radius)

- The average power emitted per turn by the beam is:

$$P_{\text{tour}} = \Delta E \frac{N}{t} = \frac{e \gamma^4}{3\pi\epsilon_0 \rho} I$$

- So, the average power emitted by the beam per unit of length is:

$$P_0 = \frac{\partial P}{\partial s} = \frac{e \gamma^4}{6\pi\epsilon_0 \rho^2} I$$

$$P_0 \propto \frac{E^4}{\rho^2} I \propto B^2 E^2 I$$

Dissipated power

- The average power emitted by the beam per unit of length is

$$P_0 \text{ [W/m]} = \frac{e}{3\epsilon_0 (m_0 c^2)^4} \frac{E^4}{2\pi \rho^2} I$$

$$P_0 \propto \frac{E^4}{\rho^2} I \propto B^2 E^2 I$$

- Electrons :

$$P_0 \text{ [W/m]} = 88.57 \frac{E[\text{GeV}]^4}{2\pi \rho[\text{m}]^2} I[\text{mA}]$$

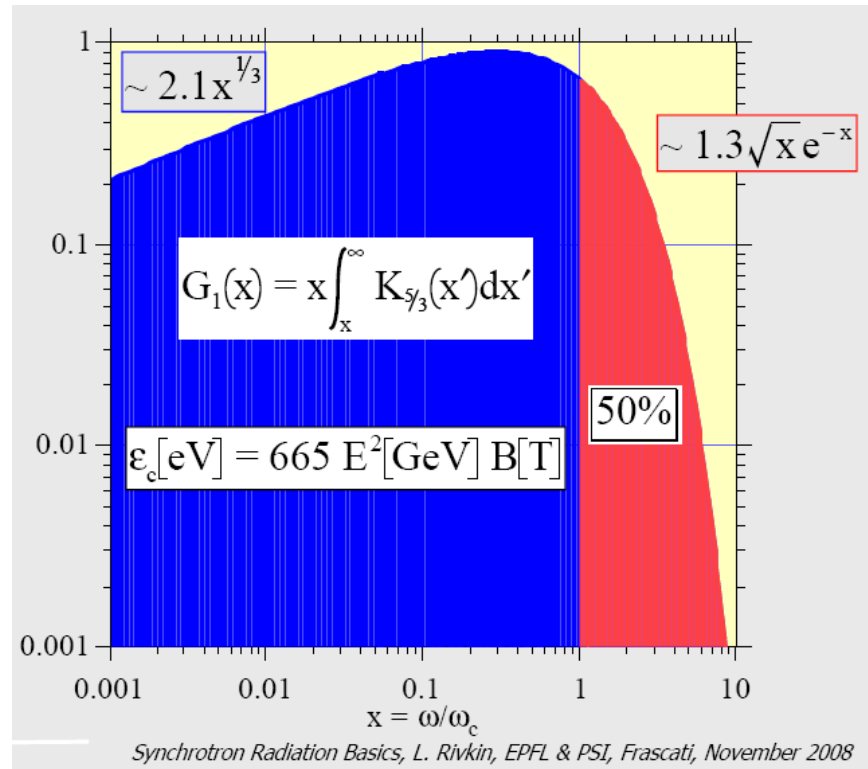
- Protons:

$$P_0 \text{ [W/m]} = 7.79 \cdot 10^{-12} \frac{E[\text{GeV}]^4}{2\pi \rho[\text{m}]^2} I[\text{mA}]$$

Power spectrum

- The SR power emitted by a particle is a function of the vertical angle and the wavelength.
- Integrating over the vertical angle, one obtains the **spectral power density** per unit of length :

$$\frac{\partial^2 P}{\partial s \partial \varepsilon} = P_0 \frac{1}{\varepsilon_c} S\left(\frac{\varepsilon}{\varepsilon_c}\right) \quad \text{with } S(x) = \frac{9\sqrt{3}}{8\pi} x \int_x^\infty K_{5/3}(z) dz \text{ ("universal function")}$$



Photon flux

- Since the photon flux is linked to the power by : $P = \dot{\Gamma} \varepsilon$
- The photon flux per unit length in a relative energy band is written:

$$\frac{\partial \dot{\Gamma}}{\partial \varepsilon / \varepsilon} = \frac{\partial^2 P}{\partial s \partial \varepsilon} = P_0 \frac{1}{\varepsilon_c} S\left(\frac{\varepsilon}{\varepsilon_c}\right)$$

- So, the total photon flux per unit of length is:

$$\dot{\Gamma} = \int_0^\infty \frac{\partial \dot{\Gamma}}{\partial \varepsilon} d\varepsilon = \frac{P_0}{\varepsilon_c} \times \int_0^\infty \left(\frac{\varepsilon}{\varepsilon_c}\right)^{-1} S\left(\frac{\varepsilon}{\varepsilon_c}\right) d\left(\frac{\varepsilon}{\varepsilon_c}\right) = \frac{15\sqrt{3}}{8} \frac{P_0}{\varepsilon_c} = \frac{5\sqrt{3}e}{12 h \varepsilon_0 c} \frac{\gamma}{\rho} I$$

$$\dot{\Gamma} \propto \frac{E}{\rho} I \propto B I$$

Linear photon flux

- The photon flux per unit of length is given by :

$$\dot{\Gamma} = \frac{15\sqrt{3}}{8} \frac{P_0}{\varepsilon_c} = \frac{5\sqrt{3}e}{12 h \varepsilon_0 c} \frac{\gamma}{\rho} I$$

$$\dot{\Gamma} \propto \frac{E}{\rho} I \propto B I$$

- Electrons :

$$\dot{\Gamma}[\text{photons.m}^{-1}.\text{s}^{-1}] = 1.28810^{17} \frac{E[\text{GeV}]}{\rho[\text{m}]} I[\text{mA}]$$

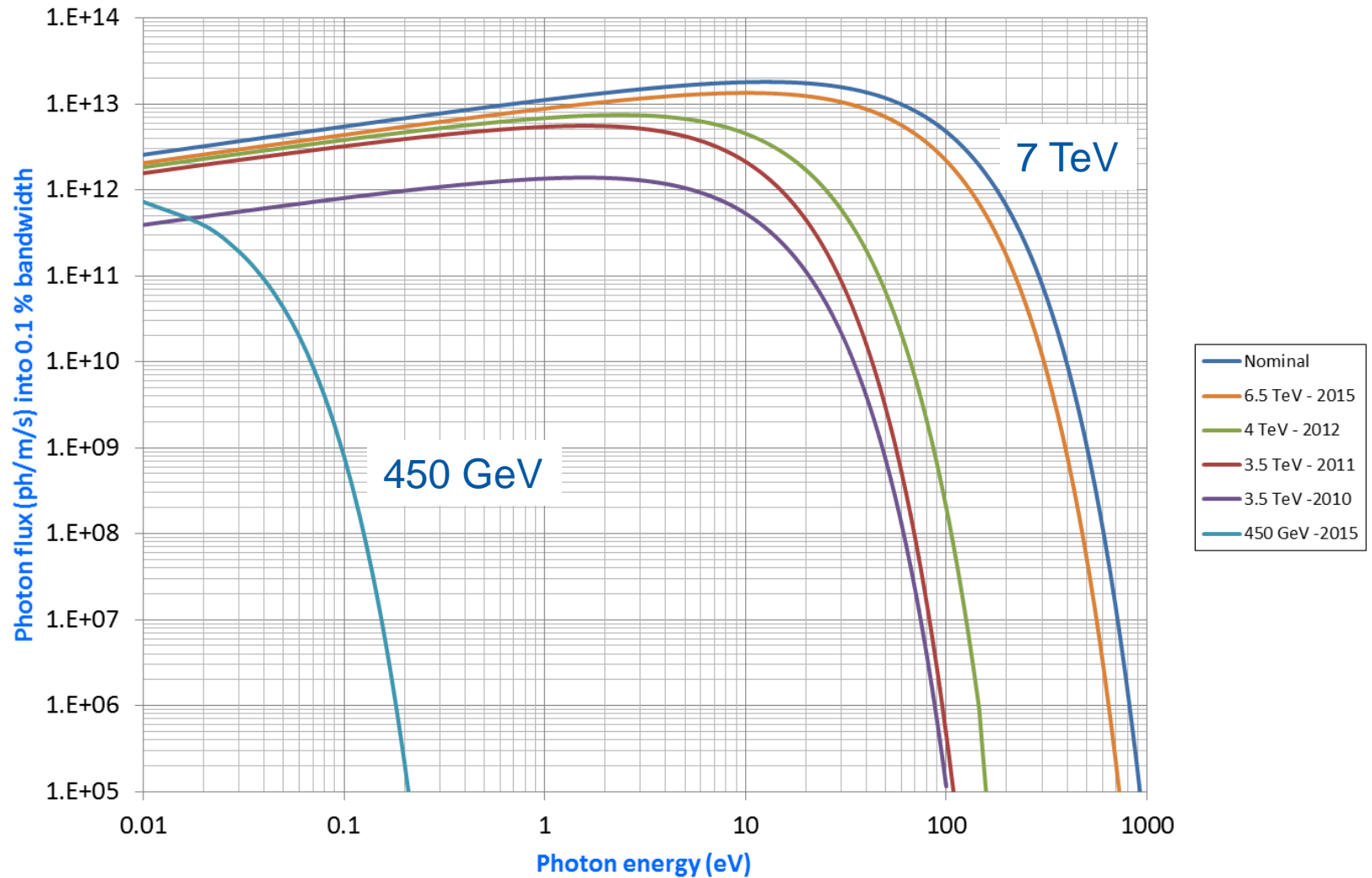
- Protons:

$$\dot{\Gamma}[\text{photons.m}^{-1}.\text{s}^{-1}] = 7.01710^{13} \frac{E[\text{GeV}]}{\rho[\text{m}]} I[\text{mA}]$$

LHC SR Spectrum : from IR to UV

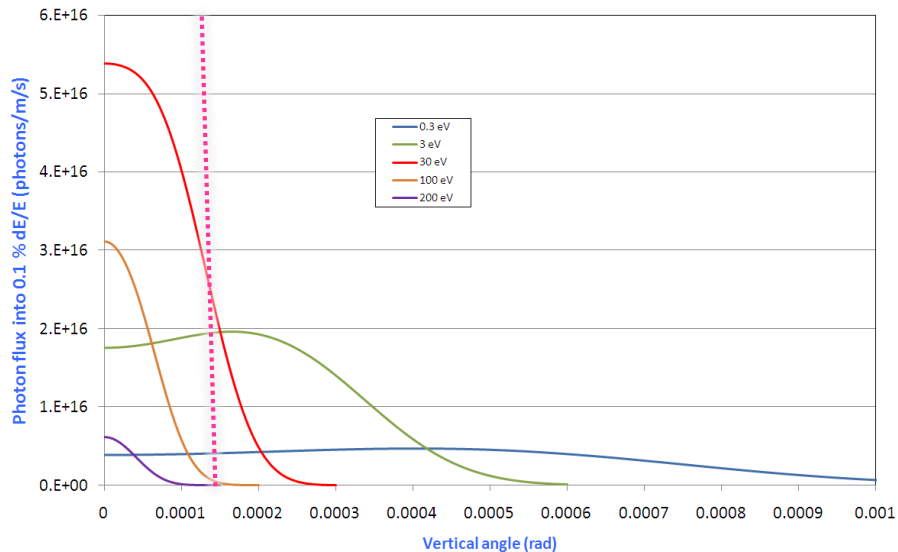
- With nominal parameters : 7 TeV and 585 mA
- 2010, 2011, 2012 and 2015 spectra

Key parameter: **photodesorption yield**

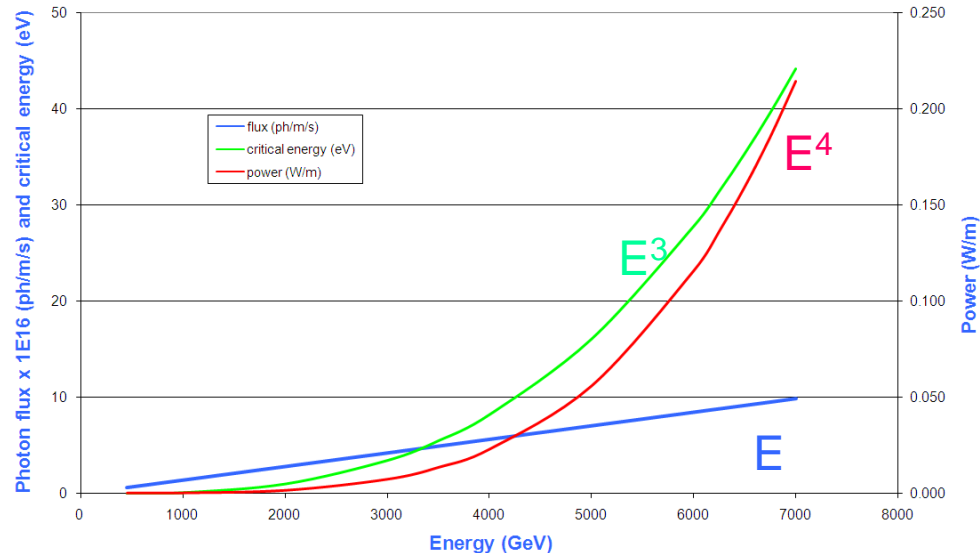


LHC SR properties

Vertical distribution of LHC photon flux

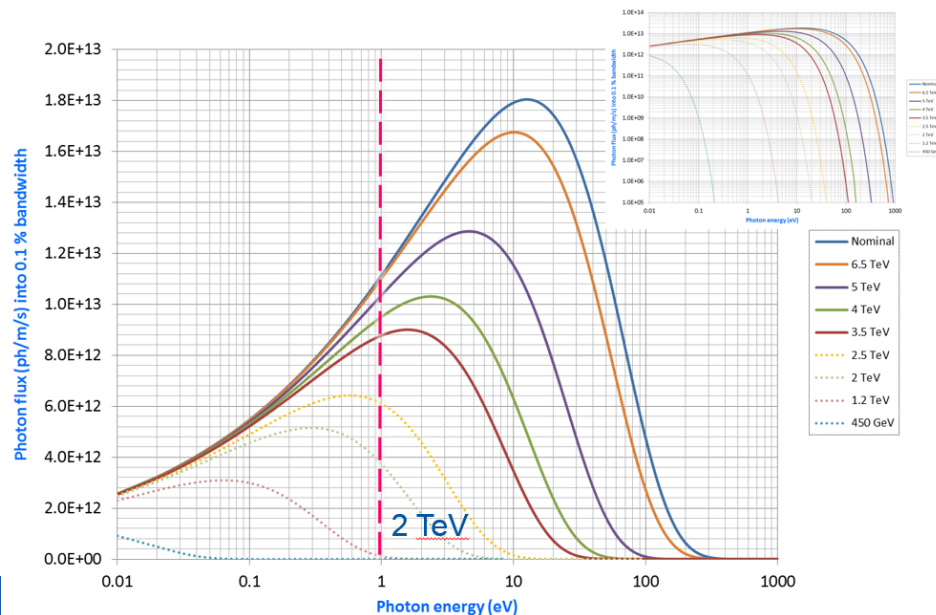


LHC synchrotron radiation at 560 mA

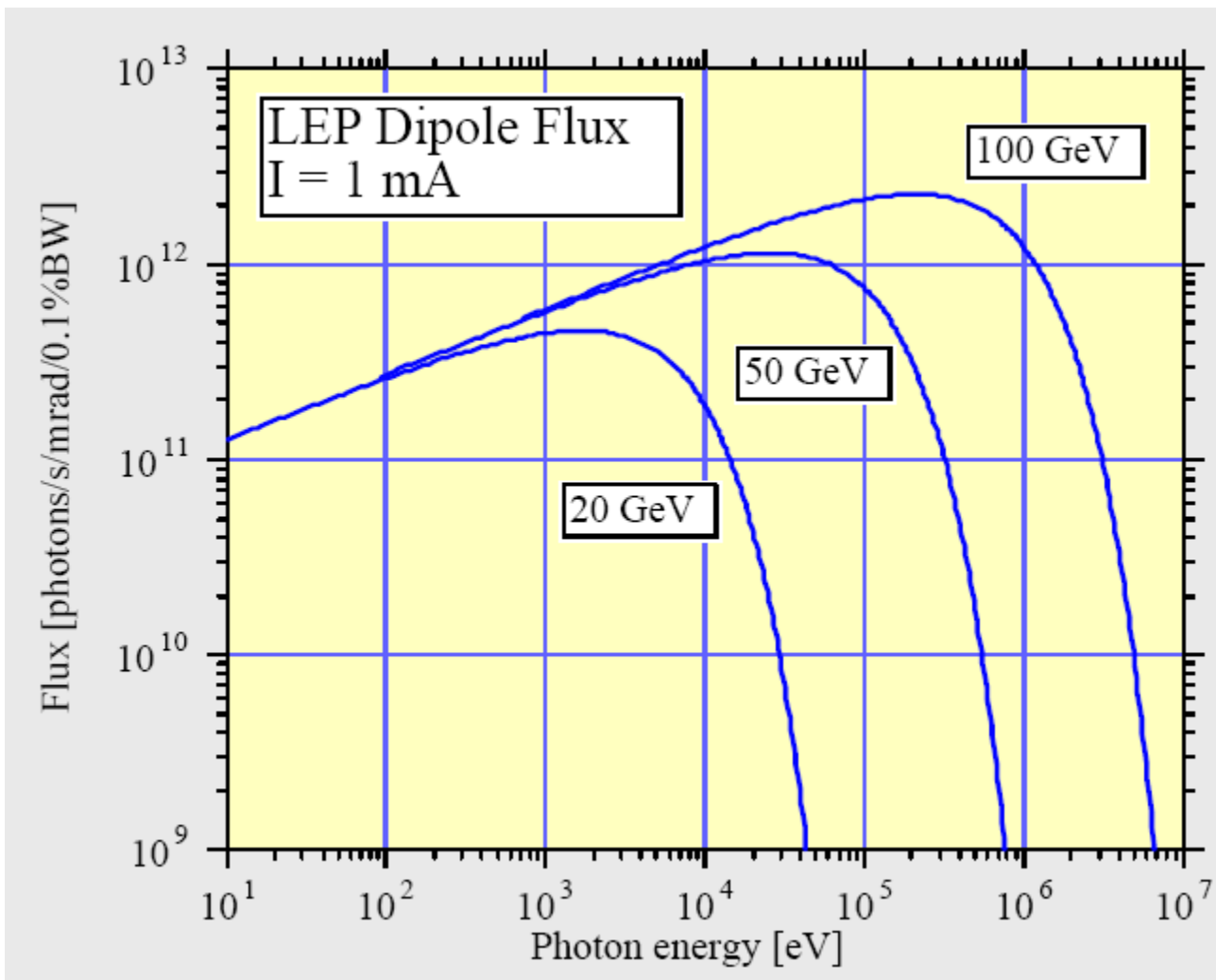


1/gamma opening angle

7 TeV
 $\epsilon_c = 44$ eV
 0.2 W/m
 10^{17} photons/m/s
 1/gamma = 0.13 mrad



LEP SR spectrum: X-rays & gamma rays



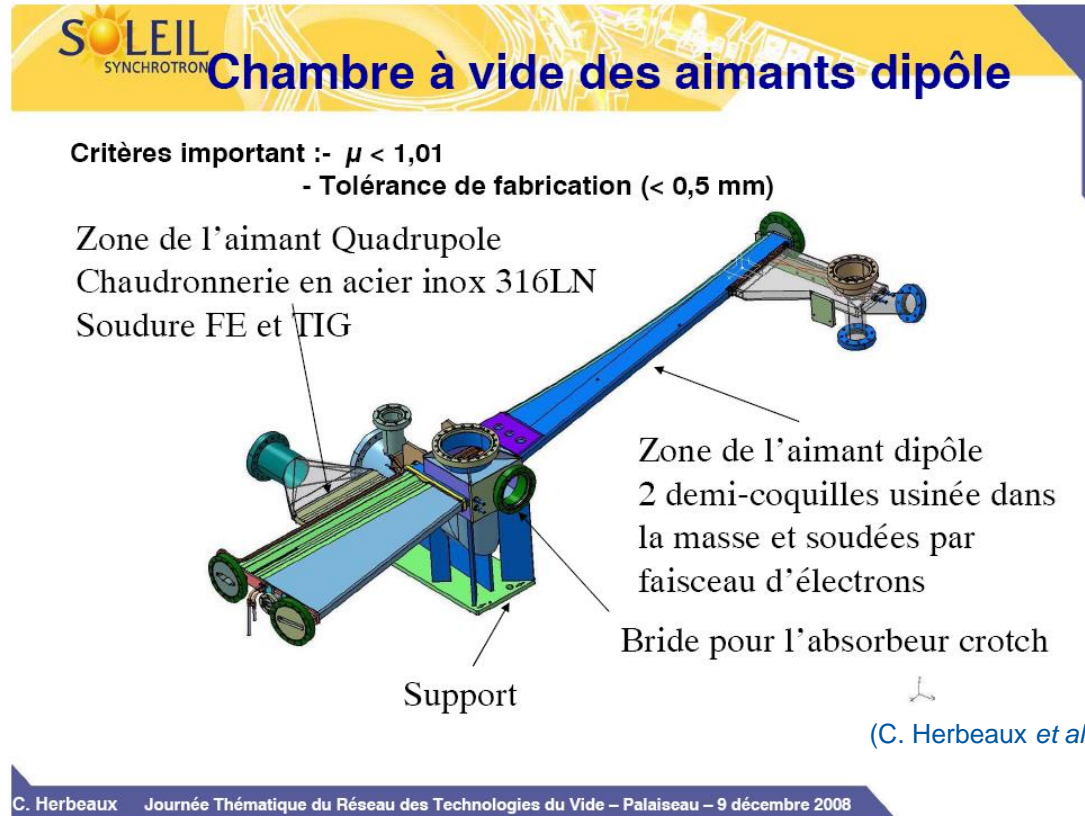
SR impact on different type of machines ...

		Soleil	KEK-B		LEP			LHC	
			LER	HER	Inj.	1	2	Inj.	Col.
Particle		e ⁻	e ⁺	e ⁻	e ⁻	e ⁻	e ⁻	p	p
Beam current	mA	500	2600	1100	3	3	7	584	584
Energy	GeV	2.75	3.5	8	20	50	96	450	7000
Bending radius	m	5.36	16.31	104.46	2962.96			2784.302	
Power	W/m	14 030	20 675	5 820	0.8	30	955	0	0.2
Critical energy	eV	8 600	5 800	11 000	6 000	94 000	660 000	0	44
Photon flux	photons/m/s	3 10 ¹⁹	7 10 ¹⁹	1 10 ¹⁹	3 10 ¹⁵	7 10 ¹⁵	3 10 ¹⁶	7 10 ¹⁵	1 10 ¹⁷
Dose at 3000 h	photons/m	4 10 ²⁶	8 10 ²⁶	1 10 ²⁶	3 10 ²²	7 10 ²²	3 10 ²³	7 10 ²²	1 10 ²⁴

- In LEP, and all synchrotron light sources, the evacuation of the **power is an issue**
- The LHC will operate at 7 TeV with ~ .6 A. **Power evacuation is an issue for the cryogenic system (1 kW/arc !!)**
- The critical energy varies from a few 10 eV to 660 keV. **Strongly bound molecules can be desorbed**
- The photon flux is large, so large gas load. **Adequate dimensioning of the effective pumping speed**
- The annual photon dose is large. **Implications on gas reduction and radiation**

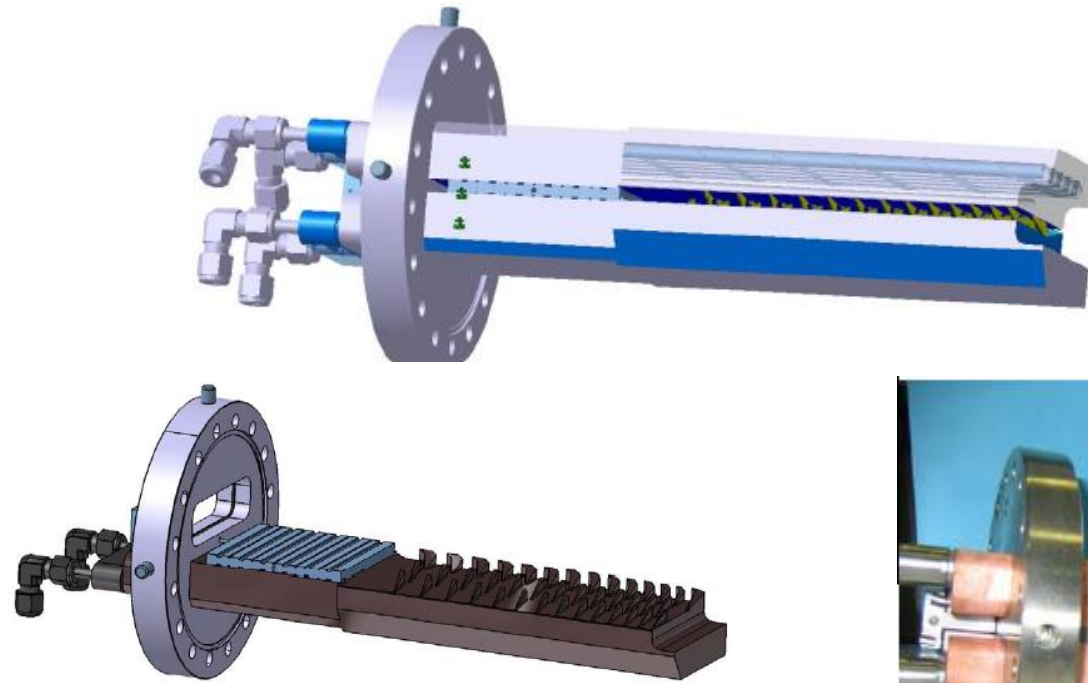
... heavy consequences on design

- Stainless steel
- NEG coated, in-situ baked to 180°C

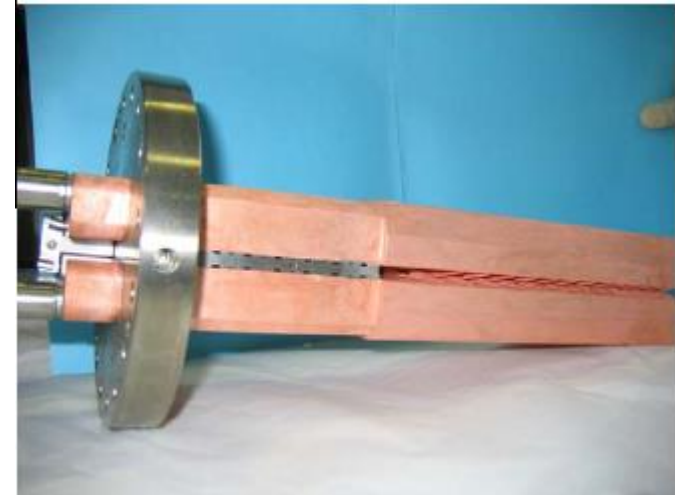


- A **complex** vacuum chamber design with a light extraction path, pumping and instrumentation ports and **power absorbers** (crotch)

... heavy consequences on design



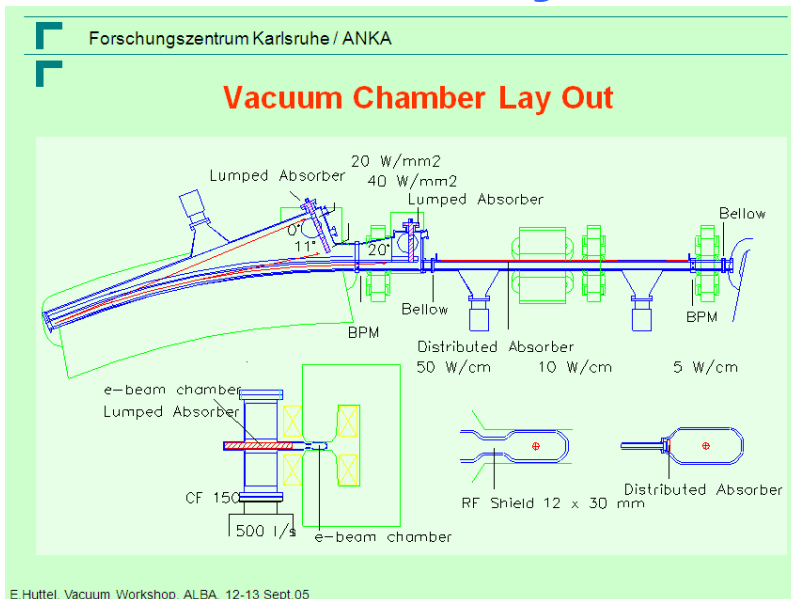
SOLEIL Design



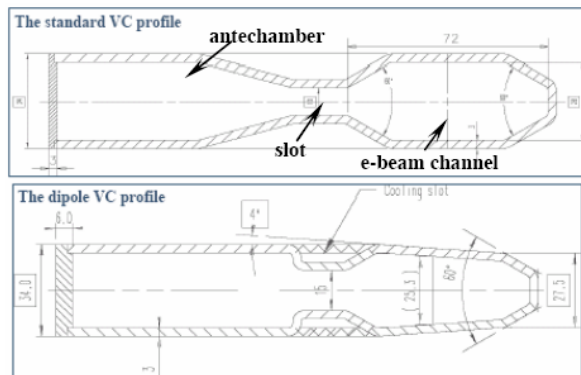
(C. Herbeaux *et al.*)

- Soleil « crotch » power absorber: Water cooled copper Glidcop (256 W/mm^2)

... heavy consequences on design

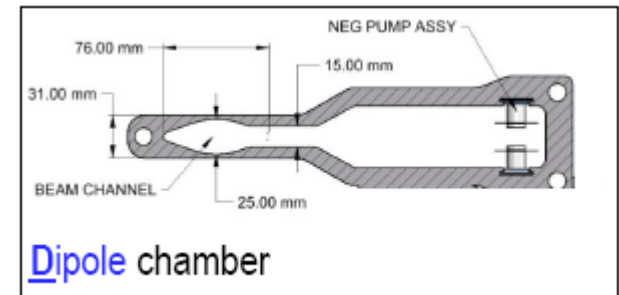


(E. Huttel et al.)



ALBA Design

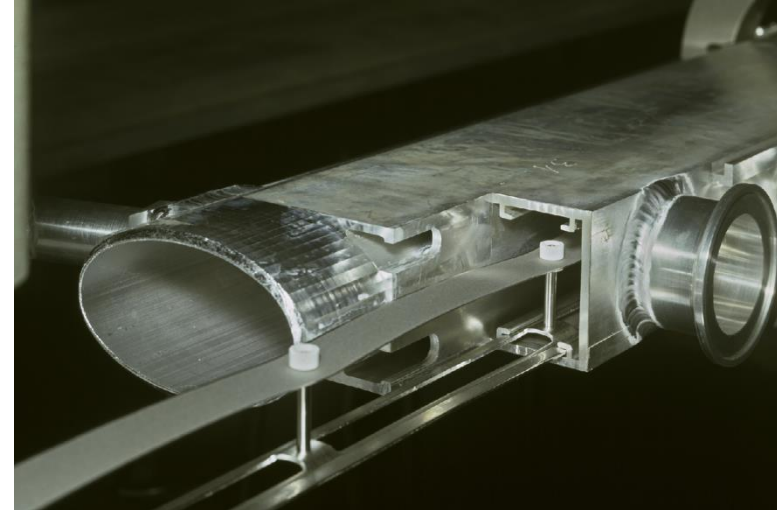
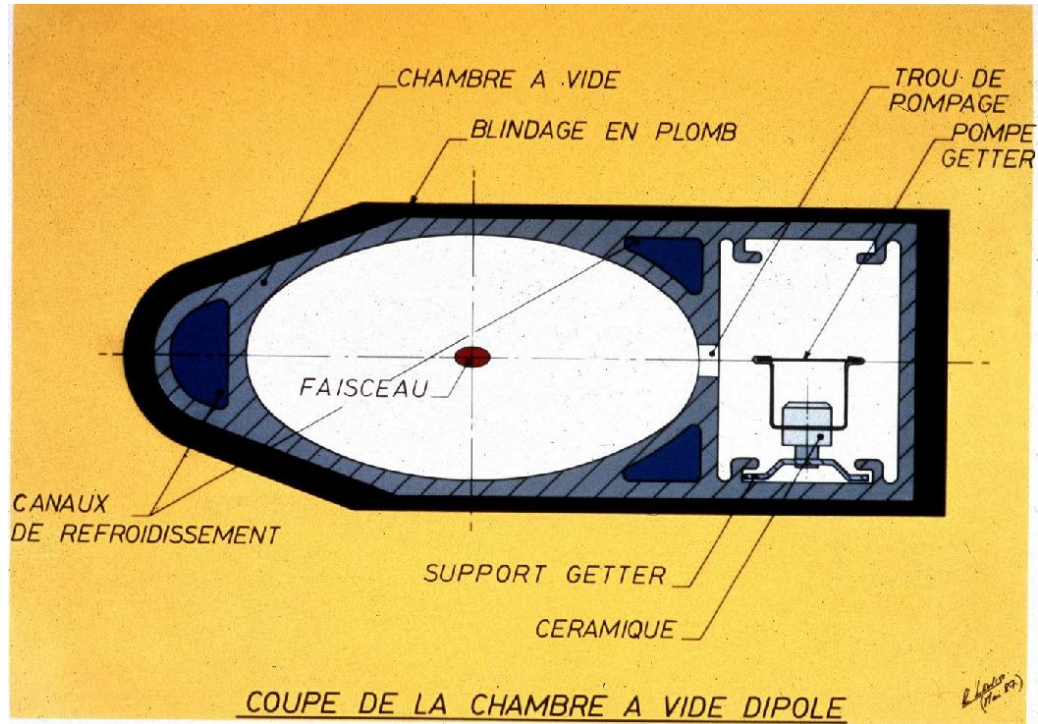
(E. Al-Dmour, EPAC 2006)



NSLS-2 Design

- **Antechamber** design to absorb the SR power externally to the beam path with the integration of a distributed pumping

... heavy consequences on design

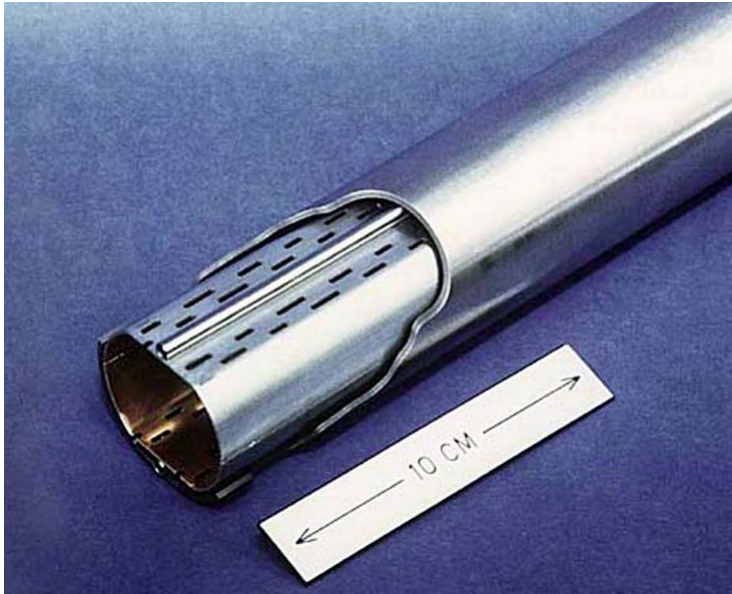


LEP Design

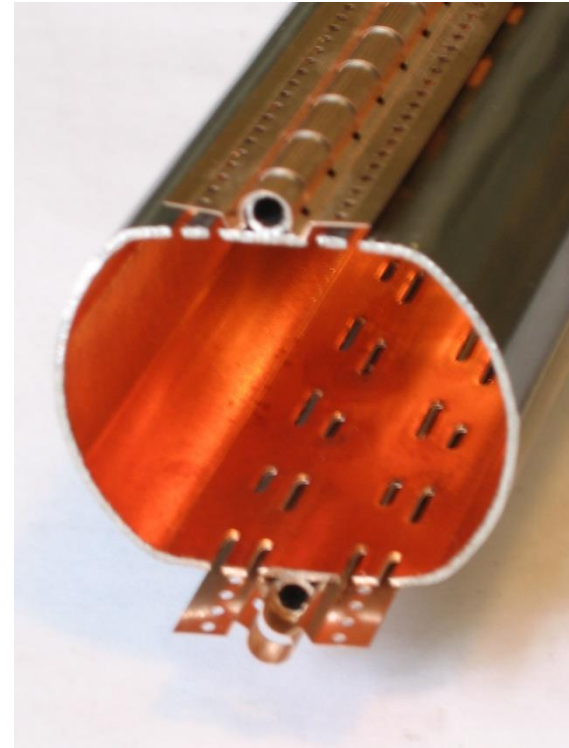
(CERN LEP Vacuum group)

- Antechamber and distributed NEG pumping, water cooling and lead shielding

... heavy consequences on design



Courtesy N. Kos CERN TE/VSC



Courtesy N. Kos CERN TE/VSC

LHC Design

(CERN LHC Vacuum group)

- **Perforated Cu colaminated beam screen** to intercept the SR power protecting the 1.9 K cold bore and to allow a distributed pumping

1.2 Photodesorption

Photodesorption

- The interaction of photons (light) with matters produce the **desorption of neutral gases** inside the vacuum system
- The photon stimulated desorption (PSD) of physisorbed (meV) or chemisorbed (eV) molecules can be direct or non-direct
- The identified transmitter are photoelectrons, secondary electrons and phonons
- The photon stimulated molecular desorption is a function of the nature of the material, its temperature, its surface state, of the photon energy and the irradiation angle.
- No model exists, therefore ***in-situ* qualification** of material is required for the design of a future machine.

Photodesorption: present understanding

- The photodesorption process is linked to the production of photoelectrons and secondary electrons
- Photoelectrons contribute to the gas load by ESD
- The **oxide and carbon layers** are believed to be the source of gas
- The diffusion of atoms into the solid and their recombination at the surface plays a role

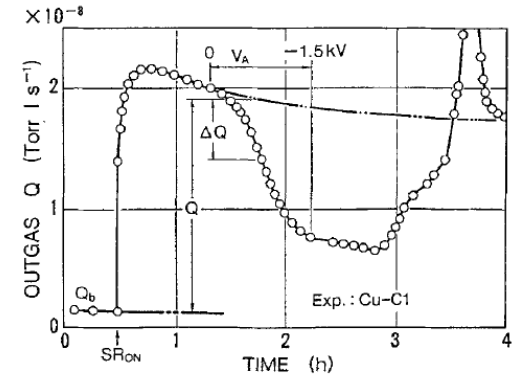


Fig. 5. Changes of outgas due to the bias voltage V_A .

T. Kobari *et al* Proc .of Vacuum Design of Synch Light Sources Conference, Argonne, 1990

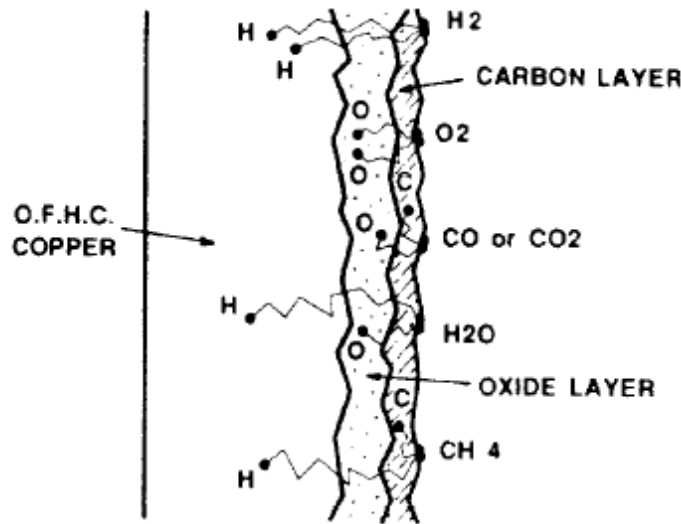
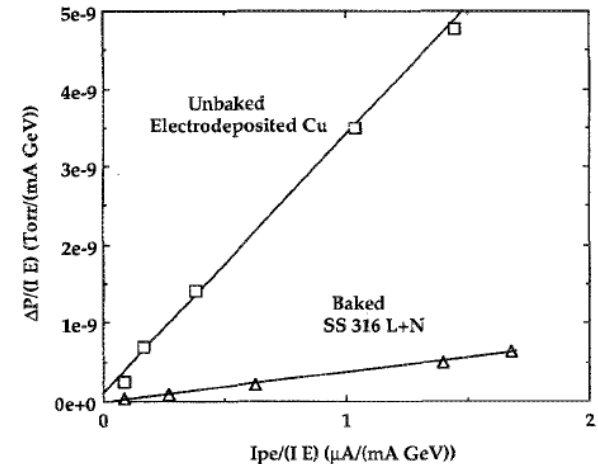


Fig. 6. Tentative Microscopic Model for PSD from OFHC Copper.

O. Gröbner *et. al.* EPAC 1992



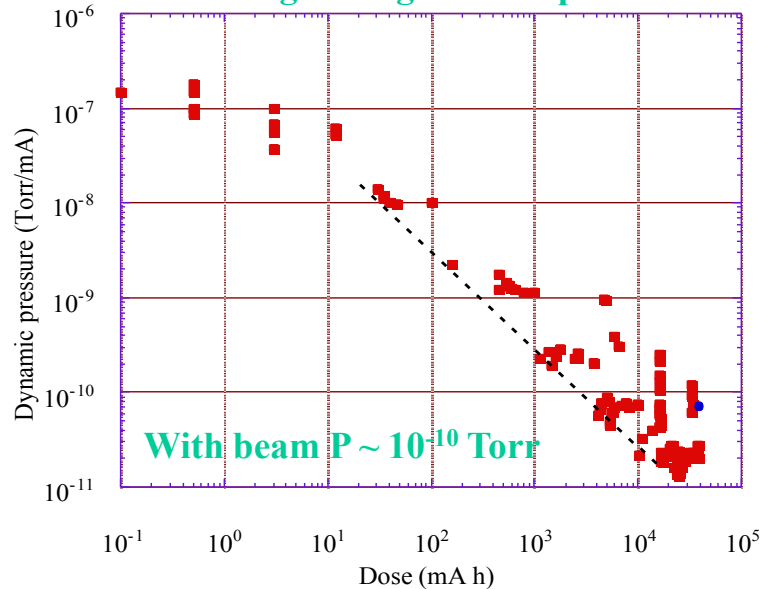
J. Gómez-Goñi *et al.* JVSTA 12(4) Jul/Aug 1994, 1714

Dynamic pressure due to PSD

- The dynamic pressure decreases by several orders of magnitude with photon dose: “**photon conditioning**”
- The photon desorption yield is characterised by η_{photon}

$$P = \frac{Q + \eta_{\text{Photons}} \dot{\Gamma}_{\text{Photons}}}{S}$$

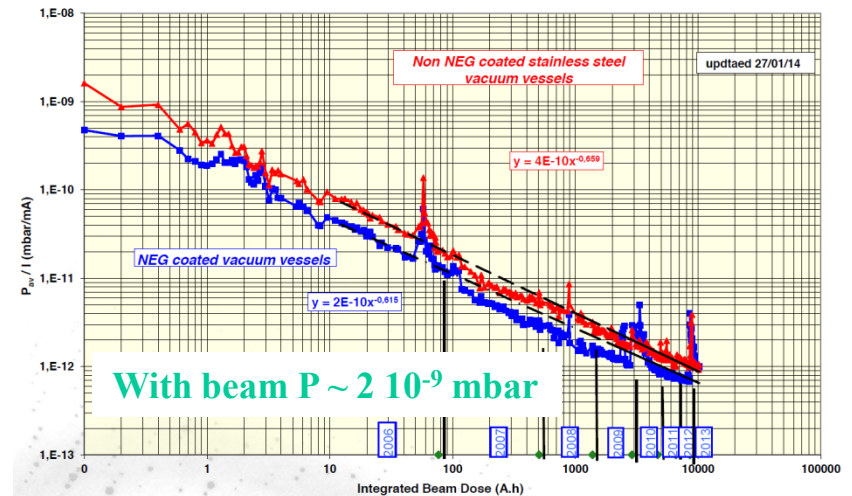
Beam cleaning during the first period of LEP



O. Gröbner. Vacuum 43 (1992) 27-30

SOLEIL

Average pressure rise in cell C07 normalized to current Vs. beam dose



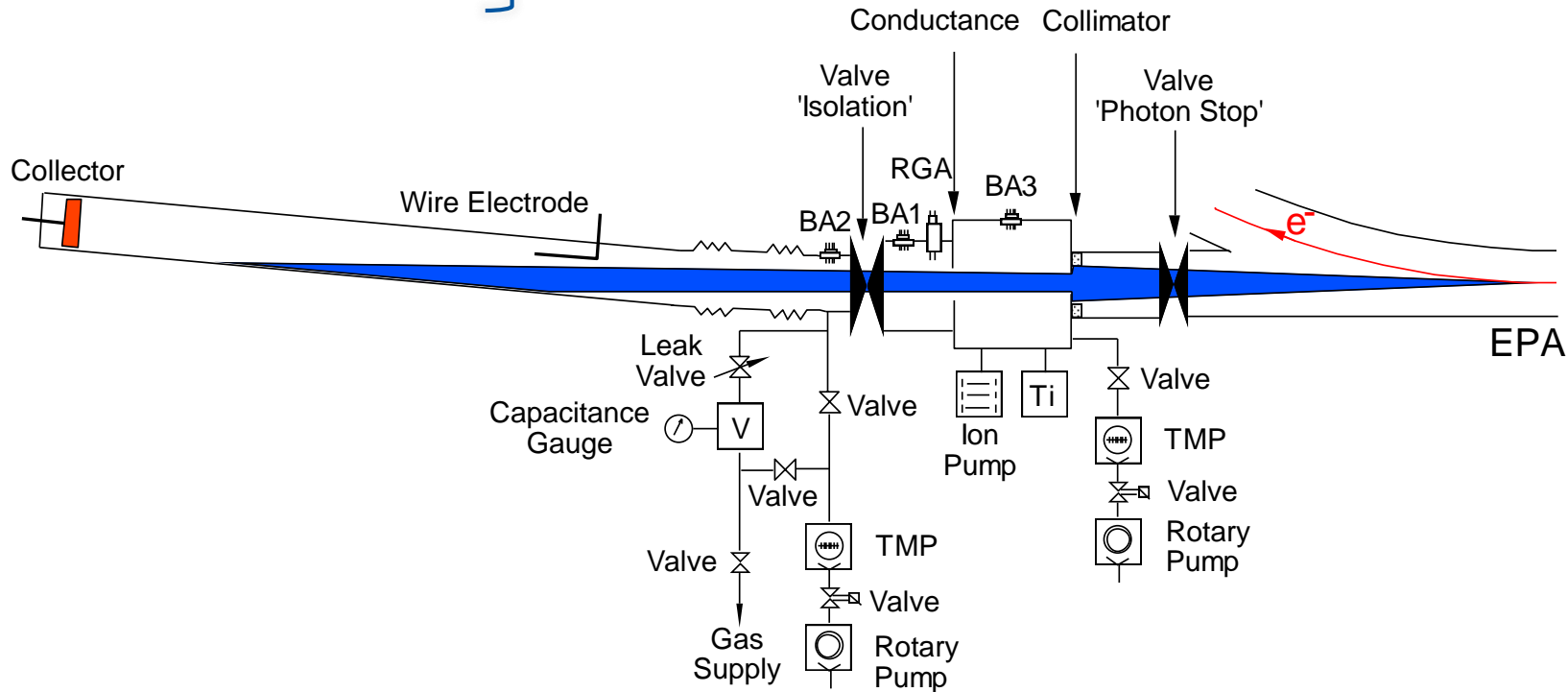
C. Herbeaux, Journée thématiques RTVide, décembre 2014

Photo-desorption yield measurement

- SR light is extracted from a dipole magnet to irradiate the chamber at ~ 11 mrad
- SR fan is vertically collimated therefore photon flux < 4 eV are attenuated
- The gas load is measured by the throughput method via a conductance (72.5 l/s for N₂)
- A wire and a collector are biased for current measurement to estimate the photon reflectivity and photoelectron yield

$$\left. \begin{aligned} Q_0 &= C (P_2 - P_1) \\ Q &= \eta \dot{\Gamma} + Q_0 = C (P'_2 - P'_1) \end{aligned} \right\} \eta = \frac{G}{\dot{\Gamma}} C (\Delta P_2 - \Delta P_1) \approx \frac{G}{\dot{\Gamma}} C \Delta P_2$$

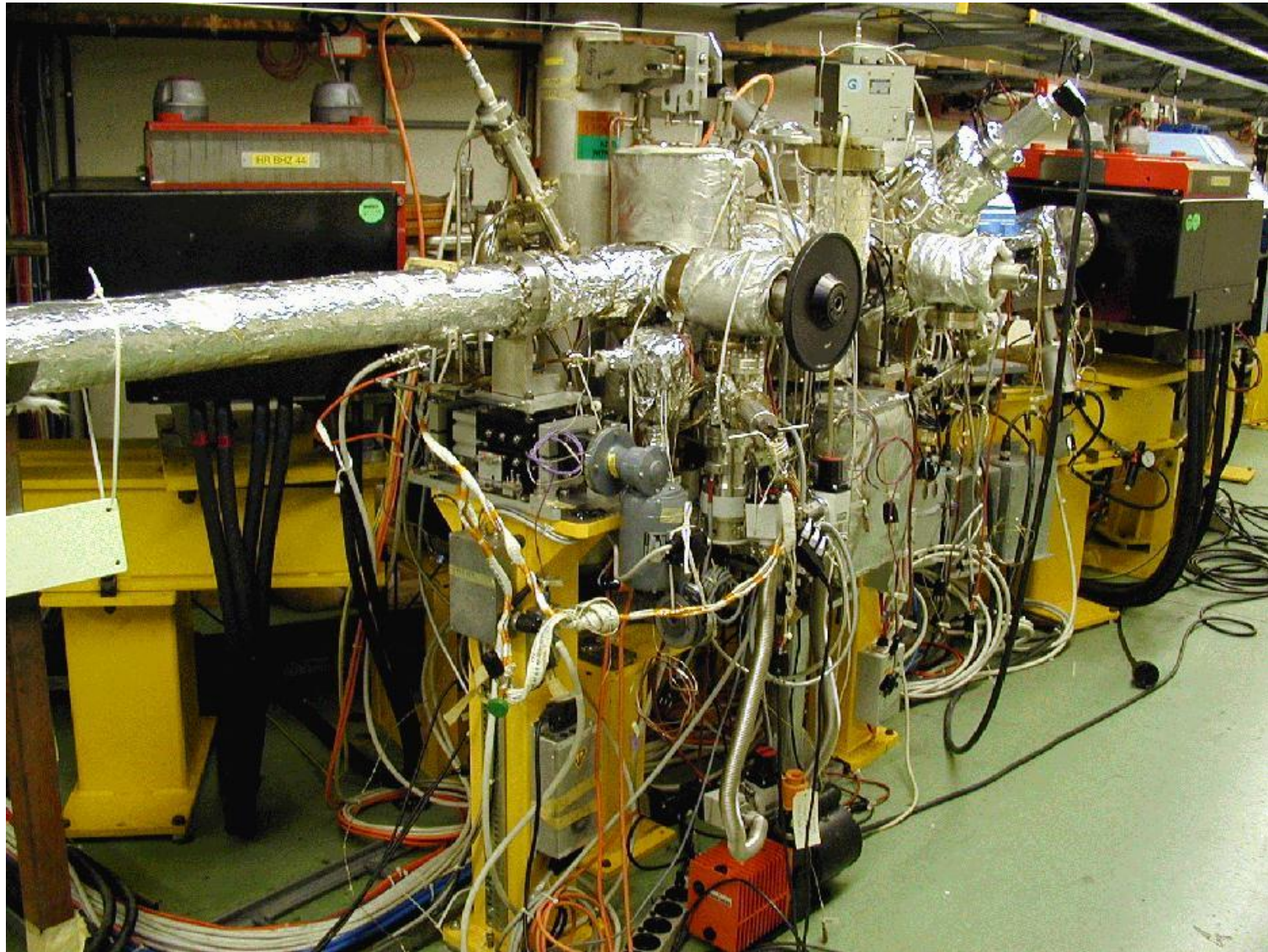
With $G = 4.3 \cdot 10^{19}$ molecules/mbar.l



J. Gómez-Goni et al. J. Vac. Sci. Technol. A 12(4), Jul/Aug 1994, 1714

V. Baglin et al. EPAC 1998, Stockholm, Sweden.

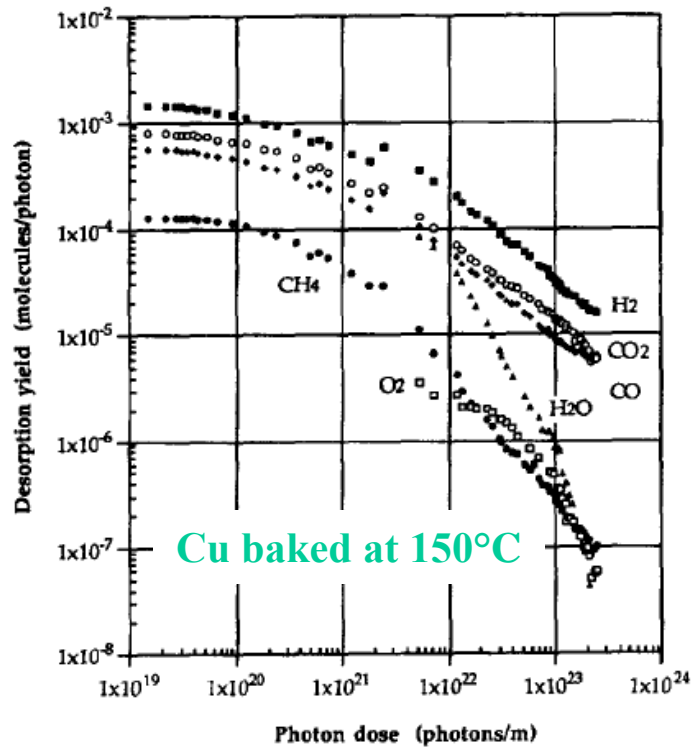
CERN EPA Synchrotron Light Facility 42 - 1999



The LEP Pre-Injector as a multipurpose facility, J-P. Potier, L. Rinolfi, EPAC 1998, Stockholm, Sweden, 1998

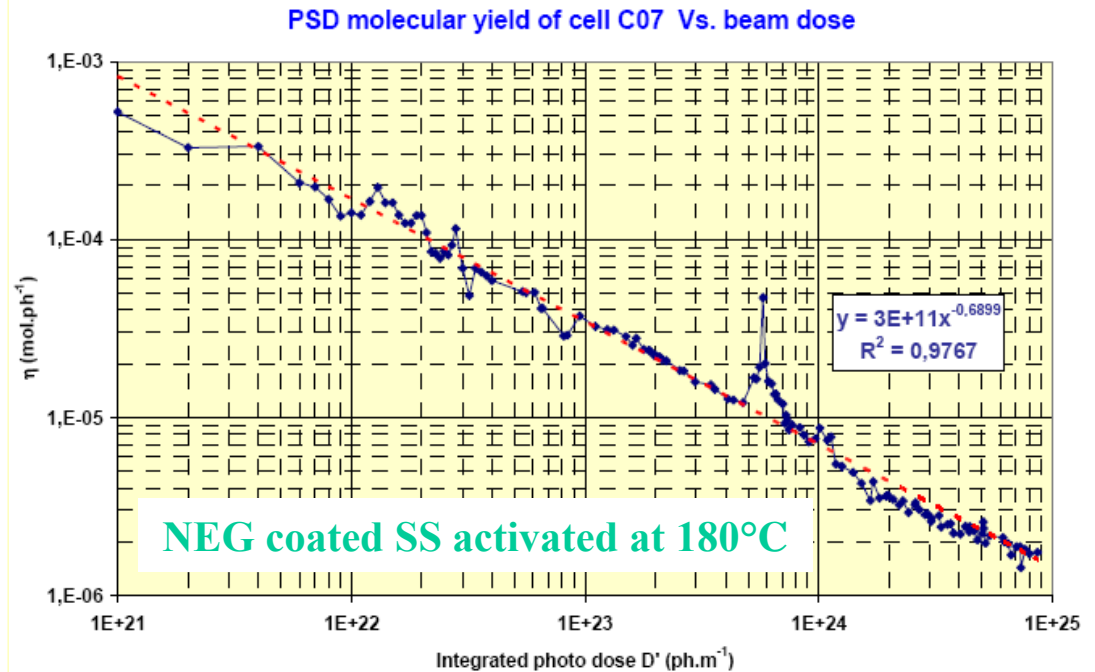
Conditioning under photon irradiation

- Typical desorption yield range: from 10^{-3} molecule/photon to 10^{-6} when conditioned



O. Gröbner *et al.*

J.Vac.Sci. 12(3), May/Jun 1994, 846-853



C. Herbeaux *et al.* EPAC 2008, Gênes, Italie

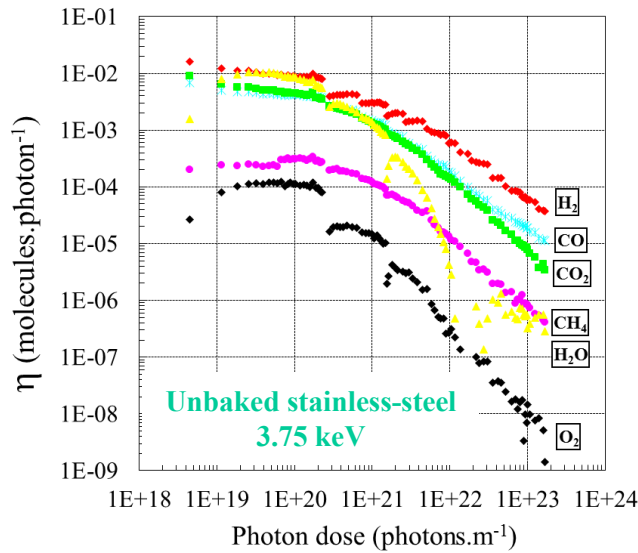
$$\eta_{Photons} = \eta_0 \left(\frac{D}{D_0} \right)^{-a}$$

- The hydrogen desorption is characterised by a diffusion process: $a = 0,5$

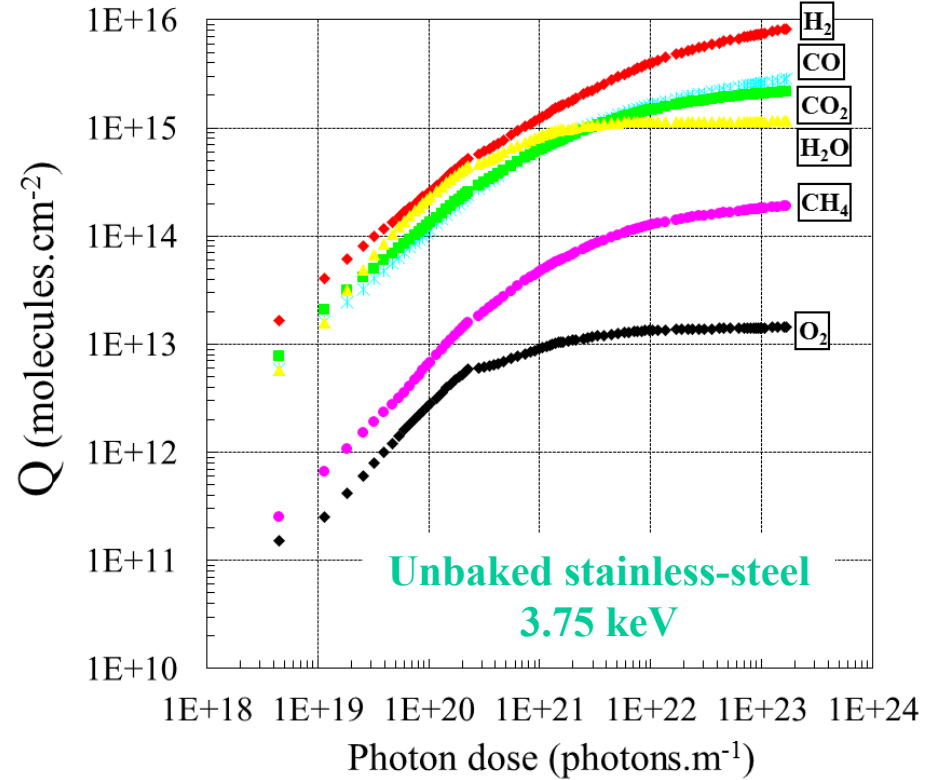
M. Andritschky *et al.*, Vacuum 38 (8-10), 933, (1988)

Gas load

- The total desorbed quantity amounts to 15 monolayers for an unbaked system



$$Q = \int \eta d\Gamma$$



Gas	H ₂	CH ₄	H ₂ O	CO	CO ₂	Total
molecules/ cm ² x 10 ¹⁵	8.1	0.2	1.1	2.8	2.2	14.4

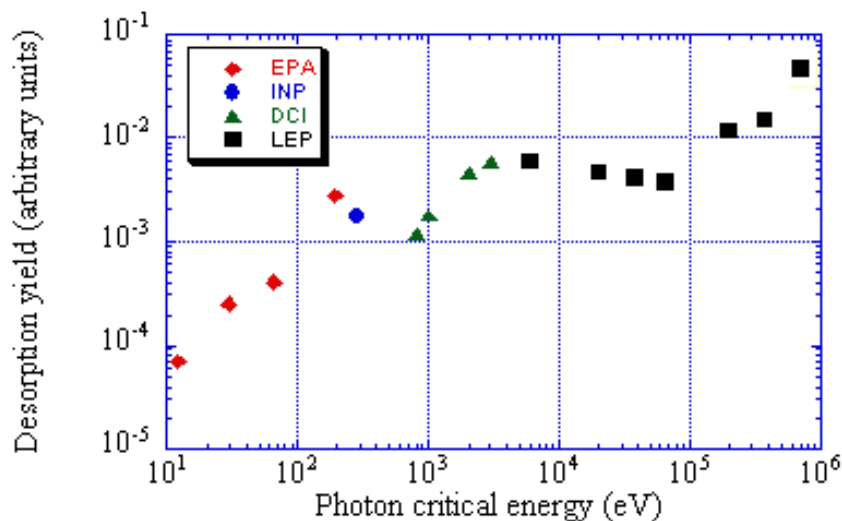
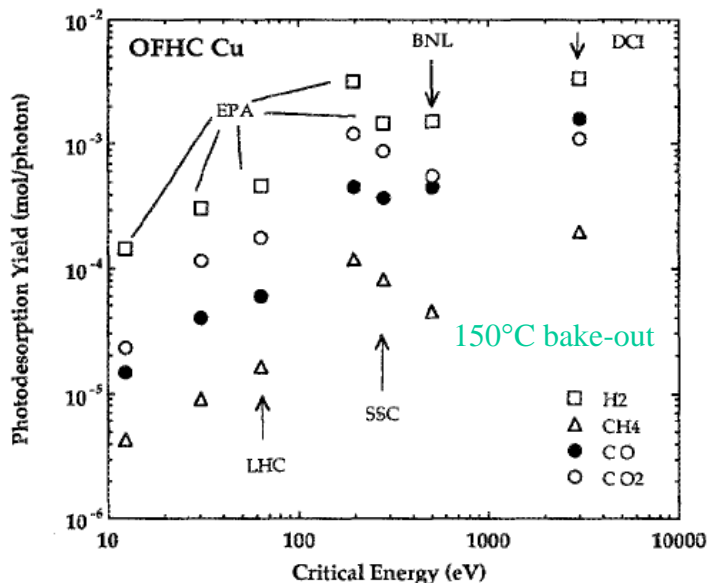
C. Herbeaux *et al.* JVSTA 17(2) Mar/Apr 1999, 635

Evolution with critical energy

- At low energy, the **photoelectric effect** dominates
- Above a few 100 keV, **Compton diffusion** dominates and produce a cascade of energetic recoil electrons with a diffusion of secondary photons

$$\eta(\text{H}_2) \sim E_c^{0.74}, \quad \eta(\text{CH}_4) \sim E_c^{0.94}$$

$$\eta(\text{CO}) \sim E_c^{1.01}, \quad \eta(\text{CO}_2) \sim E_c^{1.12}$$



O. Gröbner. CAS 99-15

J. Gómez-Goñi *et al.* JVSTA 12(4) Jul/Aug 1994, 1714

Photodesorption of NEG films

- Very low desorption yields
- Be aware of the difference between effective and **intrinsic yields**

$$\eta_{intrinsic} \approx \left(\frac{S}{C} + \sqrt{\frac{S}{C_t}} \right) \times \eta_{effective}$$

V. Baglin *et al.* CERN VTN 98-04, 1998.

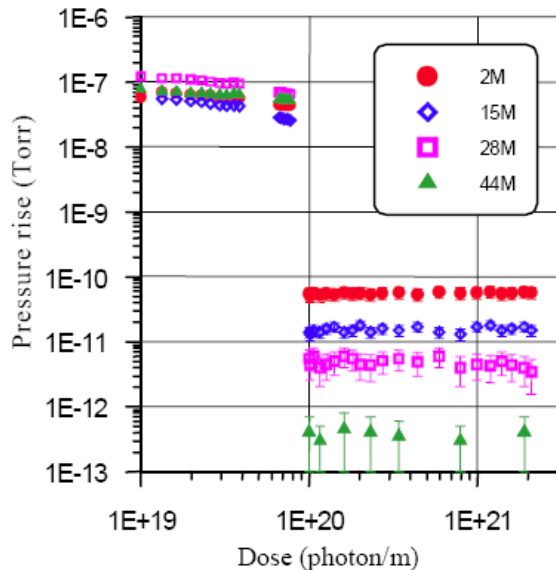


Figure 2: Pressure rise measured in the centre of the TiZrV coated test chamber before activation ($<1 \cdot 10^{20}$ photons/m) and after activation ($>1 \cdot 10^{20}$ photons/m).

TiZrV film on stainless-steel
4.5 keV

V. Anashin *et al.* EPAC 2002, Paris, France.

Table 1: Summary of results from the non-activated test chamber

Gas	Sticking probability	Photodesorption yield (molecules/photon)
H ₂	0	$1 \cdot 10^{-3}$
CH ₄	0	$2.5 \cdot 10^{-4}$
CO	0	$5 \cdot 10^{-4}$
CO ₂	0	$3 \cdot 10^{-4}$

Baked at
80°C

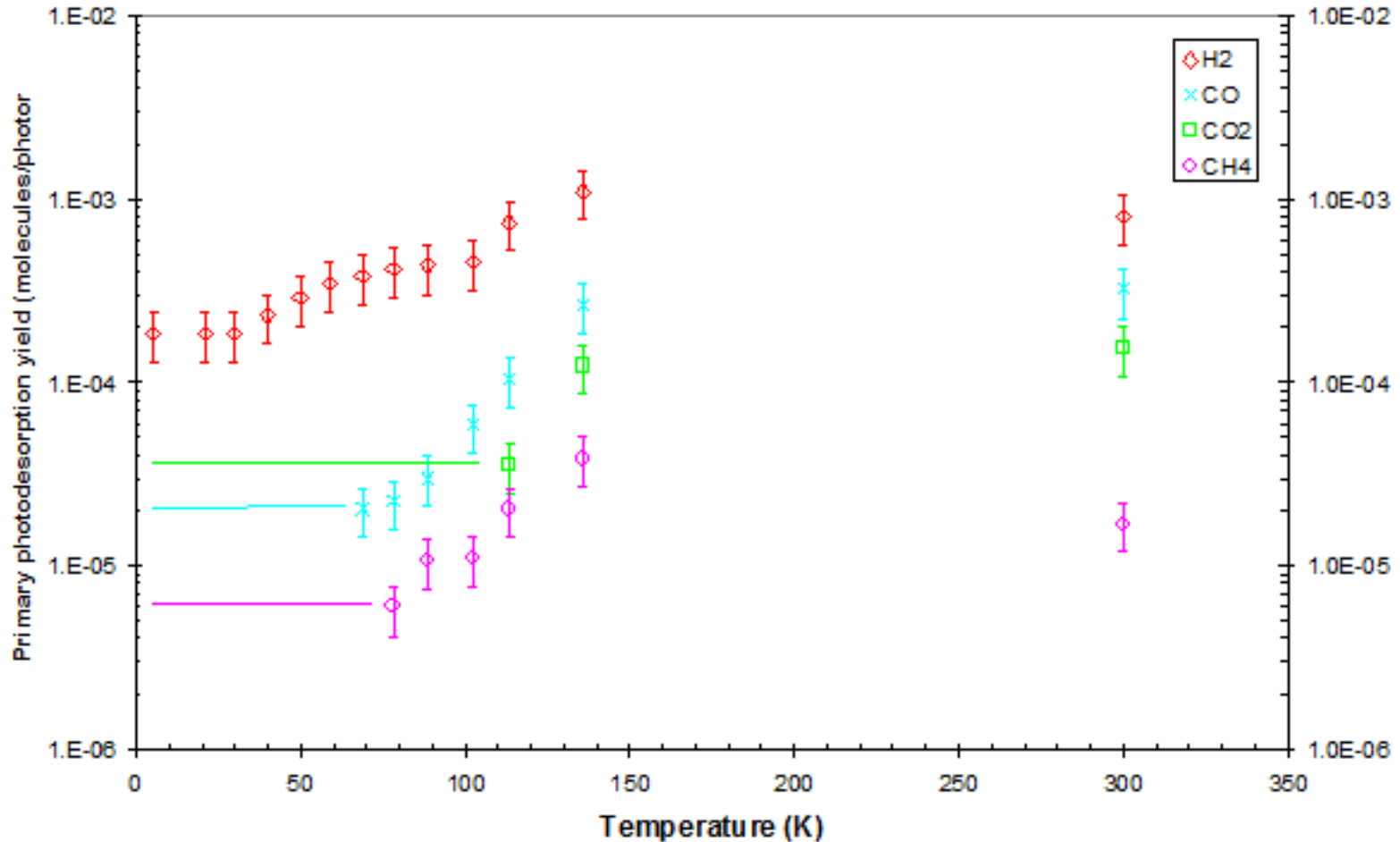
Table 2: Summary of results from the activated test chamber

Gas	Sticking probability	Photodesorption yield (molecules/photon)
H ₂	~ 0.007	$\sim 1.5 \cdot 10^{-5}$
CH ₄	0	$2 \cdot 10^{-7}$
CO (28)	0.5	$< 1 \cdot 10^{-5}$
C _x H _y (28)	0	$< 3 \cdot 10^{-8}$
CO ₂	0.5	$< 2 \cdot 10^{-6}$

Activated at
190°C

Photodesorption at Cryogenic Temperature

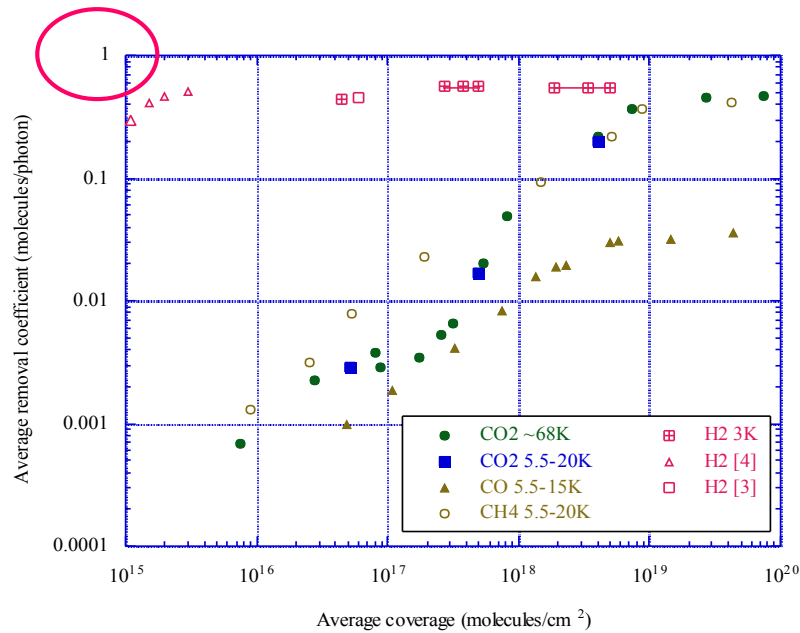
- Initial yield, η_0 , are smaller than at room temperature



V. Baglin *et al.*, Vacuum 67 (2002) 421-428

What about physisorbed molecules?

- Desorption of physisorbed molecules



V. Anashin *et al.*, *Vacuum* 53 (1-2), 269, (1999)

Stainless steel
250-300 eV
Perpendicular incidence

- Photo-cracking of molecules

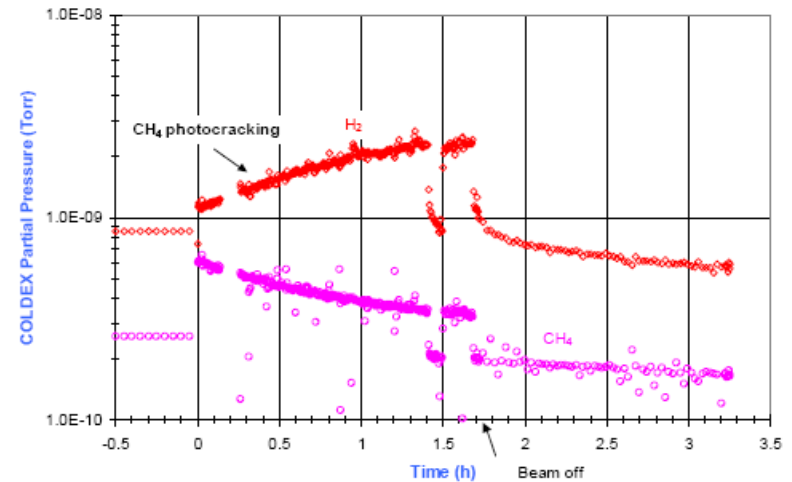


Figure 5 : ~ 10 monolayers of CH₄ condensed onto a BS without hole prior to irradiation at 6 K

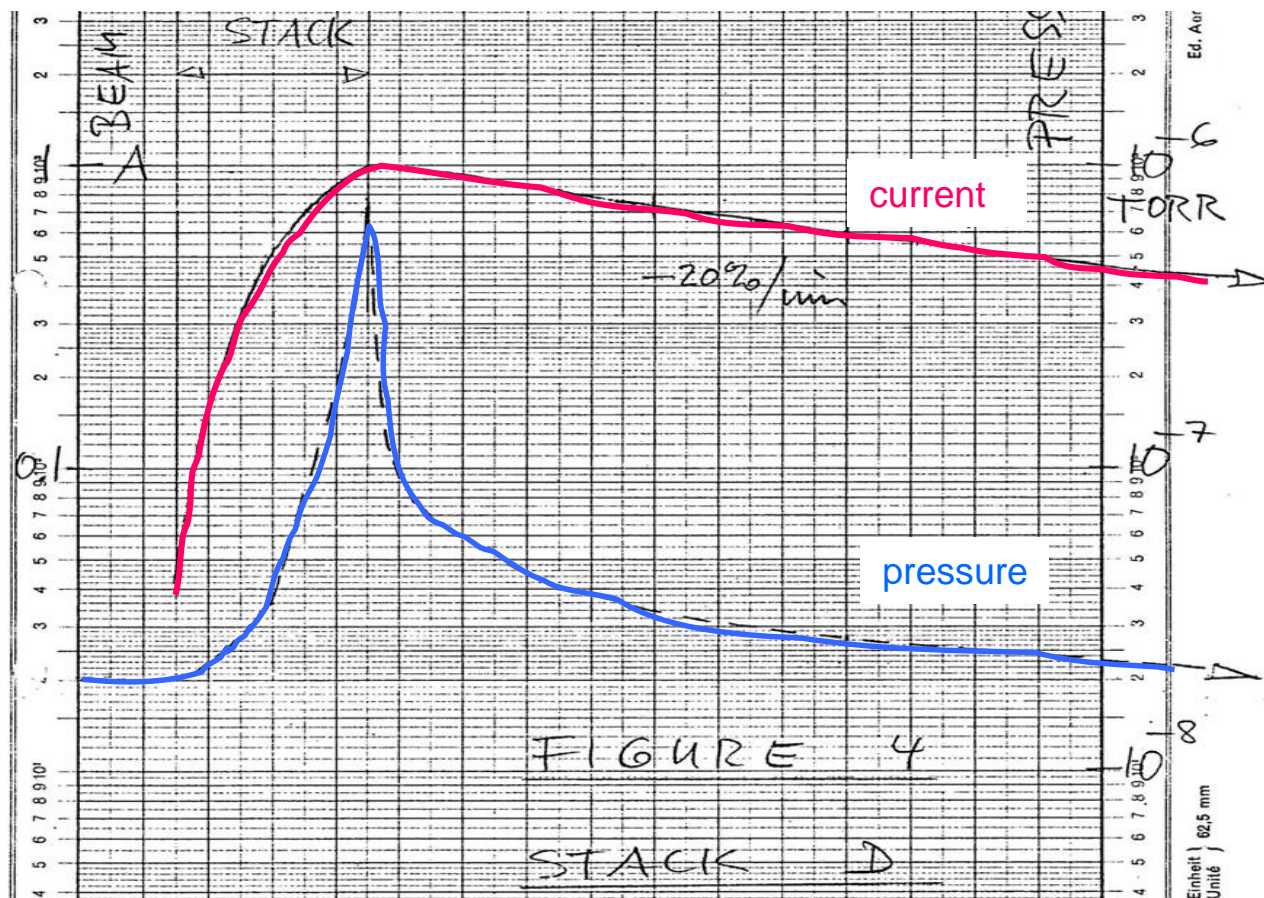
V. Baglin *et al.* EPAC 2002, Paris, France.

2. Vacuum instability and ion stimulated desorption

The phenomenon

- High current machines: ISR, LHC ...

- Beam current increase to 1 A
- Pressure increase up to 10^{-6} Torr (x 50 en une minute)
- Beam loss



First documented pressure bump in the ISR

E. Fischer/O. Gröbner/E. Jones 18/11/1970

The mechanism of vacuum instability

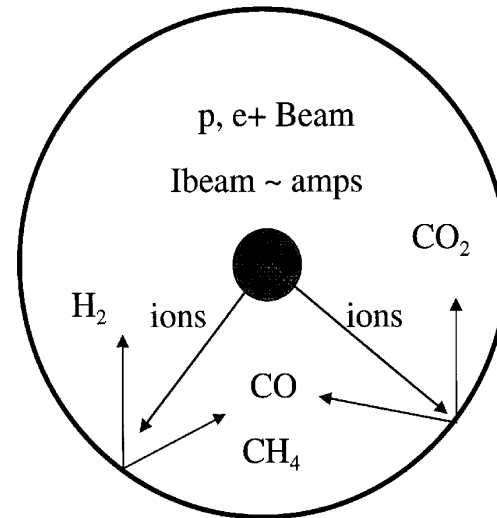
- Origin are ions produced by **beam gas ionisation**

$$V \frac{dP}{dt} = Q_0 + \eta_{\text{ion}} \sigma \frac{I}{e} P + C \frac{d^2 P}{dx^2}$$

- Quasi stationary long tube (C=0)

$$Q_0 + \eta_{\text{ion}} \sigma \frac{I}{e} P = P S_{\text{eff}}$$

$$P = \frac{Q_0}{S_{\text{eff}} \left(1 - \frac{\eta_{\text{ion}} \sigma \frac{I}{e}}{S_{\text{eff}}} \right)}$$



- When the beam current approach the **critical current**, the pressure increases to infinity

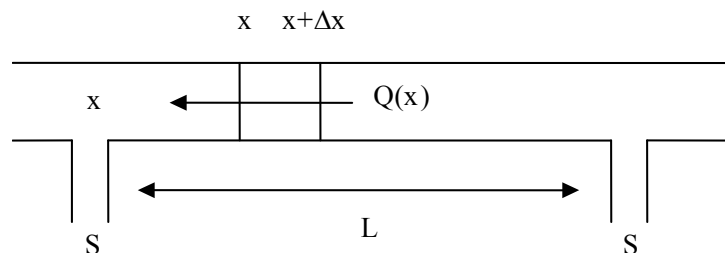
$$(\eta_{\text{ion}} I)_{\text{crit}} = \frac{e S_{\text{eff}}}{\sigma}$$

Description of the mechanism

- In the case of a machine with distributed pumping ($C \neq 0$) :

$$\frac{d^2 P}{dx^2} = -\frac{Q}{C} - \frac{\eta_{ion} \sigma}{C} \frac{I}{e} P = -\frac{Q}{C} - \omega^2 P$$

$$P(x) = \frac{a}{C \omega^2} \left[\frac{\cos(\omega(L/2 - x))}{\cos(\omega L/2) - \frac{\omega C}{S/2} \sin(\omega L/2)} - 1 \right]$$



$$\begin{cases} 2C \frac{dP(x)}{dx} \Big|_{x=0} = S P \\ 2C \frac{dP(x)}{dx} \Big|_{x=L} = -S P \end{cases}$$

- When the denominator approach zero, the pressure diverge

$$\cos(\omega L/2) - \frac{\omega C}{S/2} \sin(\omega L/2) > 0 \Leftrightarrow \omega \tan(\omega L/2) < \frac{S/2}{C} \Rightarrow (\omega L/2) < \frac{\pi}{2}$$

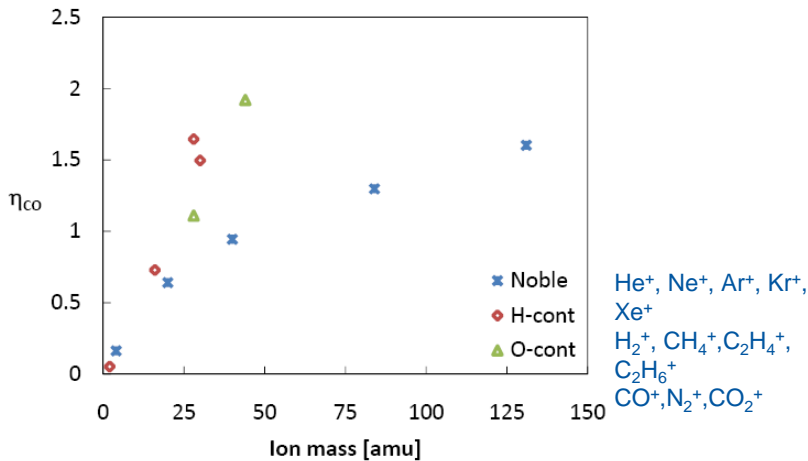
so $\eta_{ion} I < \frac{\pi^2 C e}{4 \cdot 10^3 \left(\frac{L}{2}\right) \sigma}$ therefore

$$\left(\eta_{ion} I\right)_{crit} = \frac{\pi^2 C e}{4 \cdot 10^3 \left(\frac{L}{2}\right) \sigma}$$

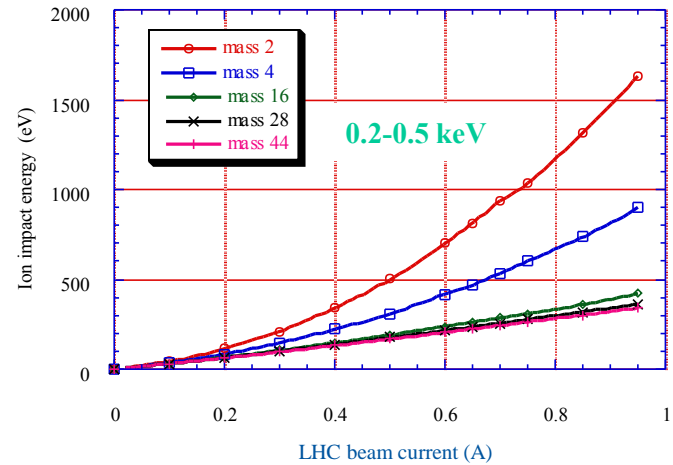
- In the case of more complex geometry, numerical tools are used

Ion desorption yield

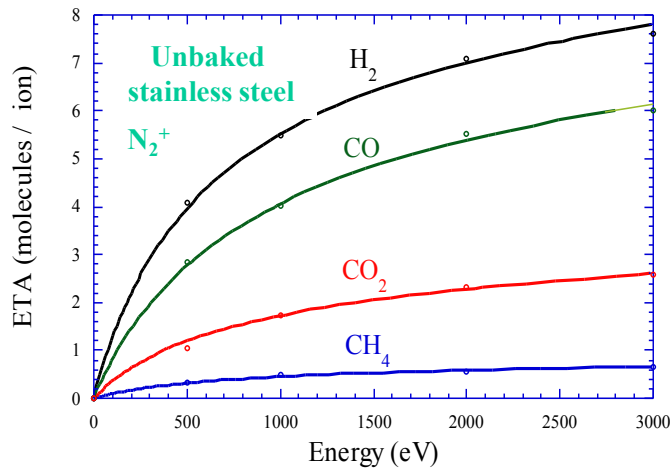
- Varies with the material, the ion energy and ion species
- Several units of molecules can be desorbed by ions → Sputtering



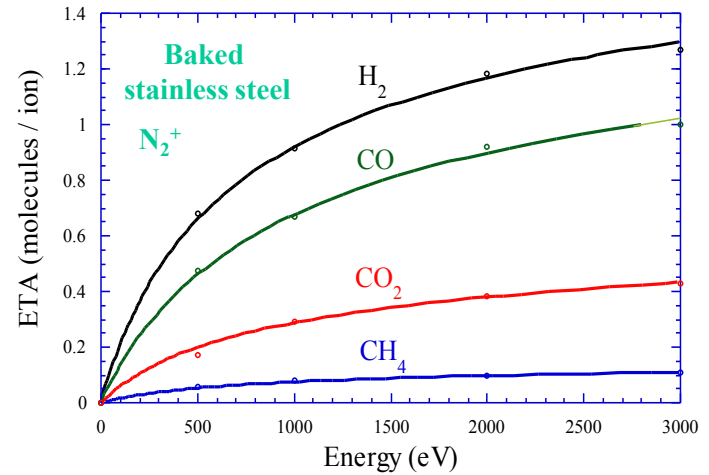
G. Hulla, PhD Thesis, Vienna Tech. U, 2009



O. Gröbner, CERN 99-05



A.G. Mathewson, CERN ISR-VA/76-5

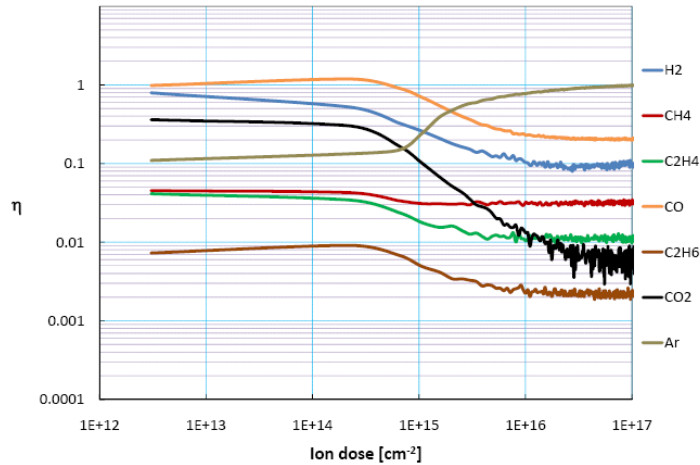


A.G. Mathewson, CERN ISR-VA/76-5

Conditioning and implantation

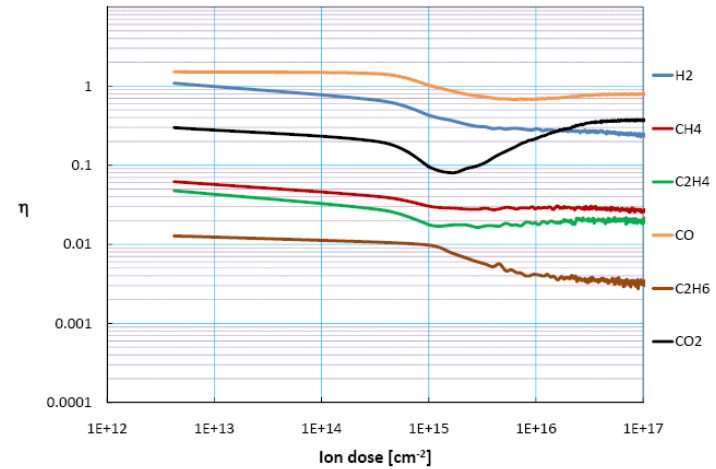
- A conditioning is observed but at high dose, some ions can be implanted !

7 keV, Cu Baked, Ar⁺



G. Hulla, PhD Thesis, Vienna Tech. U, 2009

7 keV, Cu Baked, CO⁺



G. Hulla, PhD Thesis, Vienna Tech. U, 2009

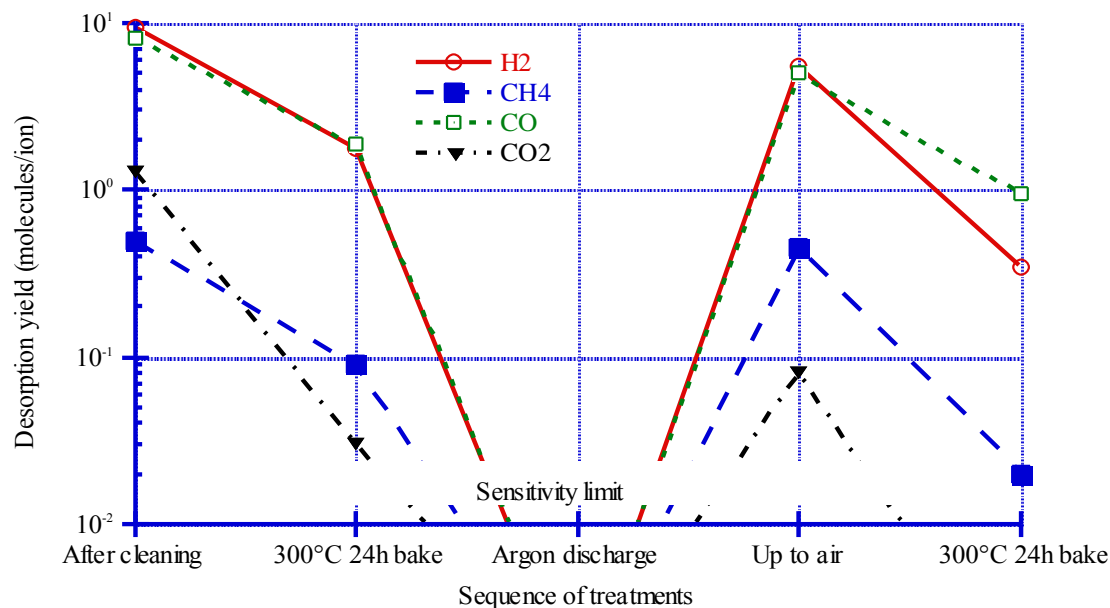
- In the LHC : the maximum flux is about $3 \cdot 10^8$ ions/($\text{cm}^2 \cdot \text{s}$) *i.e.* a dose of $3 \cdot 10^{15}$ ions/($\text{cm}^2 \cdot \text{year}$)
- **In the LHC, there is no conditioning due to ion bombardment**

How to ensure vacuum stability ?

- Beam conditioning being negligible, one must decrease the desorption yield and optimise the pumping speed

$$I_{\text{crit}} = \frac{1}{\eta_{\text{ion}}} \frac{eS}{\sigma}$$

- ISR : Argon glow discharge (Ar, 10 % O₂, ~ 400 V, 10¹⁸ Ar/cm²) with *in-situ* bakeout :

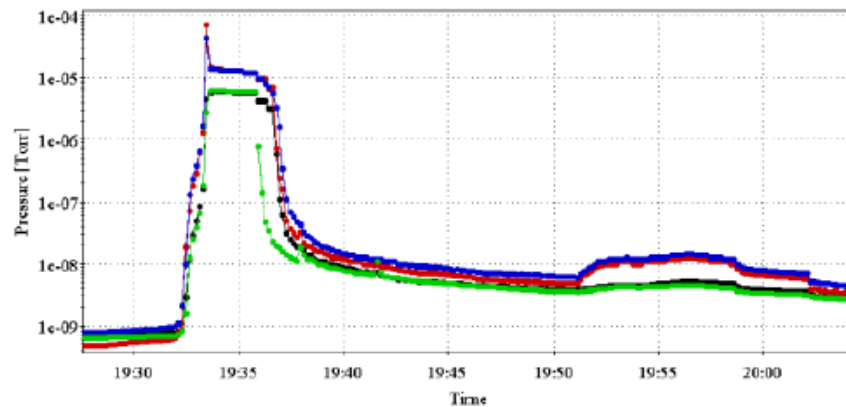
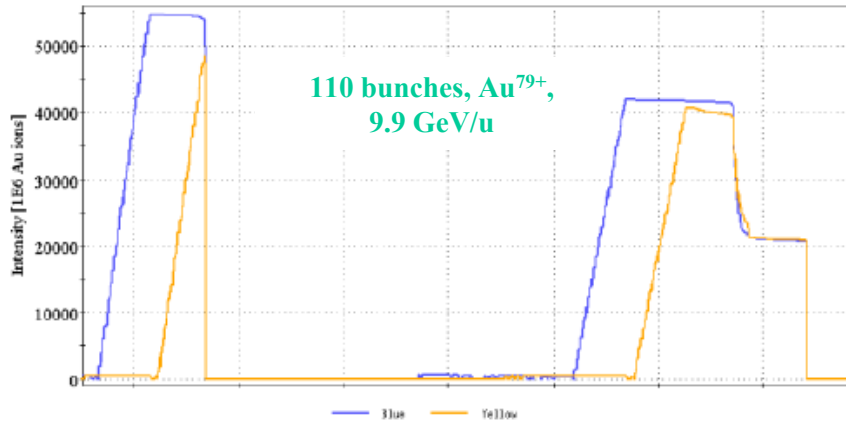


A.G. Mathewson, CERN ISR-VA/76-5

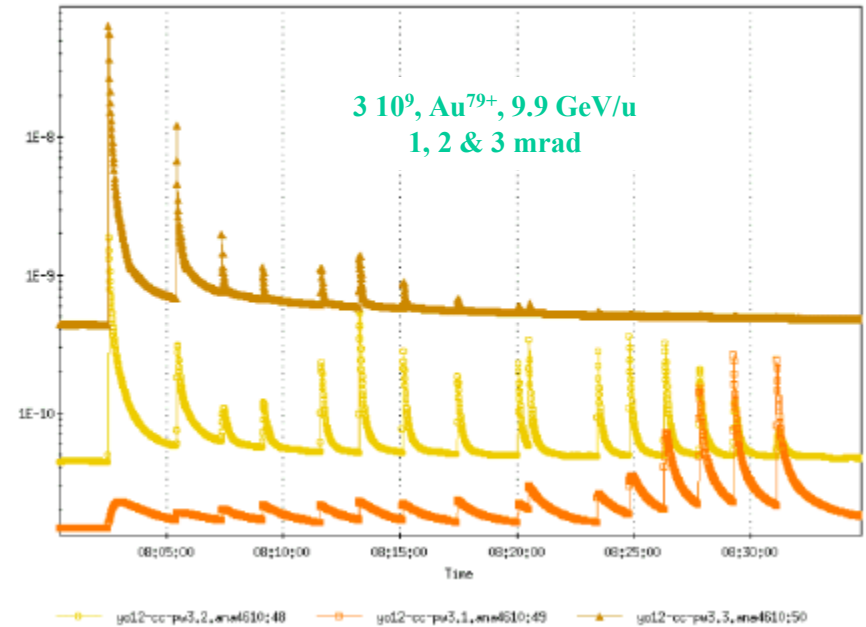
3. Particle losses and ion stimulated desorption

RHIC

- Loss of ions from a beam leads to **large** pressure increases: 10^{-8} ... 10^{-5} mbar!



W. Fischer *et. al.* EPAC 2002, Paris, France



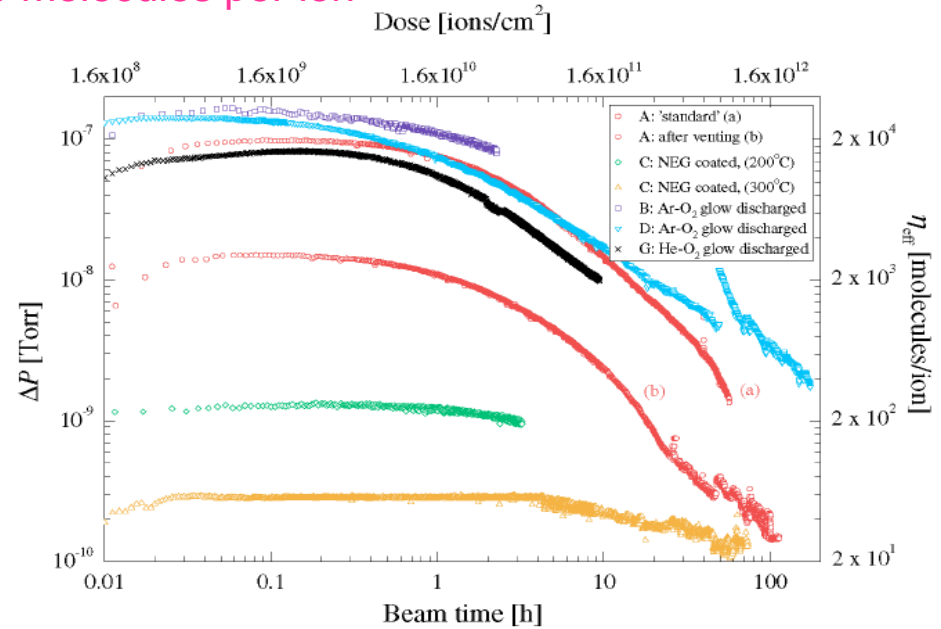
W. Fischer *et. al.* EPAC 2006, Edinburgh, Scotland

High energy ions

- Desorption yields range from 20 – 20 000 molecules per ion

Pb^{53+} , 4.2 MeV/u, 14 mrad

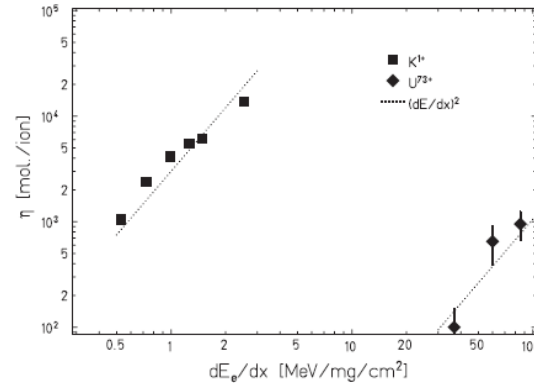
E. Mahner *et al.*,
Phys. Rev. ST Accel. Beams 6, 013201 (2003)



- The desorption is determined by the energy given to the electrons (electronic stopping force)

$$\eta_{ion} \propto \left(\frac{dE_e}{dx} \right)^2$$

L. Prost *et al.*, PRL 98, 064801 (2007)



- The desorption induced by the electrons is the responsible mechanism

Remedies

- Use of NEG films (LEIR, RHIC, GSI)
- Use of beam conditioning
- Intercept ion loss on dedicated collimators:
 - LEIR : 30 μm gold fim on SS 316 LN, perpendic
 - GSI : 0.1 μm gold film, perpendicular incidence. Absorbeur inserted in a secondary vacuum chamber. NEG film

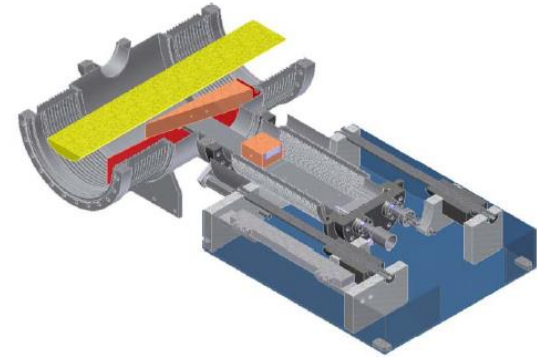
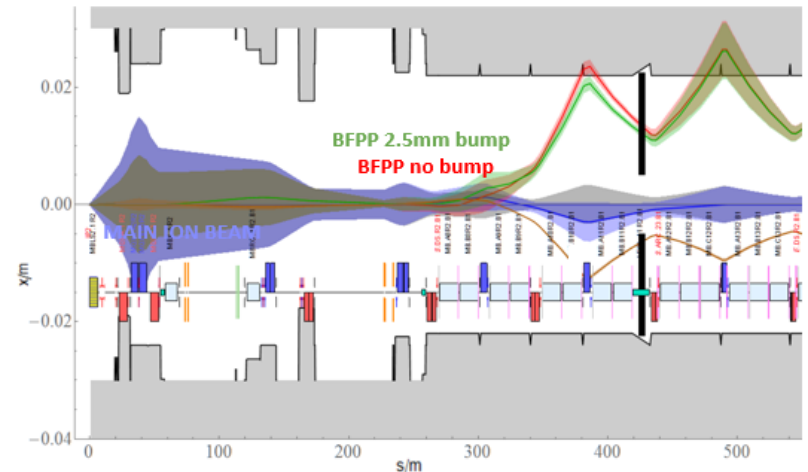


Figure 2: Horizontal cut through the installed SIS18 ion catcher prototype. Yellow: beam, red: secondary chamber, brown: beam absorbers.

C. Omet et. al. EPAC 2008, Genoa, Italy

- HL-LHC : movable collimator – 150 W of 7 ZxTeV ions coming from BFPF

BFPP:



. J. Jowett

4. Electron cloud and related surface parameters

4.1 Introduction

History: observed at the ISR

- Vacuum stability test of a baked aluminium chamber 200°C, diam 160 mm (1976-1977)
- Observation of pressure spikes, particularly during transverse displacement of a proton bunch
- The existence of the spike varies with :
 - bunch length
 - number of proton bunch
- Existence of a current threshold (120 mA for 20 bunches)
- Different gas composition (dominated by H₂ instead of CO)
- Measurement of a significant electron current on the clearing electrodes

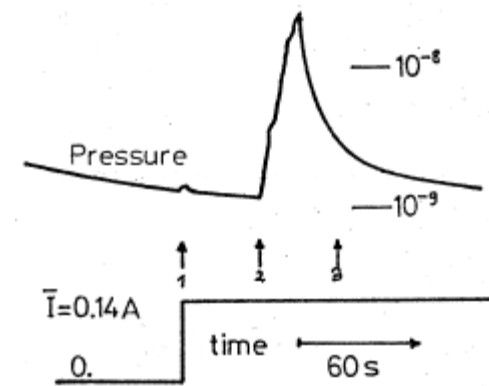


Fig. 1. Pressure spike observed during slow displacement of a bunched beam across the aperture :
1 injection - 40 mm, 2 - 10 mm and 3 + 10 mm radial position from centre of the vacuum chamber

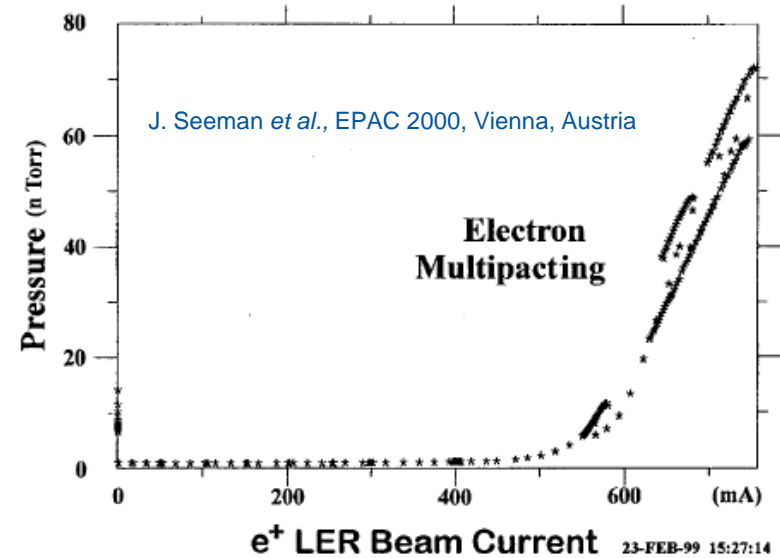
O. Gröbner, ISR-VA/77-38

- Gas desorption is stimulated by electrons
- Electrons are accelerated by the proton bunch: multipactor effect

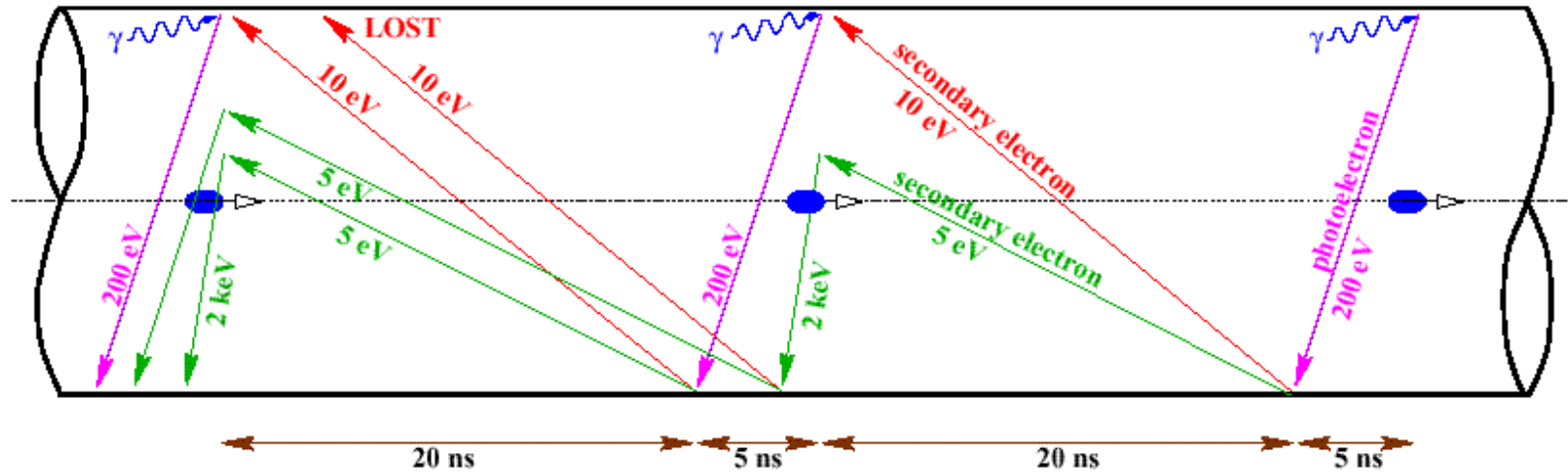
PEP-II

- Electron cloud in the positron ring was foreseen during the design phase: TiN coating on Aluminum
- emittance blow up above 800 mA (SR light)
- Observation of non linear pressure rise
- Winding of solenoids in the straight section

→ Luminosity increase



LHC mechanism



Schematic of **electron-cloud build up** in the LHC beam pipe.

F. Ruggiero *et al.*, LHC Project Report 188 1998, EPAC 98

- Key parameters:

- beam structure
- bunch current
- vacuum chamber dimension
- secondary electron yield
- photoelectron yield
- electron and photon reflectivities
- ...

$$P = \frac{Q + \eta_{Electrons} \dot{\Gamma}_{Electrons}}{S}$$

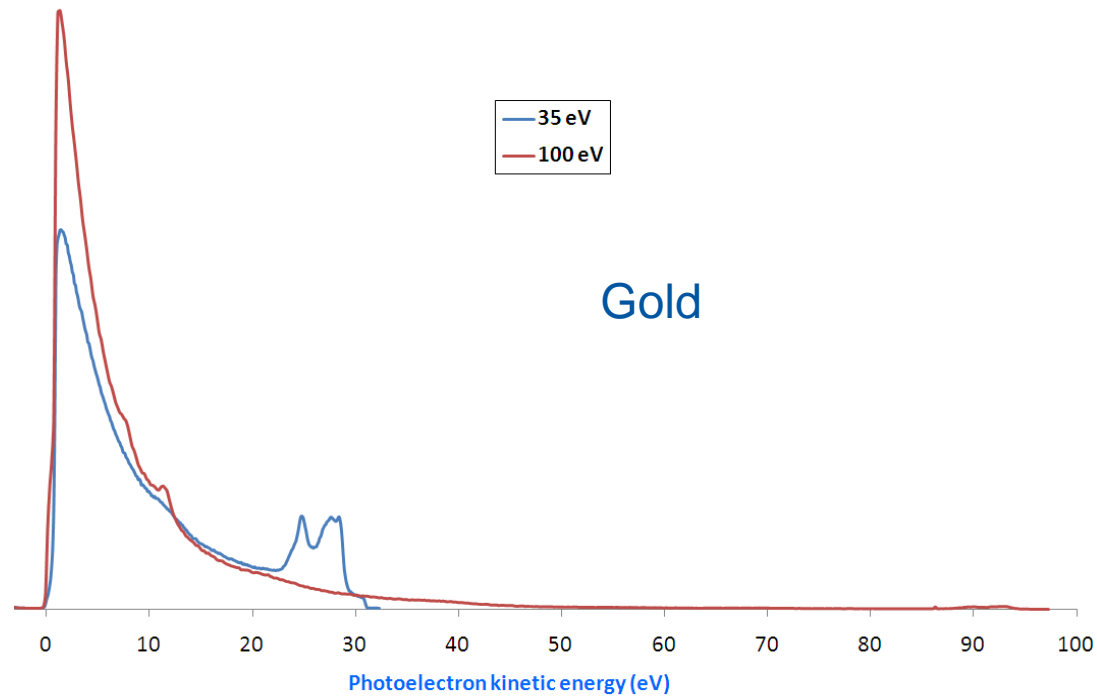
How to mitigate the electron cloud?

- Once again, play with the key parameters :
 - Reduce the photoelectron yield (grazing incidence has larger yield than perpendicular incidence)
 - Reduce the secondary electron yield (scrubbing, NEG or amorphous carbon films, geometry)
 - Reduce the amount of electrons in the system (solenoid magnetic field, clearing electrodes, material reflectivity)
 - Adapt the beam structure or the vacuum chamber dimensions to reduce the multiplication
 - ...

4.2 Photons from SR

Photoelectrons

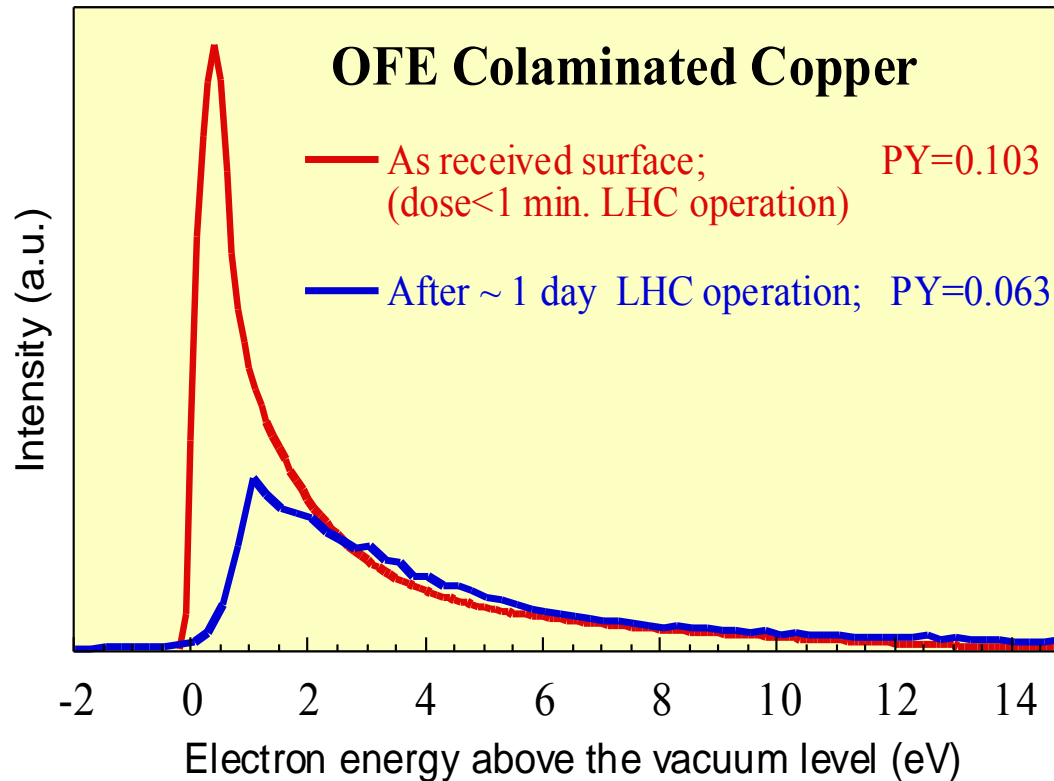
- **Photoelectric effect** : when a photons irradiates a surface with enough energy, it produces electrons
- The energy of emitted electrons varies from :
0 eV to $(h\nu - W_f)$ eV
- Most of the electrons are secondaries
- A few 0.1 % to 1 % have high energy



R. Cimino *et al.* , Phys. Rev. ST Accel. Beams 2, 063201 (1999)

EDC under SR irradiation

- EDC: Electron distribution curve
- SR dose **reduce** the amount of low energy photoelectrons
- The total yield is decreased by 40 % after 1 day of nominal LHC operation



R. Cimino *et al.* Phys. Rev. AB-ST 2 063201 (1999)

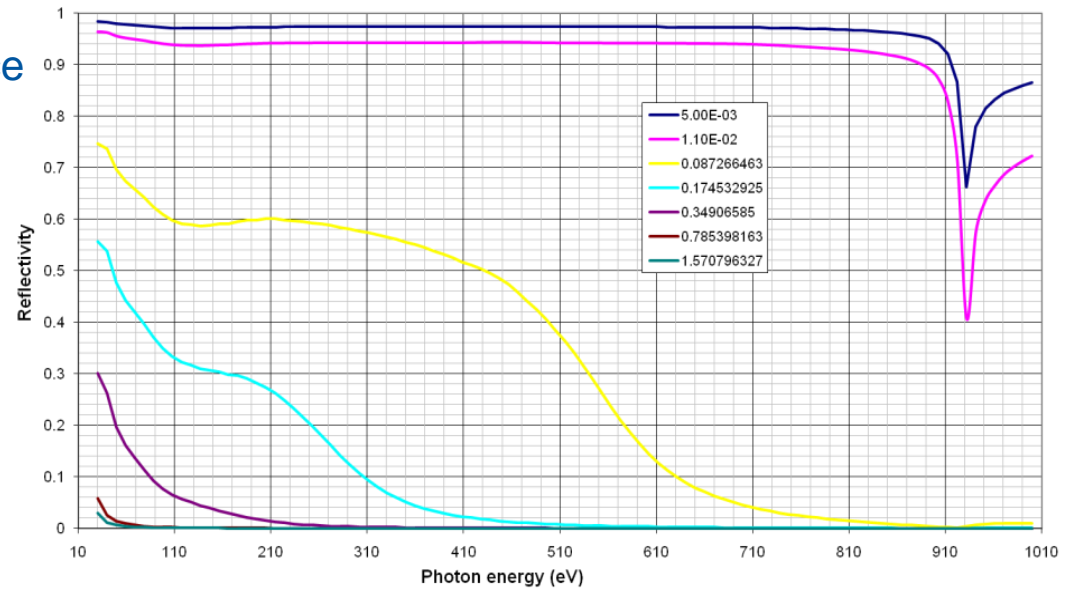
Photon reflectivity

- From 1 to 80% forward reflectivity
- Low reflectivity at perpendicular incidence
- High reflectivity at grazing incidence *i.e.* this is the case of SR in accelerators
- In LHC, 5 mrad gives more than 95% reflection
- Copper adsorption at 920 eV

Material	Status	45 eV R (%)	194 eV R (%)
Cu roll bonded	as-received	80.9	77.0
Cu roll bonded air baked	as-received	21.7	18.2
Cu electroplated	as-received	5.0	6.9
Cu sawtooth	as-received	1.8	-
	150°C, 9 h	1.3	1.2
	150°C, 24 h	1.3	1.2
TiZr film	as-received	20.3	17.1
	120°C, 12 h	19.5	16.7
	250°C, 9 h	19.9	17.4
	350°C, 10 h	20.6	16.9
	CO saturated	20.7	-

V. Baglin *et al.*, Trieste, 1998

Copper reflection for unpolarised photon with 0 Angstrom roughness



Henke databook

DCI, $E_c=3$ keV

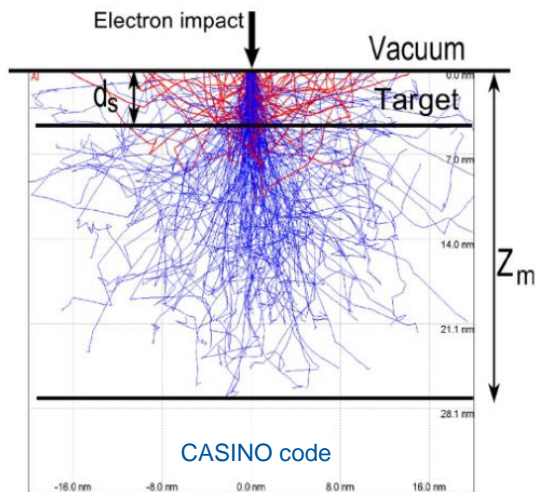


O. Gröbner *et al.*, 24-4-1988

4.3 Electrons from the electron cloud

Electron Distribution Curve (EDC)

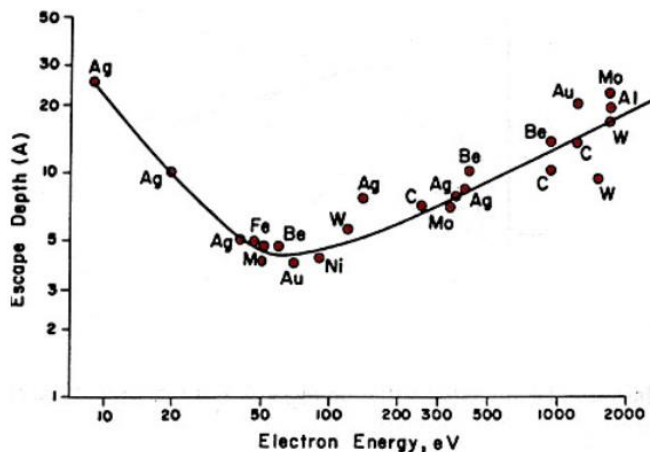
- Penetration depth: 1 – 10 nm



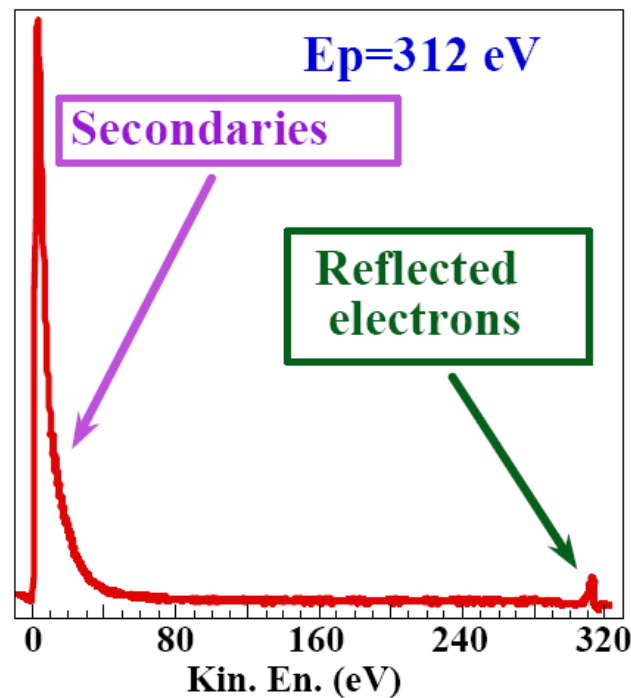
N. Balcon *et al.*,
 IEEE Trans. On Plasma Sci. 40, 2012, 282

- The electron distribution curve shows :
 - Component at reflected electron energy
 - Secondary electrons with low energy
- most of the emitted electrons have low energy

- Escape depth: <10 nm



Mean escaped depth of electrons in solids and "universal" curve.

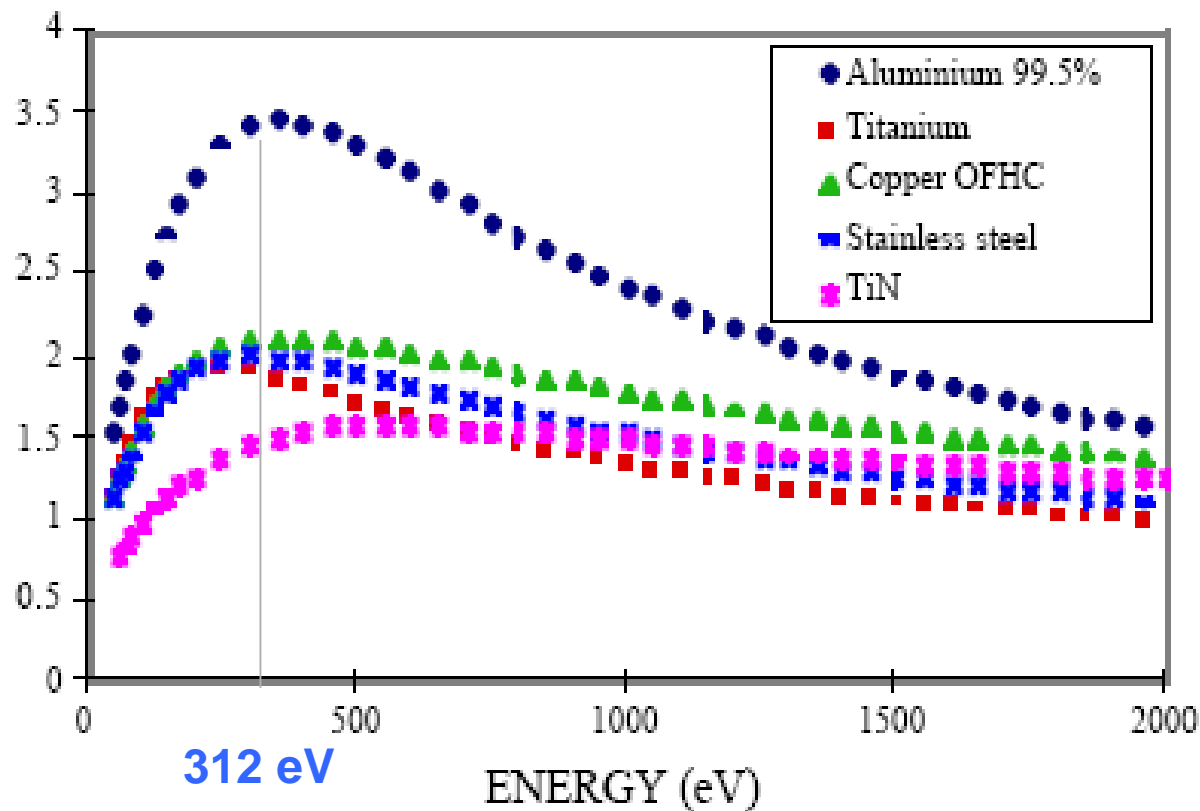


Courtesy R. Cimino

Secondary Electrons Curve

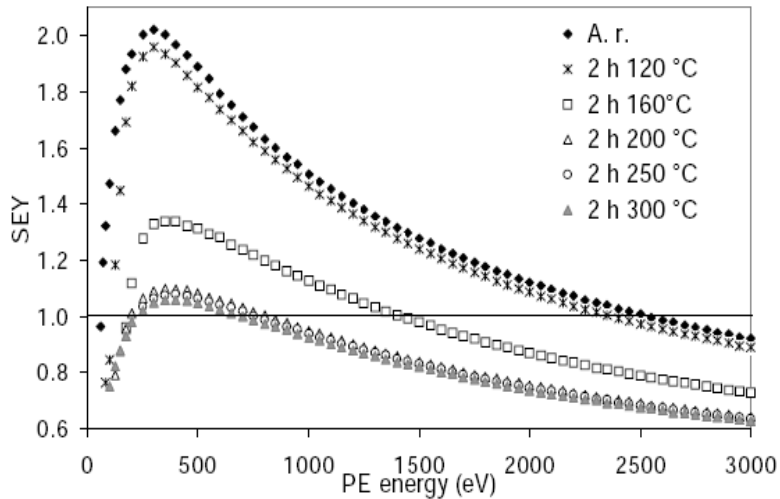
$$\delta = \frac{\text{number of produced electrons}}{\text{incident electrons}}$$

- Technical material
- Maximum around 200-300 eV
- $\delta_{\max} \sim 2$ to 3.5



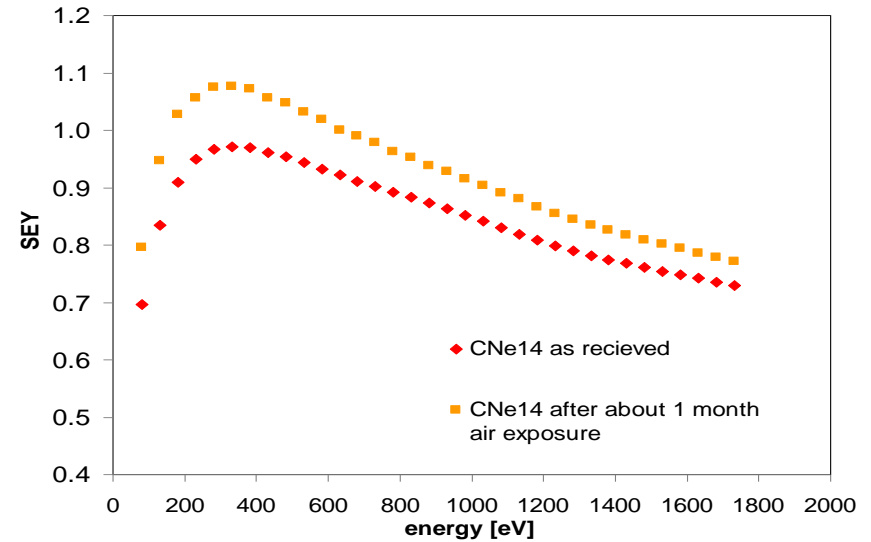
N. Hilleret *et al.*, LHC Project Report 433 2000, EPAC 00

Very low SEY



C. Scheuerlein *et al.* Appl.Surf.Sci 172(2001)

- TiZrV film



M. Taborelli *et al.*, ECM workshop, 2008

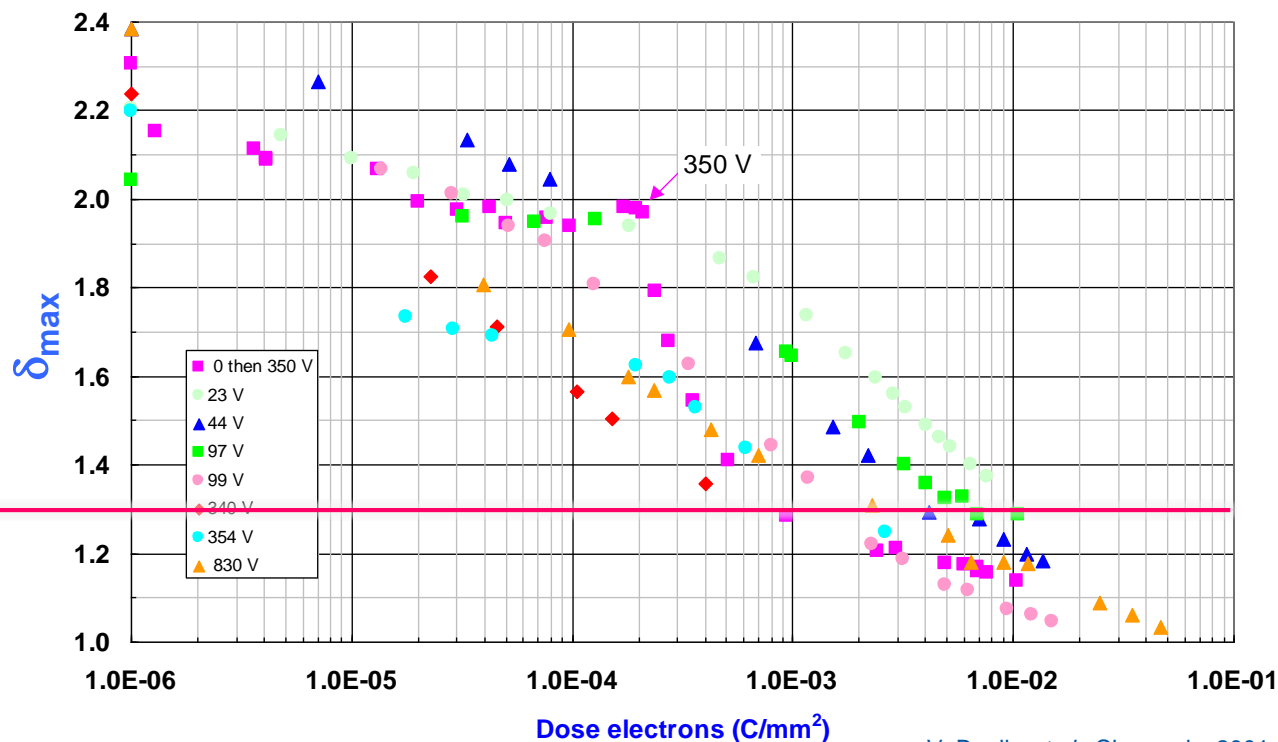
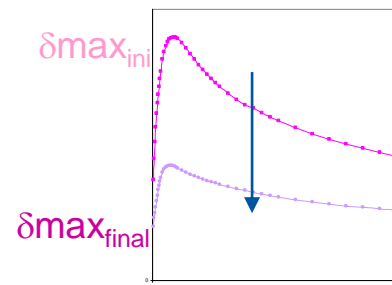
- Amorphous carbon

The origin of the low SEY is different in both case :

- nature of the surface
- smooth versus rough surfaces

LHC : Scrubbing of the Surface

- Photoelectrons produced by SR are accelerated towards the test sample
- Reduction of SEY under electron irradiation is observed
- 1 to 10 mC/mm² is required
- Growth of a carbon layer (AES, XPS)



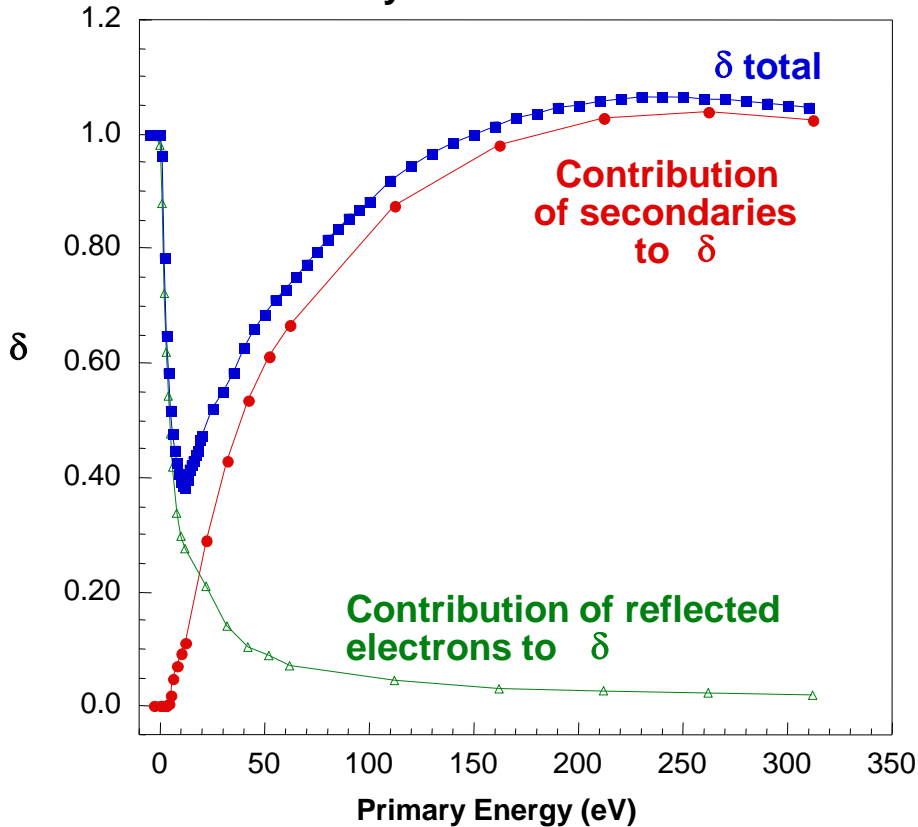
LHC design:
 $\delta_{max} \sim 1.3$

V. Baglin *et al.*, Chamonix, 2001

SEY at cryogenic temperature

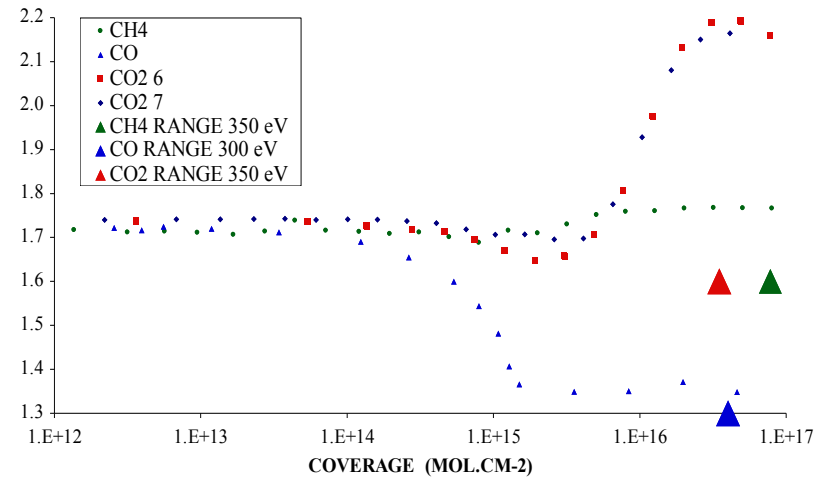
- Beam scrubbing at 10 K but SEY increases with gas condensation

Fully scrubbed Cu



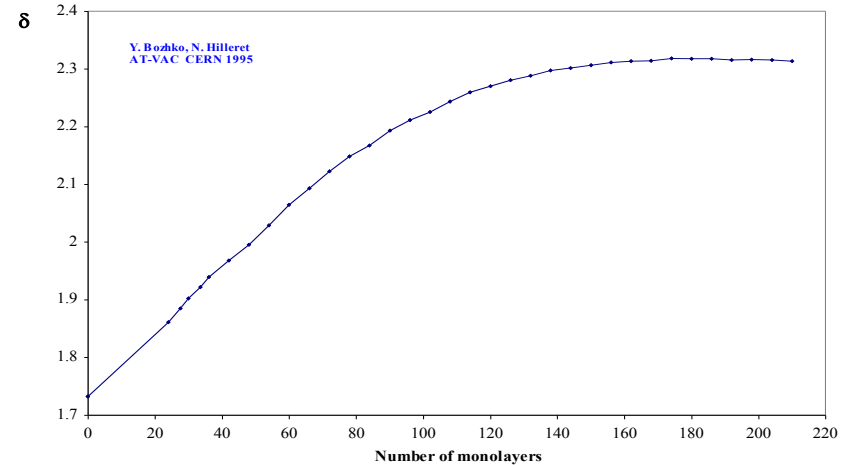
R. Cimino, I.R. Collins, *App. Surf. Sci.* 235, 231-235, (2004)

δ_{MAX} VERSUS COVERAGE



N. Hilleret. LHC MAC December 2004

Variation of maximum yield with amount of adsorbed water



N. Hilleret *et. al.* Chamonix 2000

Electron desorption yield

- Unbaked copper
- Threshold around 10 eV

$$\eta(E) = \eta_0 \left(\frac{E - E_c}{300 - E_c} \right)^{0.85}$$

Table 1: Fit parameters

	$\eta_0 / (\text{molec./e}^-)$	E_c / eV
C ₂ H ₆	1.1×10^{-1}	11.4
CH ₄	2.1×10^{-2}	7.5
CO	5.8×10^{-2}	7.2
CO ₂	2.7×10^{-1}	9.1
H ₂	1.9×10^0	12.7
H ₂ O	3.1×10^{-2}	-22.9

$$\eta = \frac{\text{number of desorbed molecules}}{\text{incident electrons}}$$

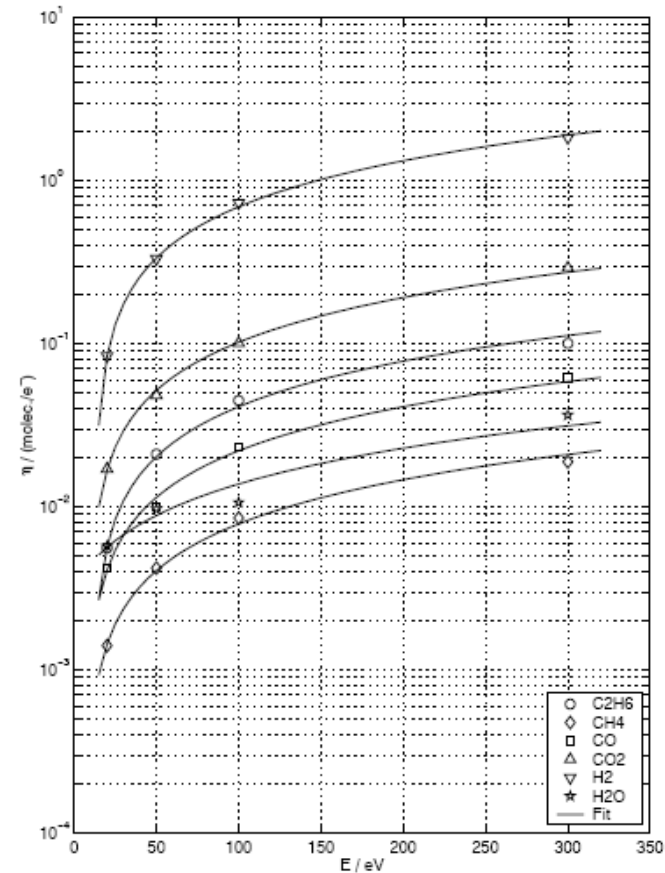


Figure 5: Electron induced desorption yield as a function of the electron energy. The values for 20, 50, and 100 eV have been obtained by interpolation between the two measurements shown in figure 4 at a constant dose of $1.4 \times 10^{14} \text{ e}^-/\text{cm}^2$.

G. Vorlaufer *et al.*, CERN VTN, 2000

Electron dose

- Reduction of the electron desorption yield with the electron dose

$$\eta(D) = \eta_0 \left(\frac{D}{D_0} \right)^{-a}$$

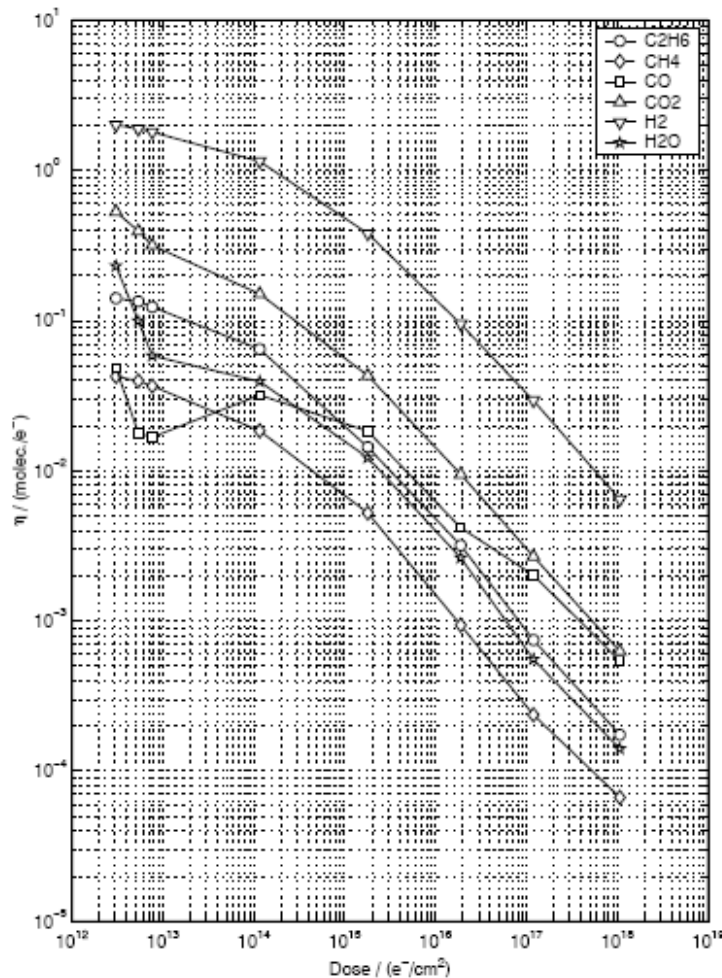


Figure 3: Effect of the electron dose on the electron induced desorption yield of an unbaked copper sample. The electron energy during bombardment and measurement was 300 eV.

	H ₂	CH ₄	H ₂ O	CO	CO ₂
η_0	$2 \cdot 10^{-1}$	$2.5 \cdot 10^{-2}$	$1 \cdot 10^{-1}$	$3.5 \cdot 10^{-2}$	$5 \cdot 10^{-2}$
D_0 $\times 10^{14}$	3	1	6	2	4
a	0.47	0.62	0.66	0.49	0.54

Electron desorption at cryogenic temperature: Cu

- The yields are very large and range from 0.1 to 50
- For a monolayer (10^{15} molecules/cm²)

	H ₂	CH ₄	CO	CO ₂
η	500	5	10	0.5

Studied for 300 eV electrons with :

- 1) Pure gas
- 2) Equimolecular mixture of 4 gases
- 3) Standard LHC gas composition

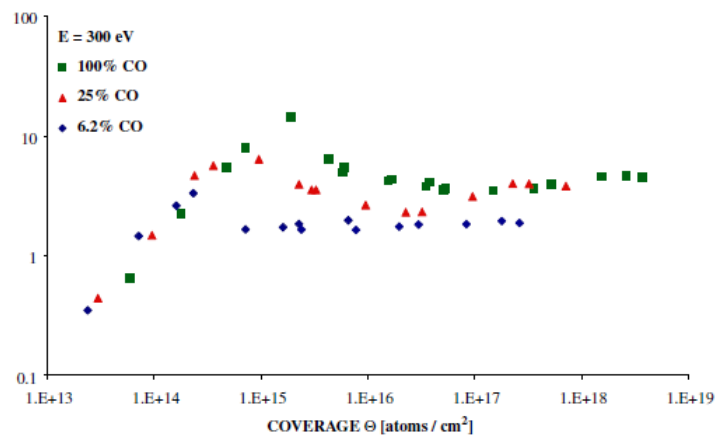


Fig. 7. The CO desorption yield as a function of CO coverage for different condensed gas composition (electron energy 300 eV).

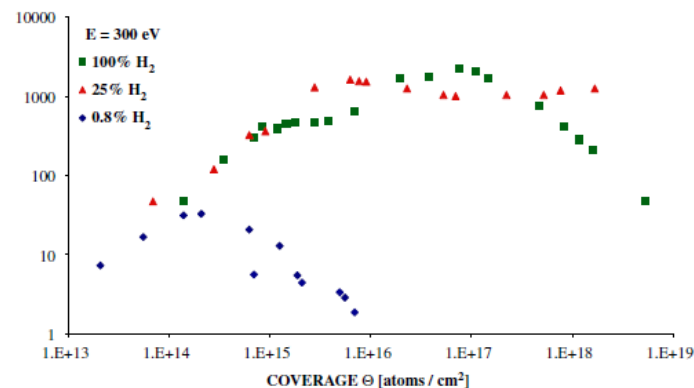


Fig. 5. The H₂ desorption yield as a function of H₂ coverage for different condensed gas composition (electron energy 300 eV).

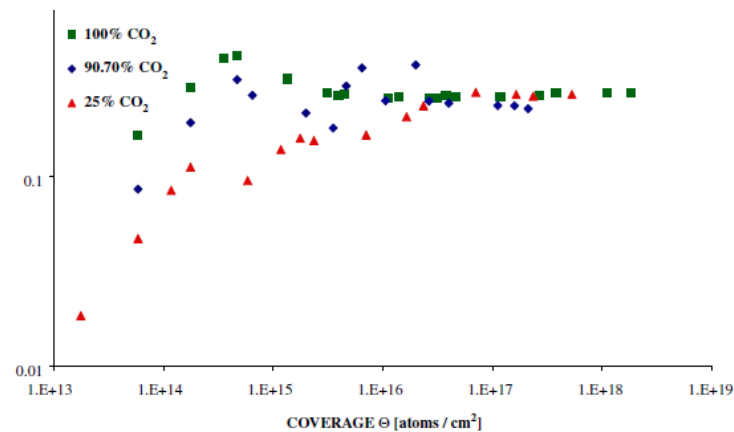
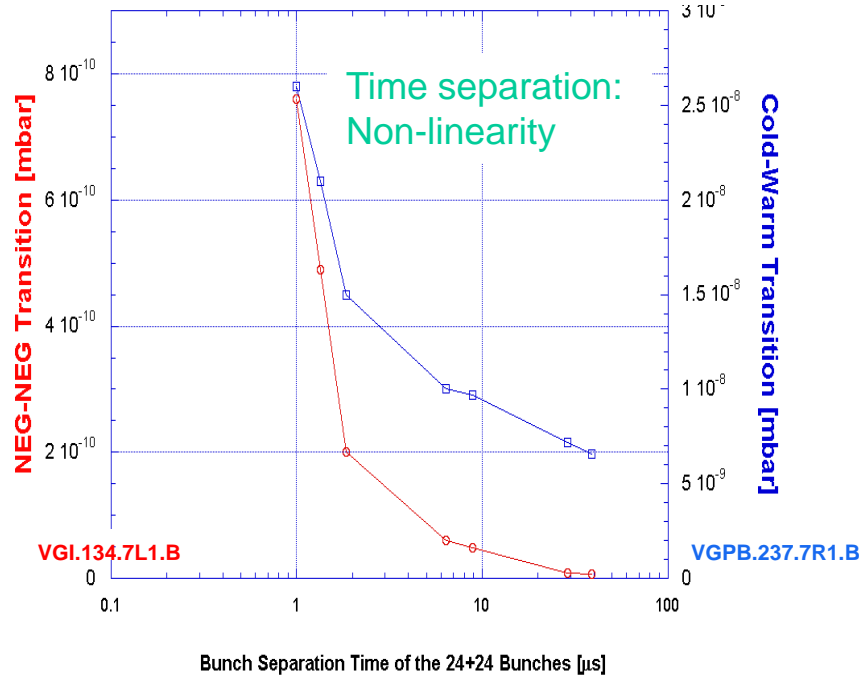
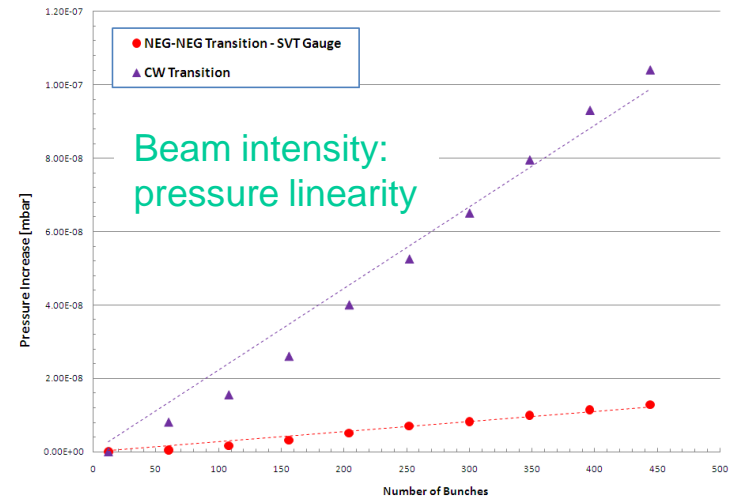
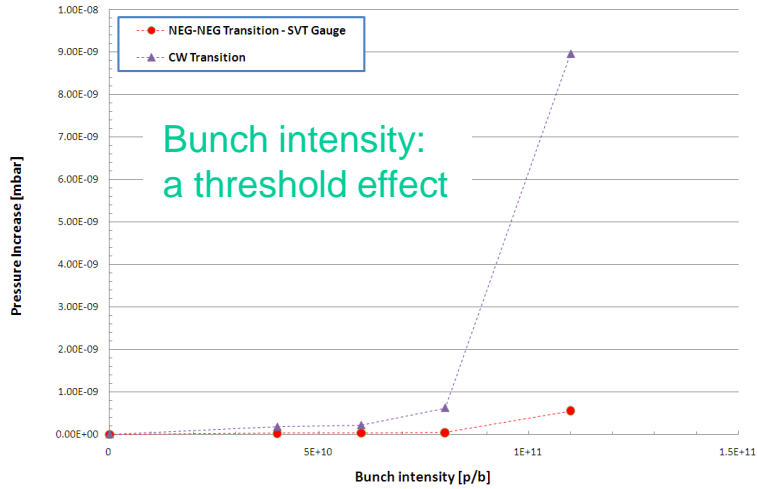


Fig. 8. The CO₂ desorption yield as a function of CO₂ coverage for different condensed gas composition (electron energy 300 eV).

H. Tratnik *et al.*, Vacuum 81, 731,(2007)

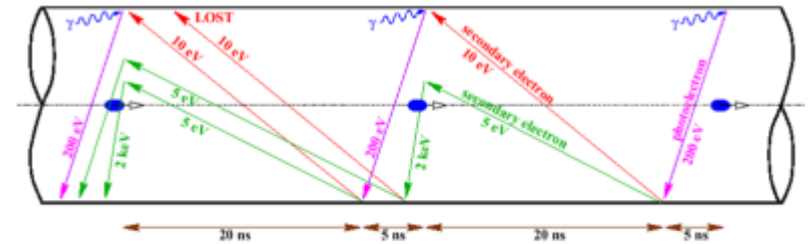
4.5 Beam structure

Multipacting: Influence of Beam Structure



G. Bregliozi *et al.*, IPAC San Sebastian, 2011

$$P = \frac{Q + \eta_{Electrons} \dot{\Gamma}_{Electrons}}{S}$$



Schematic of electron-cloud build up in the LHC beam pipe.

F. Ruggieri *et al.*, LHC Project Report 188 1998, EPAC 98

Lecture 4 summary

- In accelerators, the **circulating beam** can contribute to stimulate molecular desorption
- Those phenomenon can lead to much larger **gas load** than the thermal outgassing rate
- **Photon stimulated desorption** originates from SR
- **Ion stimulated desorption** originates from beam gas ionisation and can lead to vacuum instability
- Particle losses
- **Electron stimulated desorption** originates from an electron cloud

Some References

- Cern Accelerator School, Vacuum technology, CERN 99-05
- Cern Accelerator School, Vacuum in accelerators, CERN 2007-03
- Cern Accelerator School, Vacuum for particle accelerators, Glumsløv, June 2017

- The physical basis of ultra-high vacuum, P.A. Redhead, J.P. Hobson, E.V. Kornelsen. AVS.
- Scientific foundations of vacuum technique, S. Dushman, J.M Lafferty. J. Wiley & sons.
- Les calculs de la technique du vide, J. Delafosse, G. Mongodin, G.A. Boutry. Le vide.
- Vacuum Technology, A. Roth. Elsevier Science
- Foundations of vacuum science and technology, Ed by J.M. Lafferty. J. Wiley & sons.

Some Journals Related to Vacuum Technology and Accelerators

- Journal of Vacuum Science and Technology
- Vacuum
- Applied Surface Science
- Nuclear Instruments and Methods
- Physical Review Accelerator and Beams

Thank you for your attention !!!





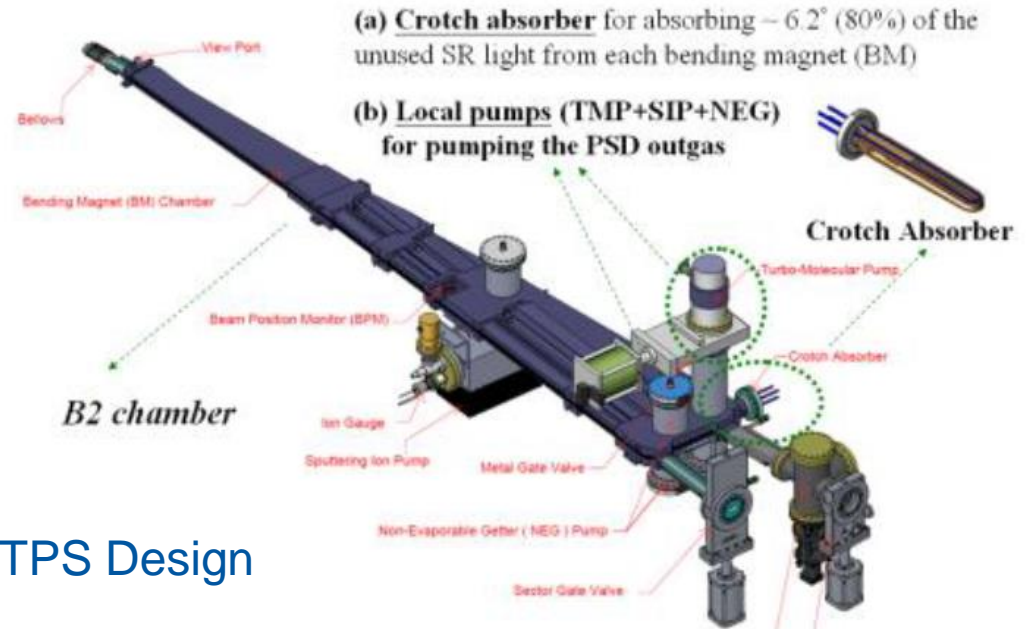
Complementary information

1.1 Synchrotron radiation

... heavy consequences on design

Complementary information

- Extruded Aluminum
- Ex-situ baked to 150°C



TPS Design

G.Y Hsiung *et al.*

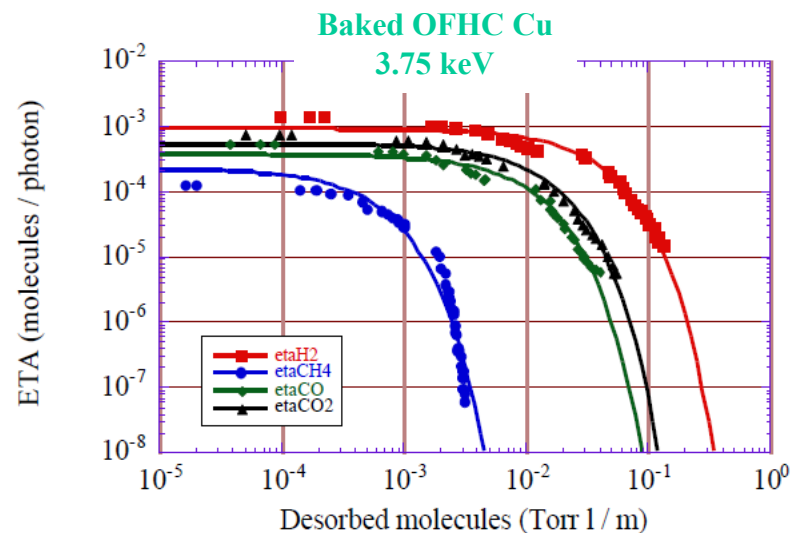
- A **complex** vacuum chamber design with a light extraction path, pumping and instrumentation ports and **power absorbers** (crotch)

1.2 Photodesorption

Desorption yield vs gas load

Complementary information

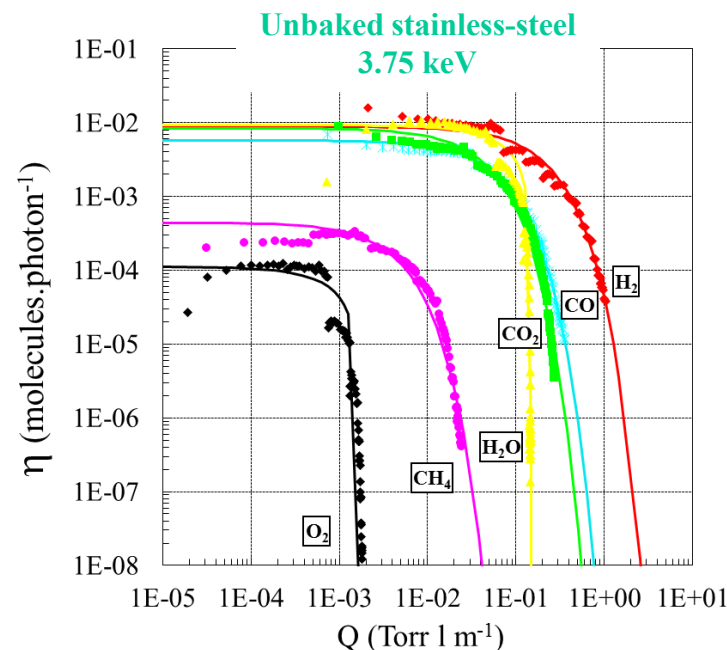
- The quantity removed during the cleaning process is a useful information to estimate intervals between getter reactivation or surface coverage on a cryogenic surface



$$\eta = \eta_0 e^{-\frac{q}{Q_0}}$$

O. Gröbner *et al.*

J.Vac.Sci. 12(3), May/June 1994, 846-853



C. Herbeaux *et al.* JVSTA 17(2) Mar/Apr 1999, 635

	H ₂	CH ₄	CO	CO ₂
η ₀ (molecules/ph)	9.2 · 10 ⁻⁴	2.3 · 10 ⁻⁴	3.7 · 10 ⁻⁴	5.5 · 10 ⁻⁴
Q ₀ (Torr l / m)	3.0 · 10 ⁻²	4.5 · 10 ⁻⁴	8.4 · 10 ⁻³	1.1 · 10 ⁻²
Q ₀ (molecules/cm ²)	2.3 · 10 ¹⁴	3.5 · 10 ¹²	6.5 · 10 ¹³	8.5 · 10 ¹³

	H ₂	CH ₄	CO	CO ₂
η ₀ (molecules/ph)	8.8 · 10 ⁻³	4.4 · 10 ⁻⁴	5.7 · 10 ⁻³	8.4 · 10 ⁻³
Q ₀ (Torr l / m)	1.9 · 10 ⁻¹	3.9 · 10 ⁻³	5.7 · 10 ⁻²	4.0 · 10 ⁻²
Q ₀ (molecules/cm ²)	1.5 · 10 ¹⁵	3.1 · 10 ¹³	4.5 · 10 ¹⁴	3.2 · 10 ¹⁴



2. Vacuum instability and ion stimulated desorption

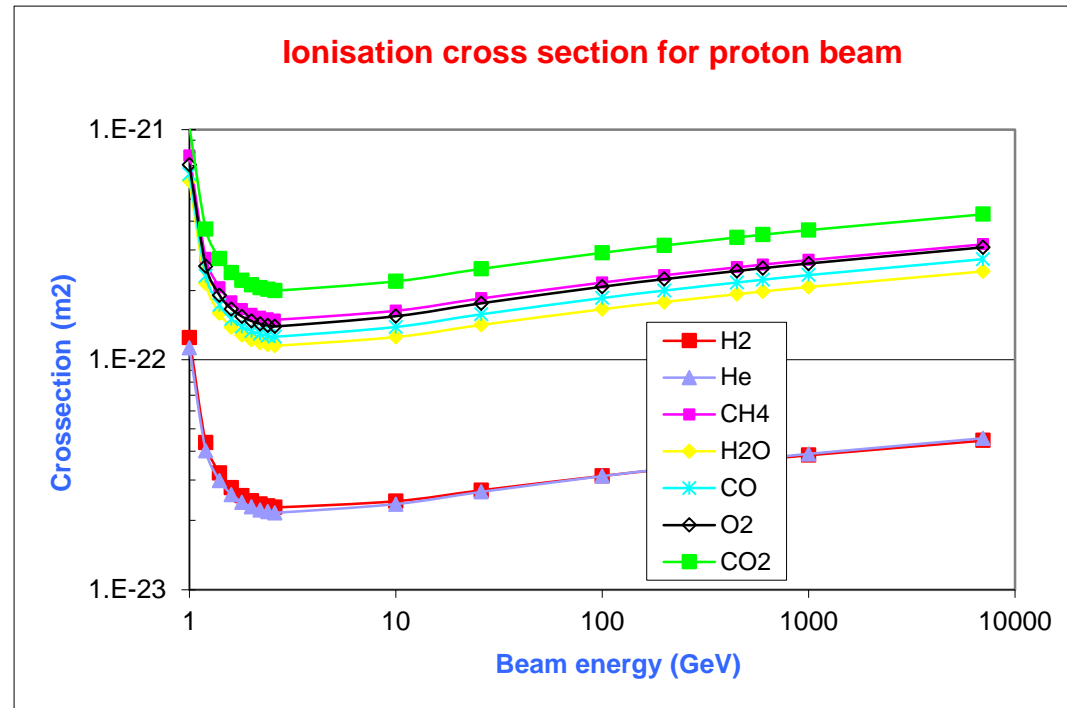
Ionisation cross section

- It is a function of the speed & the charge of the projectile and of the nature of the residual gas.

$$\sigma = 4\pi \left(\frac{h/2\pi}{m_e c} \right)^2 \frac{Z^2}{\beta^2} \left[M^2 \left(\ln \left(\frac{\beta^2}{1-\beta^2} \right) - \beta^2 \right) + C \right]$$

F.F. Rieke, W. Prepejchal, Phys. Rev. A5, 1507 (1972)

Gas	Ionisation cross-section (in 10 ⁻¹⁸ cm ²)		
	26 GeV	450 GeV	7000 GeV
H ₂	0.27	0.36	0.45
He	0.27	0.36	0.45
CH ₄	1.9	2.5	3.2
H ₂ O	1.4	1.9	2.4
N ₂	1.6	2.2	2.7
CO	1.6	2.2	2.7
O ₂	1.8	2.4	3.1
Ar	1.7	2.4	3.1
CO ₂	2.5	3.4	4.3



→ Heavy gas must be avoided

Ion desorption

S(E)

Complementary information

- Described by the nuclear and electronic stopping force (stopping power)
- Low masses (H_2) are desorbed by the electronic energy transfer to the lattice
- High masses are desorbed by the direct nuclear momentum transfer between two particles

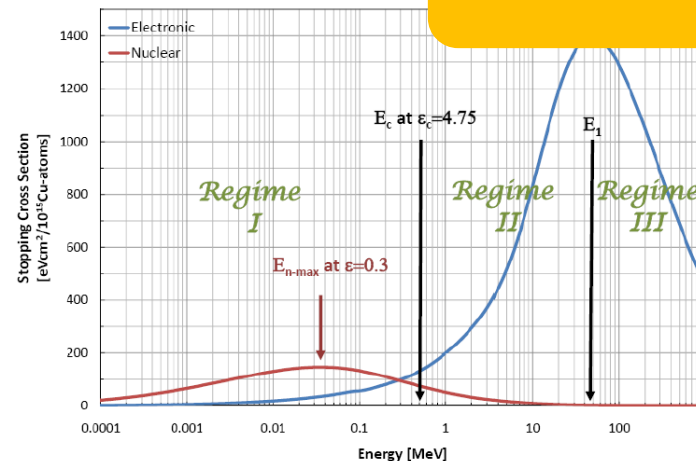


Figure 4.3: Electronic and nuclear stopping cross sections for Ar^+ -ions incident on copper.

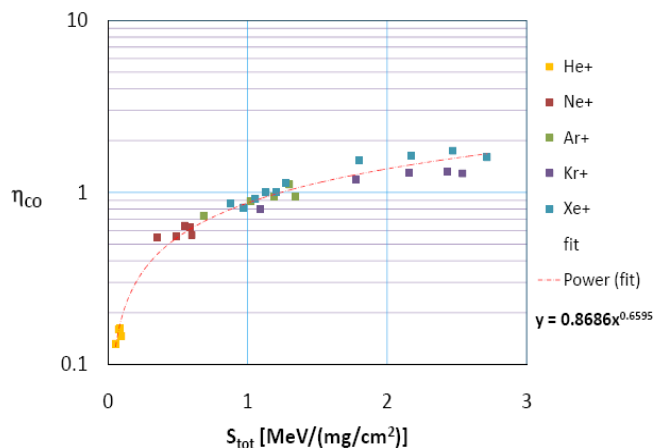


Figure 6.43: CO desorption yields as a function of the total energy loss obtained for noble gas ions incident on copper.

$$\eta = A \cdot S_{tot}^b$$

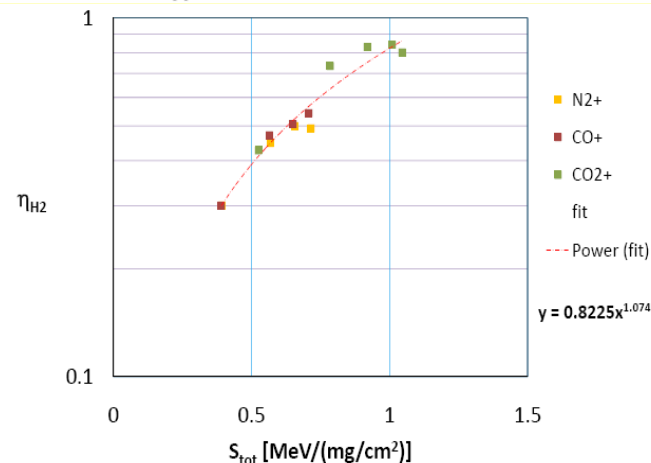


Figure 6.48: H_2 desorption yields as a function of the total energy loss obtained for N_2^+ -ions and oxygen containing ions incident on copper.

G. Hulla, PhD Thesis, Vienna Tech. U, 2009

- Desorption of physisorbed gas

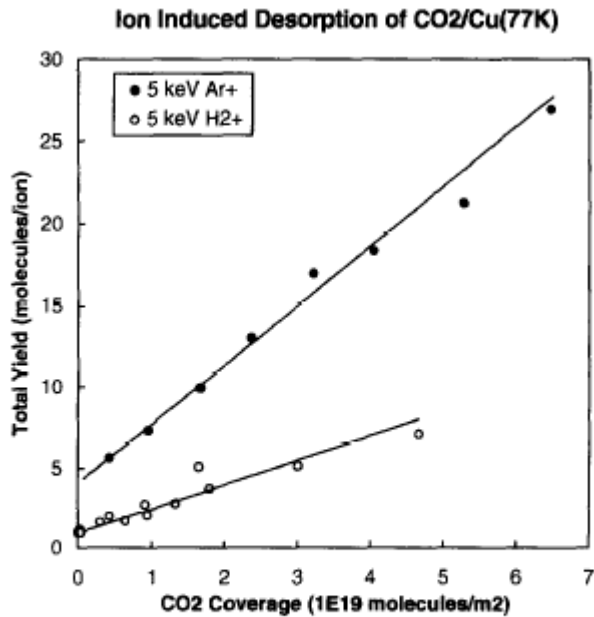
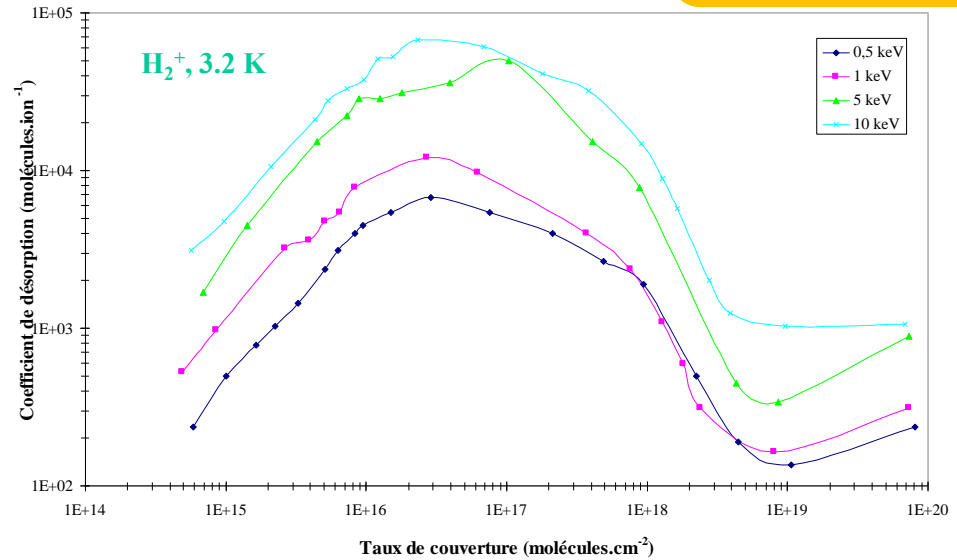


Figure 2. Total desorption yields from adsorbed CO₂/Cu(77K) induced by bombardment of 5 keV H₂⁺ and Ar⁺ ions, plotted as a function of CO₂ dose. The lines indicated are best fit lines drawn by eye through experimental points.

J. Barnard *et al.*, Vacuum 47 (4), 347, (1996)



(N. Hilleret, R. Calder, IVC, 1977)

$\eta'_{H_2} \sim 2000$
 $\eta'_{CO_2} \sim 2$
 @ 5 keV and 1 monolayer

- Critical current is changed to
$$I_c = \frac{\alpha S}{(\eta_{ion} + \eta'_{ion}) \frac{\sigma}{e}}$$

- It is a function of the geometry, the gas specie, the sticking coefficient and of the 2 desorption

LHC beam screen stability

Complementary
information

- A minimum pumping speed is provided beam the beam screen's holes

$$(\eta_i I)_{\text{crit}} = \frac{e}{\sigma} S_{\text{eff}}$$

	H ₂	CH ₄	CO	CO ₂
$(\eta I)_{\text{crit}}$ [A]	1300	80	70	35



Courtesy N. Kos CERN TE/VSC

- Beam screen's holes provide **room for LHC upgrades**

- NB : In the long straight sections, vacuum stability is provided by TiZrV films and ion pumps which are less than 28 m apart

Pressure increase in LHC due to ions ?

Complementary
information

- The ion flux is a function of the pressure and the beam current

$$\dot{\Gamma}_{\text{ion}} = \sigma \frac{I}{e} P \cong 310^8 \text{ ions/cm}^2/\text{s} = 310^{11} \text{ ions/m/s}$$

- For nominal parameters, $P \sim 10^{-8}$ mbar and $I \sim 600$ mA
- Ion energy will be about 100 eV, so the desorption yield about 2 molecules/ion

$$Q = \frac{\eta \dot{\Gamma}}{3.310^{19}} = 2 \cdot 10^{-8} \text{ mbar} \cdot \ell/\text{s/m}$$

- Beam screen pumping speed, S

$$S = 3.63 \text{ A} \sqrt{\frac{T}{M}} \cong 1000 \ell/\text{s/m}$$

- Pressure increase due to ion:

$$\Delta P = \frac{Q}{S} = 10^{-11} \text{ mbar}$$

→ No visible pressure increase in LHC

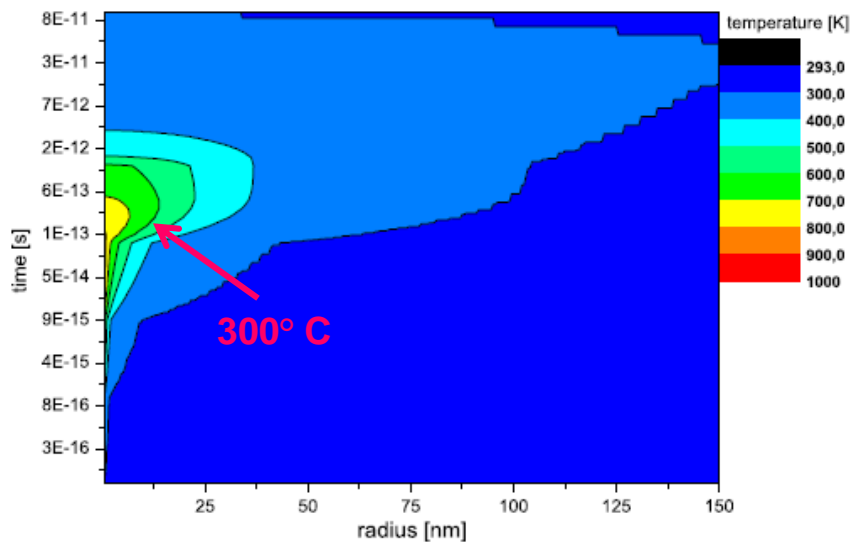
3. Particle losses and ion stimulated desorption

- Surface effect (except diffusion H₂) due to a thermal activation
- « Inelastic thermal spike model » : a temperature map coupled to the thermal desorption model

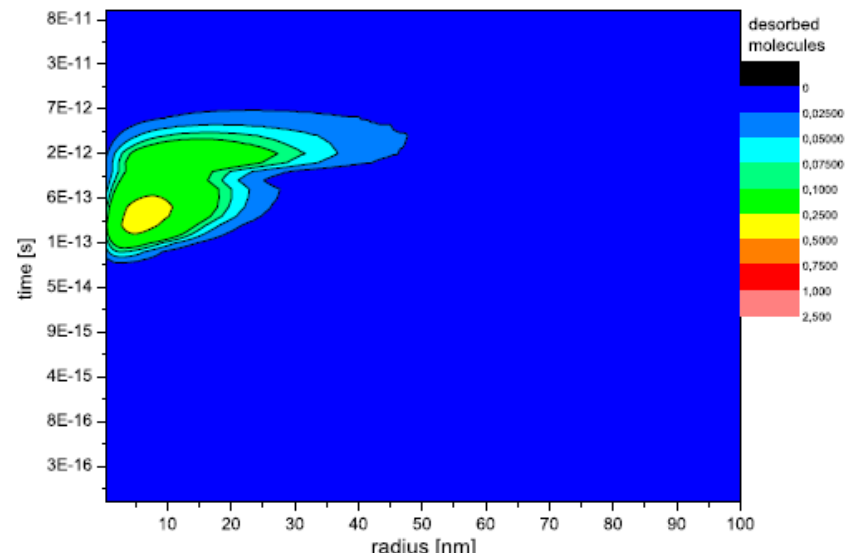
$$\eta = \int_0^{t_{max}} \int_0^{r_{max}} v_0(T(r,t)) \cdot \bar{n}(r,t) \cdot \exp\left(-\frac{E_{des}}{k_B \cdot T(r,t)}\right) \cdot 2\pi \cdot r dr dt,$$

M. Bender *et al.*, NIM B 267 (2007) 885-890

Xe²⁹⁺, 1.4 MeV/u, Perpendicular



Temperature of atomic Cu subsystem after Xe impact



Desorbed particles per Xe per dt

$$\eta_{calculated} = 185$$

4. Electron cloud and related surface parameters

4.1 Introduction

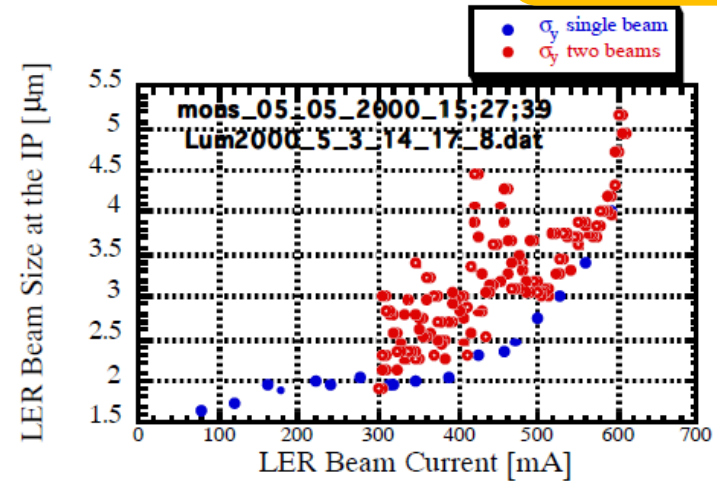
- Cu OFHC vacuum chamber, unbaked, NEG pumping
- Emittance blow up in the vertical plane of the positron beam
- Positron bunch instability due to the cloud of photoelectrons
- Observed in multibunch mode

K. Ohmi, F. Zimmermann, PRL 85, 3821 (2000)

- Installation of permanent magnets then solenoids

→ Luminosity increase

Observation at IP



Y. Funakoshi *et al.*, EPAC 2000, Vienna, Austria



KEKB LER Solenoids

- Stainless steel vacuum chamber baked at 250°C in the straight sections
- Stainless steel vacuum chamber cooled at 4 K in the arcs
- Pressure increase with protons and ions beams
- NEG, bakeout, solenoids, beam structure

→ Luminosity increase

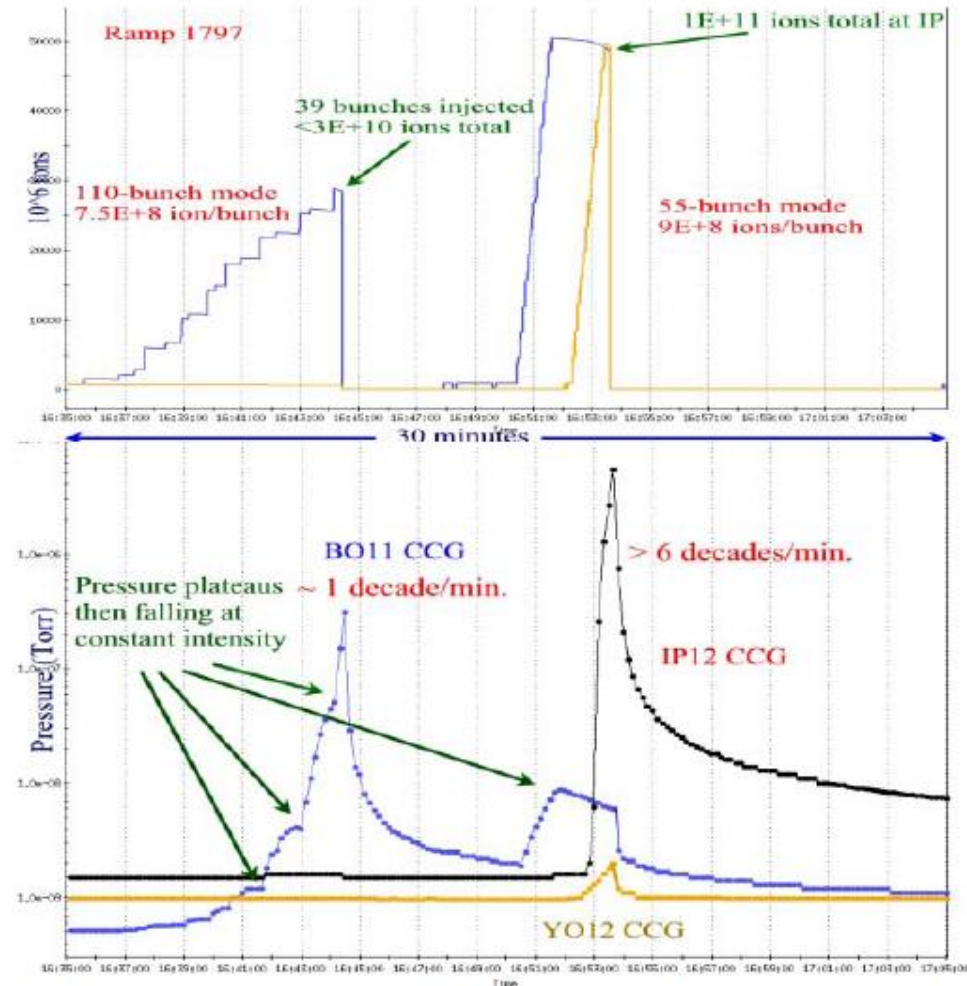
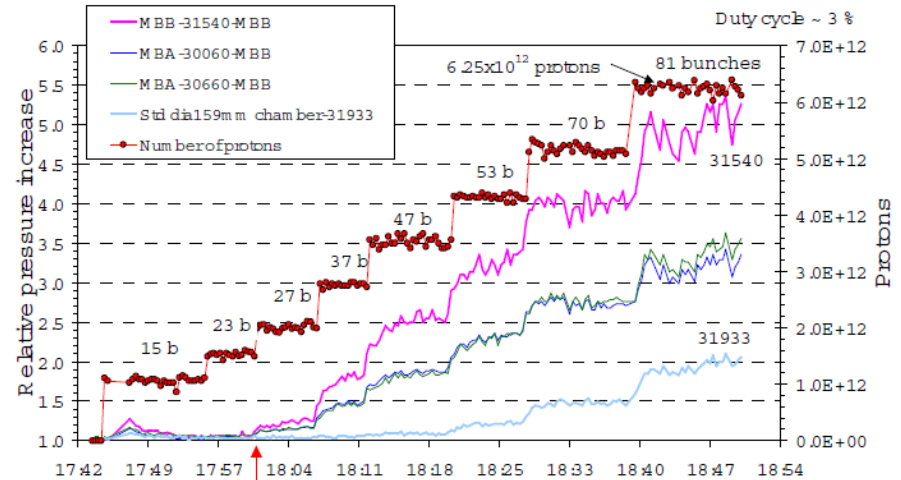


Fig 2. Pressure rises during 110-bunch and high intensity 55-bunch mode Au operations. H. Hseuh *et al.*, EPAC 2002, Paris, France

- Unbaked stainless steel vacuum chamber
- Pressure increase observed with LHC type beams
- Measurement of electron current on a pick up

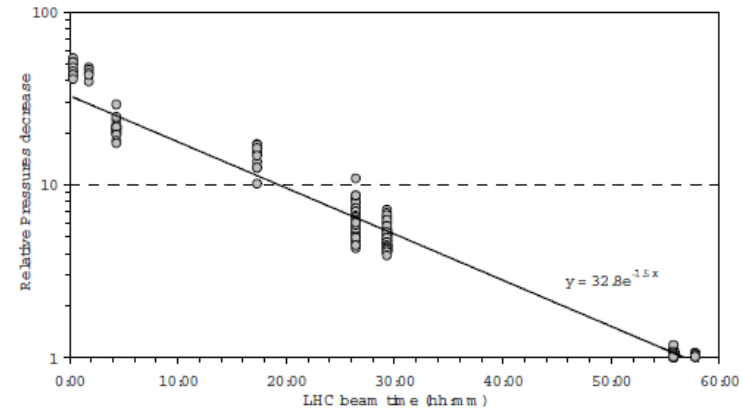
7.7 10¹⁰ protons/bunch



J.M. Jimenez et al., EPAC 2000, Vienna, Austria

- 60 h of beam conditioning

→ Ok for LHC beam injection



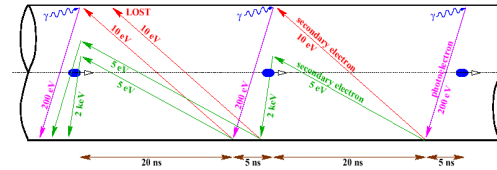
J.M. Jimenez et al., EPAC 2000, Vienna, Austria

Simple model

Complementary information

- Synchronism condition:

$$\frac{2r_p}{\Delta v} \leq t_{bb}$$



Schematic of electron-cloud build up in the LHC beam pipe.

- Speed increment due to the kick

$$\Delta v = \frac{\Delta p}{m} = 2cr_e \frac{n_b}{r}$$

- Intensity threshold:

$$n_b = \frac{r_p^2}{r_e L_{bb}}$$

- Enough energy gain due to the kick to produce secondaries:

$$\Delta W = \frac{\Delta p^2}{2m} = 2 \frac{mc^2}{e} r_e^2 \left(\frac{n_b}{r} \right)^2$$

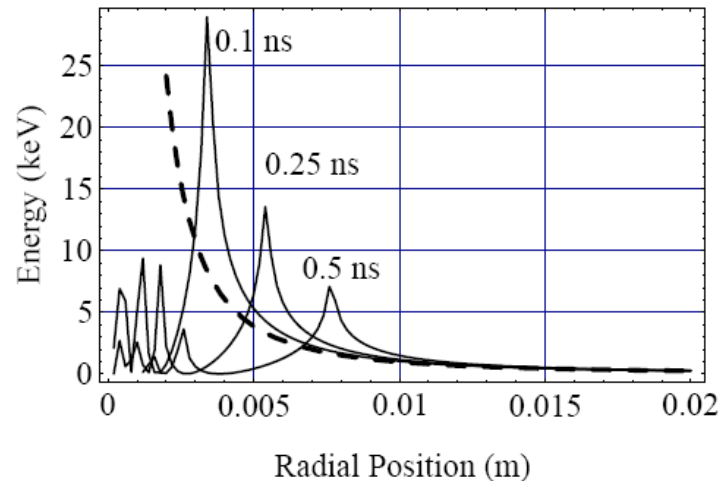


Figure: 1 Electron energy after the passage of a bunch in LHC versus the initial radial position for 0.1, 0.25 and 0.5 ns bunch length. The dotted curve is calculated for the stationary electron approximation.

O. Gröbner. PAC 97, Vancouver, Canada

Electrons in the vacuum chamber wall vicinity receive a kick of 190 eV, those in the beam vicinity receive 15 keV.

4.2 Photons from SR

- SR irradiation at EPA
- Grazing incidence, 11 mrad
- The photoyield **increases** when increasing critical energy.
- Photon reflectivity **slightly decreases** when increasing critical energy
- PY*: photoelectrons per absorbed photons

Material	Status	45 eV		194 eV	
		R (%)	PY* (e/ph)	R (%)	PY* (e/ph)
Al	unbaked	-	0.11	-	0.32
Cu-smooth	unbaked	81	0.11	77	0.32
Cu-electrodeposited	unbaked	5	0.08	7	0.08
Cu-sawtooth	unbaked	8	0.03	7	0.04
TiZr	unbaked	20	0.06	17	0.08
TiZr	activated at 350°C	20	0.02	17	0.03

I.R. Collins *et al.* EPAC 1998, Stockholm, Sweden

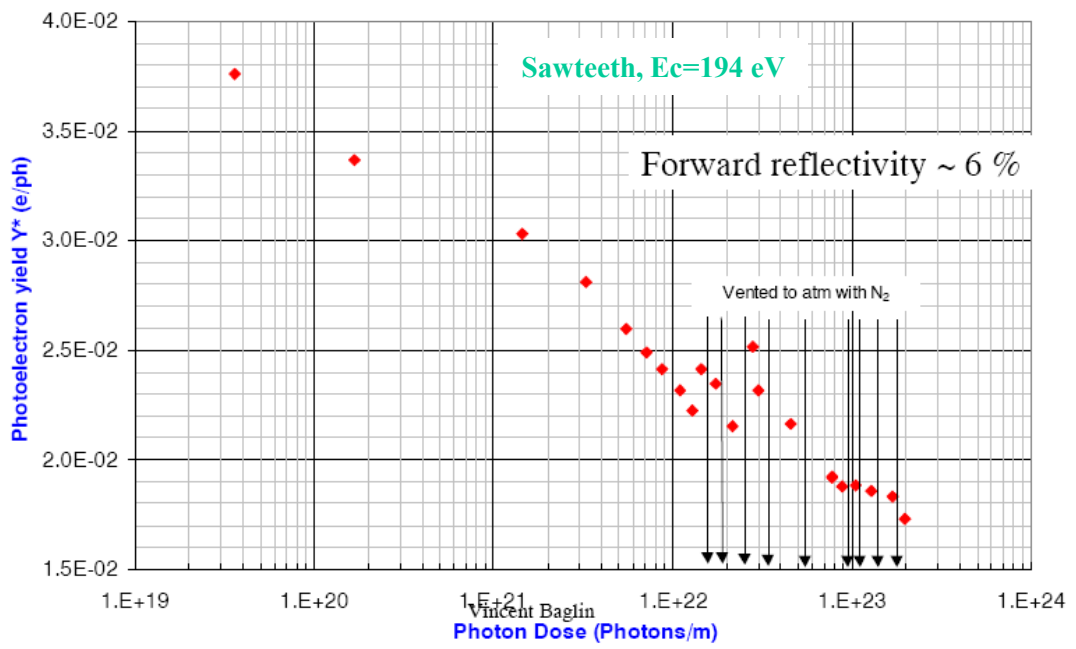
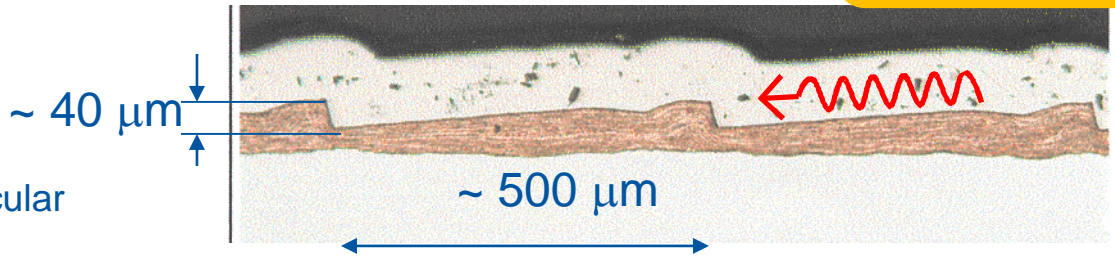
NB : molecular desorption yields are linear in the range, 10 – 300 eV.
So the photoelectron yield should be also proportional to critical energy

$$PY^* \sim E_c$$

Photoelectrons for a LHC type beam screen

Complementary information

- The Photoyield decrease with **beam conditioning**
- It varies from 1 to 4 % under perpendicular incidence

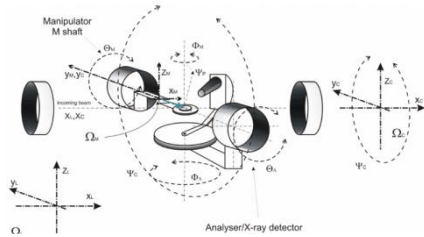


V. Baglin *et al.*, Chamonix, 2001

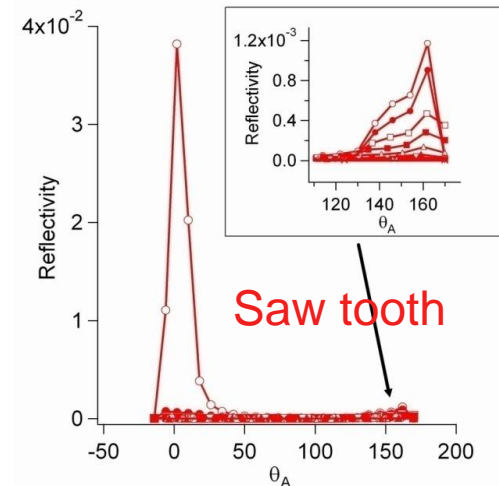
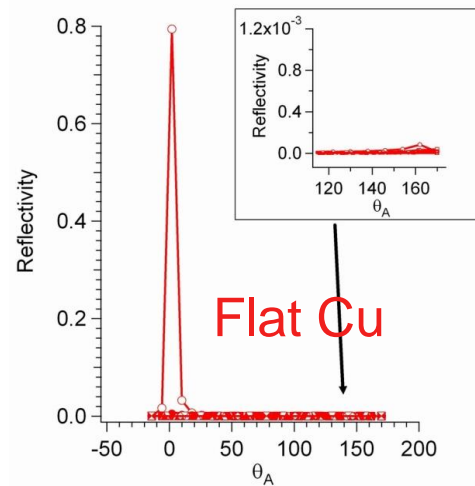
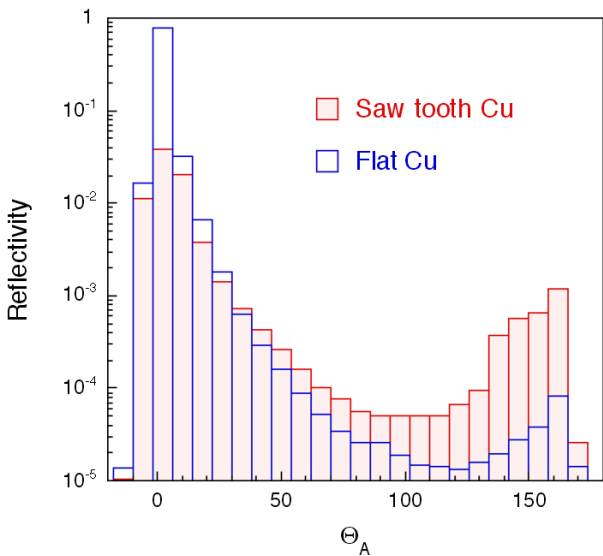
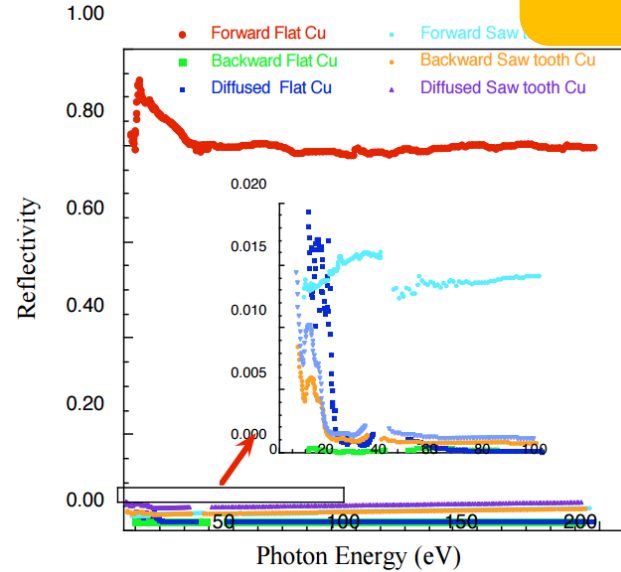
Photon reflectivity of LHC type material

Complementary information

- The saw tooth structure reduces the reflectivity



	Flat sample	Saw-tooth sample
Forward scattering	80 %	4 %
Back scattering	0 %	2 %
Diffused	2 %	4 %
Total	82 %	10 %



N. Mahne *et al.* App. Surf. Sci. 235, 221-226, (2004)

4.3 Electrons from the electron cloud

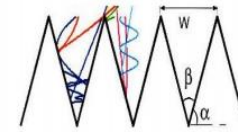
Geometrical effect

Complementary information

- After a coffee discussion, a drilled sample by the VAC workshop (H. Kos)

- $\varnothing \sim 1 \text{ mm}$, 92 holes/cm²

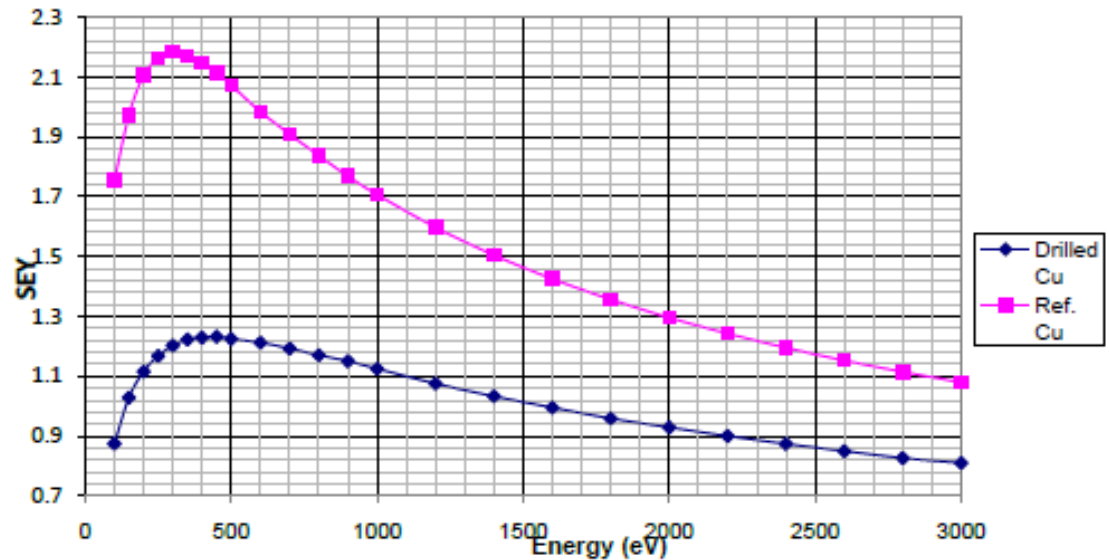
- Original idea with groove only:



By A. Krasnov and
By L Wang et.al

SEY max < 1.3 for Cu unbaked !!

Drilled Cu vs. air exposed Cu



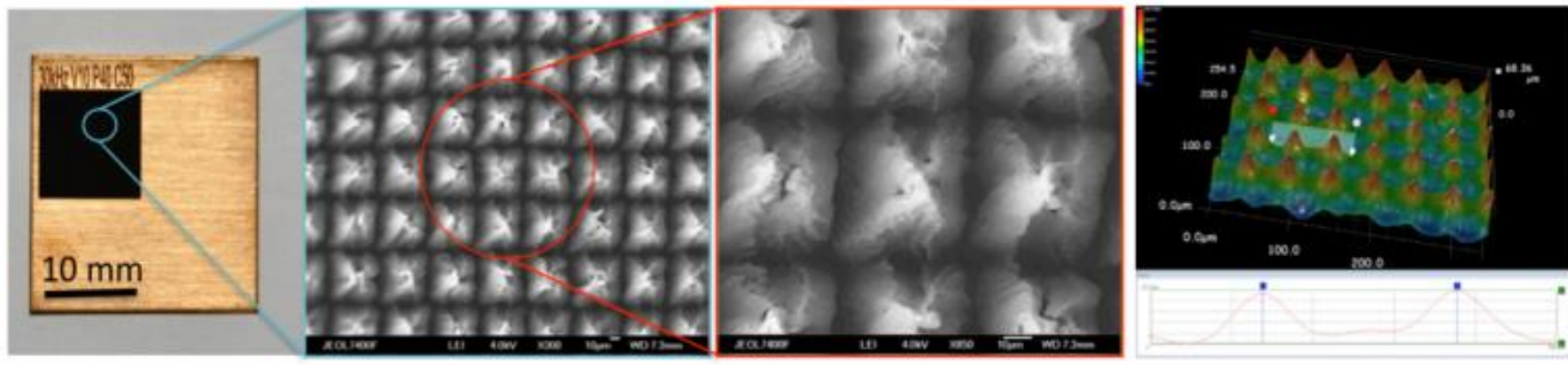
Measurement courtesy A. Kuzucan

A fancy effect or a real application ?

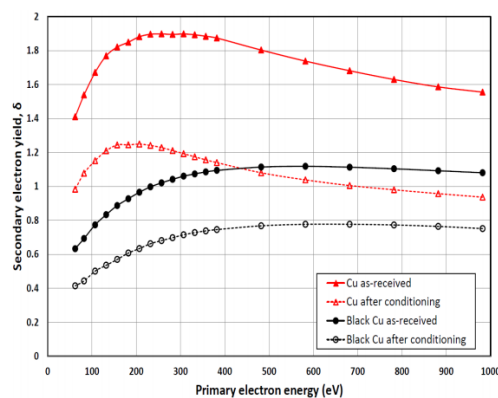
Laser Engineered Structure Surface

Complementary information

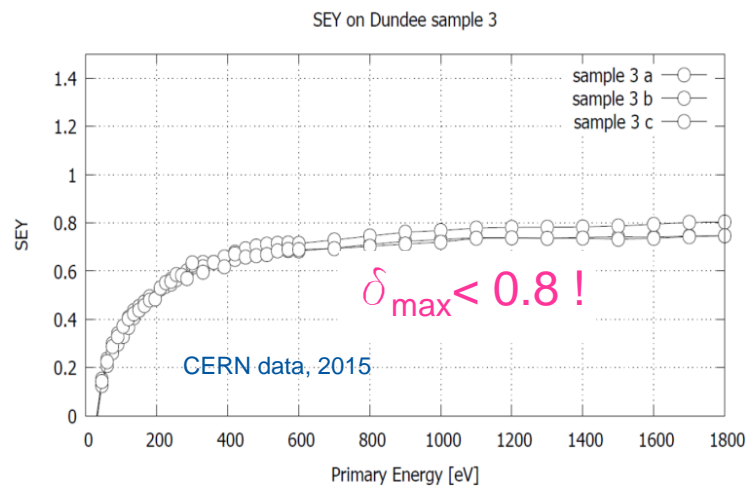
- Principle: laser treatment of a tube at atmospheric pressure
- Production of a micrometric structure



Appl. Phys. Lett. 101, 2319021 (2012). Physics Highlights – Physics Today (February 2013). Opt. Mater. Exp. 1,1425 (2011).



Applied Physics Letters 12/2014; 105(23): 231605

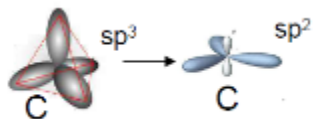


- Still under development by STFC and Dundee university, so it came too late for the LHC construction !

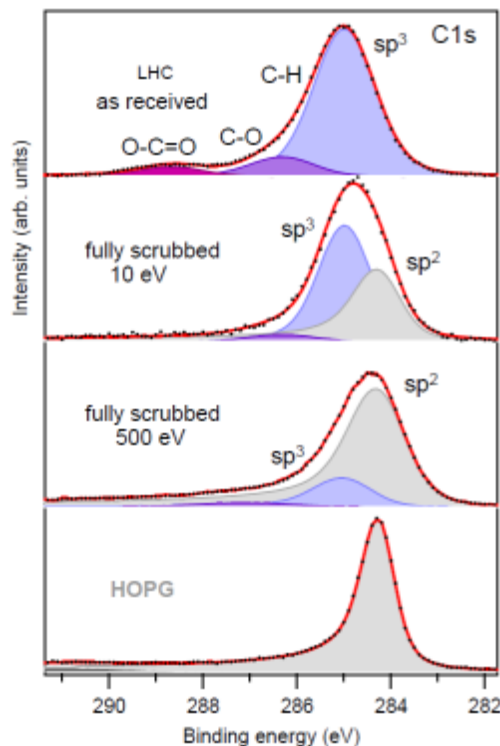
Origin of the SEY reduction at 300 K

Complementary information

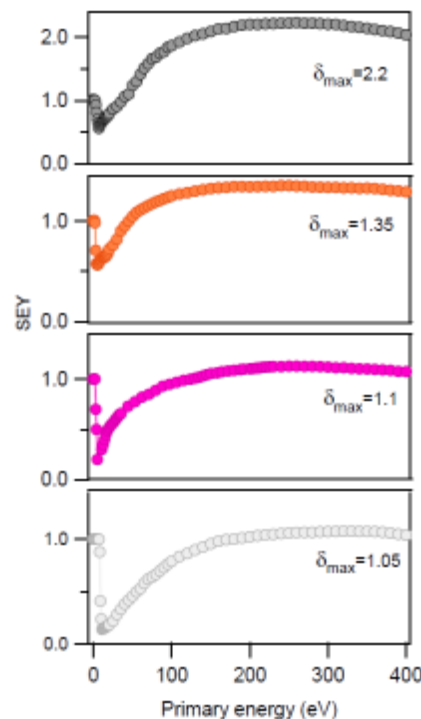
R. Cimino *et al.* PRL **109**, 064801(2012)



- Modification of C1s core level
- Conversion $sp^3 \Rightarrow sp^2$
- High energy electrons increase the number of graphitic like C-C bounds



HOPG : highly oriented pyrolyty graphite



δ_{\max}

2.2

1.35

1.1

1.05

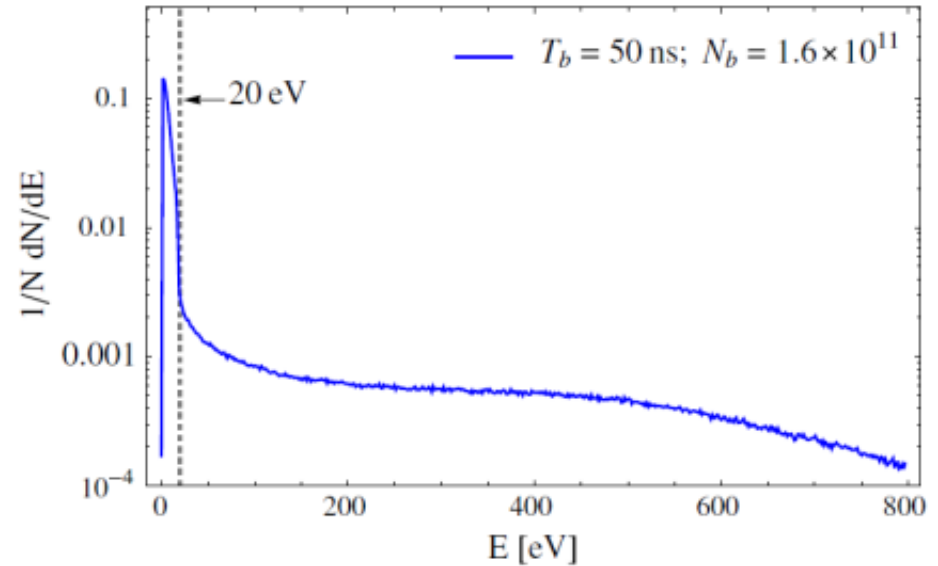
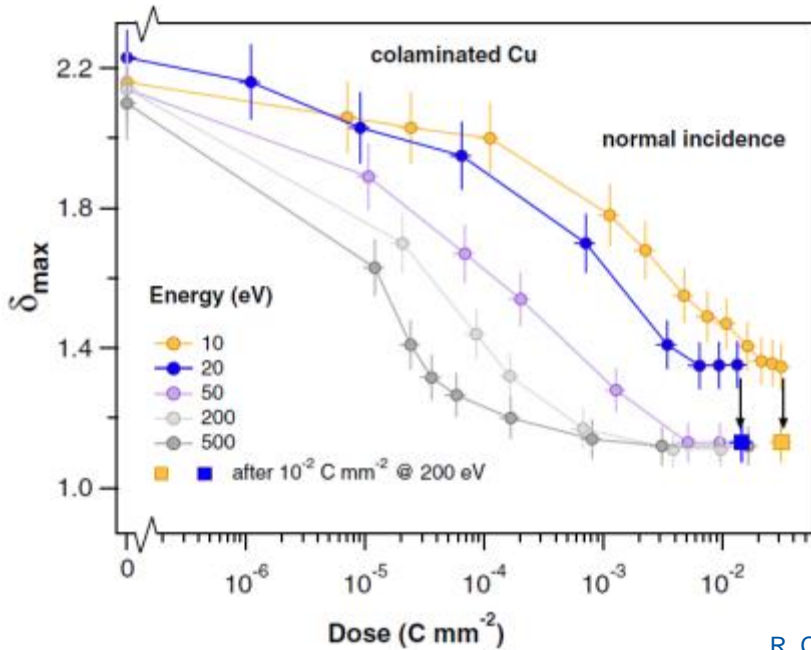
Graphitization of the carbon contamination layer under electron irradiation

Conditioning and electron energy

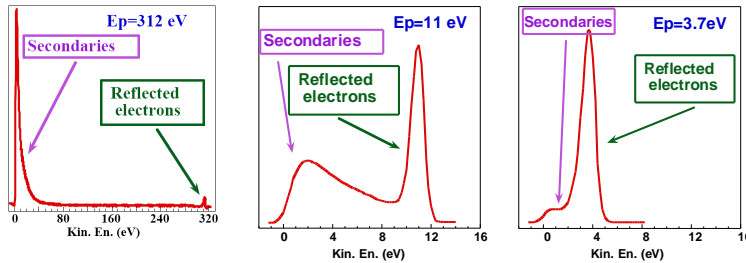
Complementary information

- At 300 K, the scrubbing efficiency of **low energy** electron is less than high energy electrons

- Electron energy distribution at the LHC vacuum chamber wall
- ~ half of the electrons have $E < 20$ eV



R. Cimino *et al.* PRL 109, 064801(2012)



R. Cimino, I.R. Collins, App. Surf. Sci. 235, 231-235, (2004)

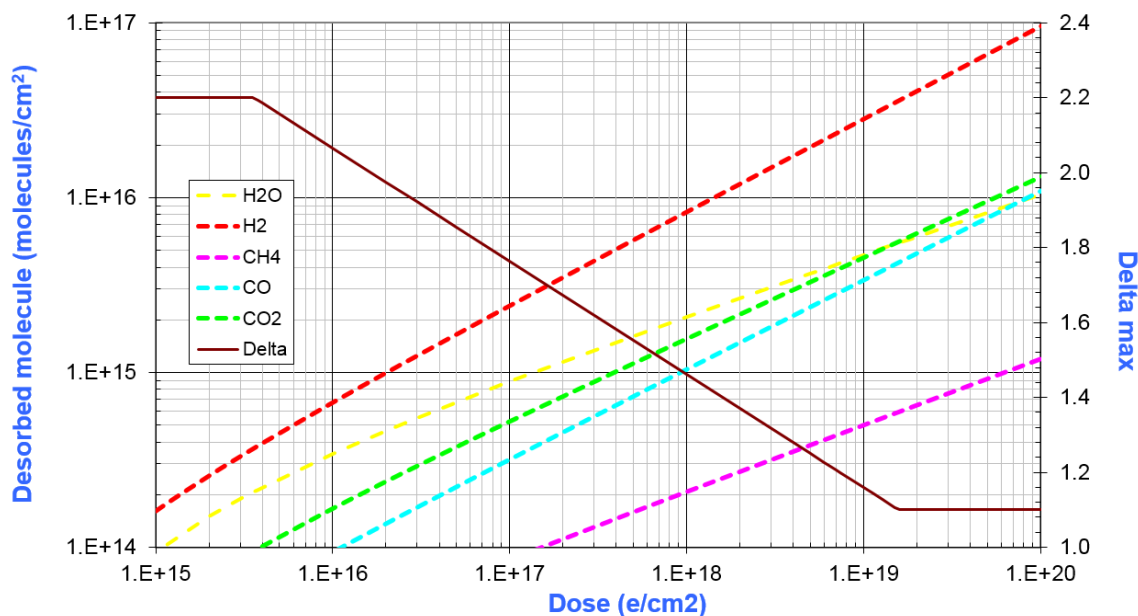
Knowing the energy distribution of electrons is of paramount importance

Electron scrubbing

Complementary information

- After a dose of $\sim 5 \cdot 10^{18}$ e/cm² i.e. 8 mC/mm², the maximum of SEY equals ~ 1.3
- The scrubbing process desorbs several monolayers of gas from the surface
- Potential impact on:
 - frequency of NEG activation
 - increase of SEY due to gas condensation

Unbaked Cu - ESD - 300 eV



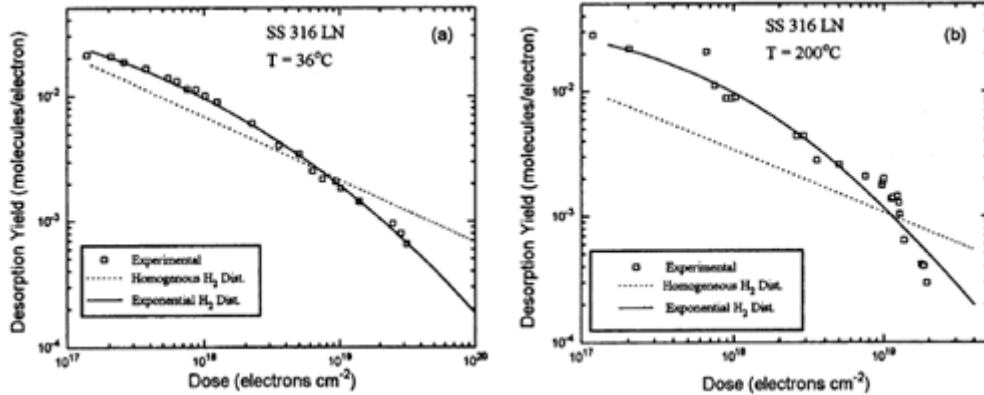
	H ₂	CH ₄	H ₂ O	CO	CO ₂
Q x 10 ¹⁵	19	0.4	4	2	3

→ several monolayer of gas are desorbed when a surface is conditioned

Electron desorption studies at different temperature

Complementary information

- Hydrogen desorption



J. Gómez-Goñi, A.G. Mathewson. J. Vac. Sci. Technol. A 15(6) (1997) 3093

- H₂ electron desorption can be explained by a **diffusion model with a non-uniform concentration** *i.e.* H is produced by dissociation of hydroxydes under electron bombardement

However, the diffusion coefficients taken for RT and 200°C were the same

- No **obvious correlation** between the surface composition determined by AES and desorption yields as a function of temperature : No changes in AES spectra vs 1 to 3 orders of magnitude decrease for the yields.

- The thickness of the oxide layer is more than 3 monolayers (AES scanning depth).

A porous surface oxide layer provide the reservoir of gas

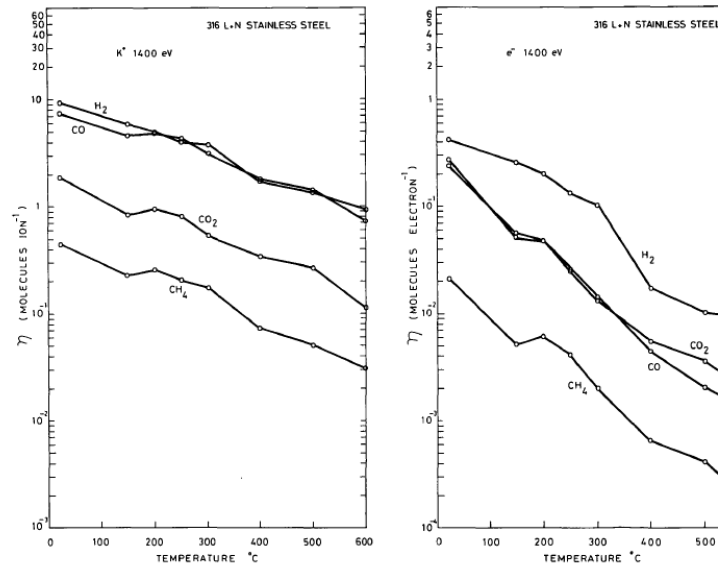


Figure 1. Electron and ion induced desorption coefficients for 316 L + N stainless steel.

M.H. Achard *et al.*, Vacuum 29-2, 53,(1978)

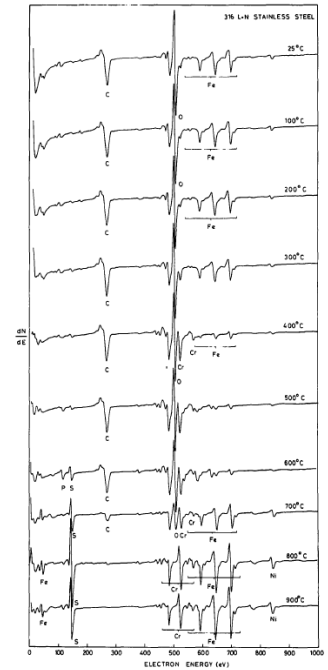


Figure 7. Auger spectra for 316 L + N stainless steel as a function of temperature.